ABSTRACT

WILSON, ANDREW REUBEN. Using a Soil Survey Approach to Understand the Fate of Blue Carbon in a Microtidal Estuary. (Under the direction of Dr. Matthew C. Ricker).

The Albemarle-Pamlico Estuary System (APES) is the second largest estuary in the United States, located in North Carolina and southern Virginia. The APES contains 607,028 hectares of estuarine waters, connected to over 14,484 kilometers of freshwater rivers. The salinity gradient in the APES provides for diverse coastal wetlands: tidal forest (mean water salinity, 0.16 – 1.64 ppt), degraded oligohaline, or 'ghost', forest (4.32 – 8.32 ppt), and mesohaline tidal marsh (12.0 – 15.5 ppt). All ecosystems are affected by climate change, whether its sea level rise (SLR), salinization, or storm-surge driven erosion. This study used a timeline-transect approach to analyze twelve tidal wetlands and the change in soil characteristics upon conversion to open water. Terrestrial, or *in situ*, pedons were compared to analogs along the transect which recently converted to open water (<5 years) and those points converted to open water over 20 years ago. Soil properties including soil organic carbon (SOC) content and bulk density were quantified in relation to position on the transect; subsequently, investigation of total hectares lost by coastal wetland type was performed. Tidal forests lose 420 ± 170 Mg C ha^{-1}, ghost forests lose 446 ± 70, and tidal marshes lose 308 ± 86 upon recent conversion to open water. The immediate loss of SOC between ecosystems was not significantly different ($p = 0.69$) but accounted for 40% of terrestrial SOC in tidal forests; 78% in ghost forests, and 43% in tidal marshes. Approximately 20 years after conversion to open water, further losses of 272 ± 22 Mg C ha^{-1} are observed in tidal forests, 128 ± 133 in ghost forests, and 282 ± 59 in tidal marshes with no significant difference between wetland types ($p = 0.38$). Results suggest large losses of SOC stocks upon land submersion within all wetlands of the APES. Based on remote sensing, 33

hectares of tidal forests, 883 hectares of ghost forests, and 1713 hectares of tidal marshes converted to open water over a 40-year time-period within the APES.

^{210}Pb and ^{14}C accretion rates were also calculated for each wetland type and associated carbon sequestration rates. Short-term (^{210}Pb) accretion rates (cm y^{-1}) in tidal forests were 0.49 ± 0.04, ghost forests 0.38 ± 0.02, and tidal marshes 0.42 ± 0.03. Short-term accretion rates in tidal forests were significantly higher than ghost forests ($p = 0.048$). Soil carbon sequestration rates (kg C yr^{-1} m^{-2}) in tidal forests were 0.18 ± 0.02, ghost forests 0.12 ± 0.004, and tidal marshes 0.08 ± 0.003. Tidal forests sequestered significantly more carbon than ghost forests and tidal marshes ($p < 0.001$). Comparing ^{14}C (long-term) accretion rates from 600 to 3000 years before 2021 (cm yr^{-1}), tidal forests accreted 0.12 ± 0.01, ghost forests accreted 0.13 ± 0.02, and tidal marsh accreted 0.07 ± 0.01. Tidal marshes accreted at significantly lower rates than tidal forest and ghost forest in long-term accretion ($p = 0.048$). There were no significant differences among long-term carbon sequestration rates (kg C yr^{-1} m^{-2}) for these three ecosystems ($p = 0.151$), with tidal forests sequestering (0.05 ± 0.01), ghost forests (0.05 ± 0.02), and tidal marshes at (0.03 ± 0.01). Based on analyses conducted and projected SLR scenarios for 2050 and 2100, none of the ecosystems will keep pace at current levels of accretion and net erosion/submersion is expected in the future. Information from this study provides significant insight into the pedogeomorphology of coastal wetlands, chemically and physically, when undergoing salinization driven by SLR. The results from this study allow land managers allocate resources and understand which ecosystems should be prioritized and preserved in the face of encroaching sea level in the 21st century.

Using a Soil Survey Approach to Understand the Fate of Blue Carbon in a Microtidal Estuary

by
Andrew Reuben Wilson

A thesis submitted to the Graduate Faculty of
North Carolina State University
in partial fulfillment of the
requirements for the degree of
Masters of Science

Soil Science

Raleigh, North Carolina
2025

APPROVED BY:

Matthew C. Ricker Committee Chair	Ben O. Kisila
Lonnie Leithold	Ekrem Ozlu

BIOGRAPHY

Reuben was born and raised in Bakersville; a town of approximately 350 people nestled deep within the Blue Ridge Mountains of Western North Carolina. He grew up the fourth out of five children on a cattle and Fraser fir farm, enjoying the outdoors, exploring the land, and playing baseball. His passion for soil science was cultivated at a young age from being on the farm and his father's service in the Mitchell County Soil and Water Conservation District. He attended North Carolina State University for his undergraduate degree, double majoring in Plant and Soil Sciences and Natural Resources, with a minor in Agricultural Business Management. His participation in collegiate soil judging and Alpha Zeta agricultural honors fraternity further cemented his desire and interest to serve and enhance the field of soil science. Upon graduation, he worked as a Research Technician for the Pedology and Land Use Lab at North Carolina State University before accepting a job as a Soil Scientist for the USDA-NRCS in Raleigh, North Carolina where he currently works.

ACKNOWLEDGMENTS

I would like to thank Dr. Matthew Ricker for formulating the research idea and helping me refine, enlighten, and further improve the way in which I analyze soils and the world within them. I would also like to thank him for providing me with the opportunity to be his research technician and ultimately exposing me to the world of Coastal Zone Soil Survey and the job I currently have with the USDA. What he has taught me about coastal wetlands and the soils has certainly allowed me to flourish and find a career which I love, and I will be forever grateful for that. I would also like to thank Dr. Ben Kisila, Dr. Lonnie Leithold, and Dr. Ekrem Ozlu for their feedback and serving on my committee.

I would like to thank Greg Taylor for seeing the potential in me and willingness to take a chance on a kid that had spent the first 23 years of his life nowhere near a boat and knew next to nothing about them. The opportunities and experiences you have provided me with the USDA were a dream I never knew I had. Specifically, thank you for letting me prove to you what I could do and letting me run with it. I would also like to thank him again, along with Dean Shields, Zach Butler, and Matt Duval for assistance in extracting the subaqueous soil cores.

I would be remiss if I didn't acknowledge Shannon Bradley and Lori Gorczynski, who encouraged me to go further and enjoy soil science in all its shapes and sizes while working on their respective graduate projects. Sure, there were tough days when heatstroke was imminent, or cottonmouths were swimming around the boat, but we had fun, and we enjoyed what we did.

I would also like to thank Dr. Rich McLaughlin, Adam Howard, and the late Chris Niewoehner for welcoming me into the world of research and being a research technician. Especially to Chris who was always able to answer any questions I had, fix any equipment that I couldn't figure out for myself, and taught me the basics of running and fixing a boat in a three-

hour timespan. People like Chris and Adam are the reason research continues to be conducted, and all the gears don't grind to a halt.

I would also like to thank my dad, Steve Wilson, for inspiring a respect for the land and the bounty for which it can provide. The lessons were almost always non-verbal or spoken in cryptic Shakespeare, but I learned much about hard work and being loyal to what made you. Thank you for continuing to nudge me along in making sure I completed what I started. I would also like to thank the rest of my family as well including my mother, Cynthia Wilson, for making sure I always had what I needed and behaved. Your sacrifices did not go unnoticed, and I will be indebted in perpetuity for when you and dad went without so that I didn't have to.

I would also like to thank the love of my life and ultimate cheerleader, Gracie. Thank you for being willing to listen, commiserate, and reprimand as needed when I started feeling discouraged about the process or anything in general. What began as trauma-bonding about being a research technician ultimately bloomed into a loving, hard-working relationship and I look forward to everyday with you.

Finally, I would like to thank my dog, Chip, for being there from the beginning and growing with me in this process. Thank you for all the afternoon walks clearing my head and always being happy to see me, no matter what kind of day I had or how I was feeling. Thanks, little buddy.

TABLE OF CONTENTS

LIST OF TABLES

LIST OF FIGURES

CHAPTER 1

A Soil Survey Approach to mapping Terrestrial and Subaqueous Blue Carbon in Dynamic Ecosystems

Introduction

Climate change is disrupting ecosystems globally; destabilization and departure from homeostasis in these environments often leads to temporal reduction in plant net primary productivity or eventual evanescence (IPCC, 2022; Nicholls et al., 2007). The main drivers of these changes include global mean sea level change, increased intensity and frequency of extreme weather and climate events, and increasing ocean acidification (IPCC, 2022; Camelo et al., 2020; Conner et al., 2007; Hoegh-Guldberg et al., 2007; Michener et al., 1997). The underlying cause of the aforementioned factors is the increase in anthropogenic carbon dioxide, methane, and other greenhouse gases in the Earth's atmosphere (IPCC, 2022; Montzka et al., 2011; Scenarios, 2000; Mitchell, 1989; Arrhenius, 1896). Due to the heat-absorbing effect of these carbon-centric gases, a collective effort exists across scientific disciplines and public policy groups to better understand the associated carbon flux and fate in a range of environments. Thus, the inception of a global endeavor to better understand the carbon cycle and inform climate change mitigation and adaptation efforts.

Estuaries are a subset of environments and ecosystems which play an outsized role in regulating the global carbon cycle. Estuaries occur at the interface of freshwater from terrestrial sources and saltwater from marine sources. This interaction creates diverse ecological communities, globally including coastal mangroves, seagrass meadows, and tidal marshes (Thrush et al., 2013; Perillo, 1995; Fairbridge, 1980; Pritchard, 1967). In the Southeast United

States, the dominant estuarine environments are tidal forests, 'ghost forests', and tidal marshes, with their corresponding ecotones (Stedman and Dahl, 2008). The Albemarle-Pamlico Estuary system (APES) is the second largest estuary in the United States and is in this region within North Carolina and southern Virginia (Giese et al., 1985). This estuary exhibits the same gradient of coastal wetland systems from tidal fresh to polyhaline moving from the west (inland) to the east towards the Atlantic Ocean. The APES is a flooded river valley and characterized as a restricted lagoonal system. The outer ring of barrier islands, also known as the Outer Banks, limit lunar tidal exchange and salinity due to interspersed inlets (Riggs and Ames, 2003). These factors lead to water levels and currents being largely driven by wind, primarily in the Pamlico Sound (Luettich et al., 2002). Albemarle Sound on the north end of the APES is less saline because of its distance from tidal inlets and seasonal flow from the Chowan and Roanoke Rivers (Giese et al., 1985). The Pamlico Sound exhibits higher salinity due to influence from adjacent inlets of Oregon, Hatteras, and Ocracoke (Eulie, 2014).

Carbon sequestration is often cited as the preeminent ecosystem service in coastal wetlands due to its role in mitigating climate change. Efforts to preserve and enhance estuarine environments for carbon sequestration are currently limited by lack of knowledge of carbon sequestration in these systems (Fest et al., 2022; Young et al., 2018). Therefore, accounting of 'blue carbon', a term used to describe carbon stored in the world's coastal zone and marine ecosystems, is lacking (Lovelock and Duarte, 2019; Krauss et al., 2018; Mcleod et al., 2011). Currently, there is a national cooperative effort in the United States headed by the Natural Resources Conservation Service (NRCS), an agency of the United States Department of Agriculture (USDA) to map and better understand blue carbon distribution on the landscape, as well as its fate as sea level rises and submerges coastal lands. The coastal zone is defined as the

land surface influenced by marine processes; it extends from the inland limit of inundation by tides, waves, and wind-blown coastal dunes and then seawards to the depth of closure where waves no longer significantly impact the seabed (Short, 2012).

Most blue carbon studies focus on terrestrial carbon stocks in tidal marshes, and some have extended into shallow sampling in subaqueous seagrass meadows (Zhong et al., 2023; Thomas, 2014), but few studies have documented the fate of blue carbon *in situ* and how it changes upon shoreline erosion, submersion, and conversion to open water. The APES contains a large area (>1.5 million ha) of tidal freshwater forested wetlands, degraded forested wetlands, and mesohaline marshes which store a significant amount of carbon (Gorczynski et al., 2024). Because of this, the APES is an ideal location for a case study of what happens to organic carbon in these three coastal wetland systems upon conversion to open water as relative sea level rises. Coupling this with a soil survey approach allows for identification of areas recently submerged (<5 years) and areas converted to open water for an appreciable amount of time (>20 years) by using soil surveys and shorelines published in the latter half of the 20th century. Building on this approach, the use of historical soil survey information allows for an evaluation of what the subaerial soil was prior to submersion and the associated ecosystem that was converted to open water.

Projected sea level rise for the Southeastern United States is currently following the Intermediate to Intermediate-High scenarios put forth by Sweet et al. (2022) with a predicted range of 28 to 58 cm by 2050. Using these same scenarios, the region could witness sea level rise as much as 110 to 160 centimeters by 2100 (Sweet et al., 2022). Using the IPCC (2022) Intermediate model, predicted sea level rise in North Carolina is 31 to 39 cm by 2050 and 72 to 88 by 2100. With the continued projection of sea level rise and subsequent erosion and

conversion of coastal wetlands to open water, carbon storage and the efficacy of coastal wetlands to be carbon sinks is expected to be significantly reduced (Sapkota and White, 2021; Sierra et al., 2018; DeLaune and White, 2012). We hypothesize SOC stocks will be significantly lower in submerged soils compared to the terrestrial corollary within the APES due to physical erosion of stored SOC. The overall goal of this research was to use a timeline-transect approach, building from historic soil survey data, to quantify and understand the fate of blue carbon in distinct coastal wetland ecosystems of the region.

Area of Interest

The Albemarle-Pamlico Estuary system (APES) contains 607,028 hectares of estuarine waters that is connected to over 14,484 kilometers of freshwater rivers within the greater watershed (Riggs and Ames, 2003). The resulting three dominant types of coastal wetlands are tidal forests, ghost forests, and tidal marshes. Each coastal wetland is influenced by different landscape factors, and they are therefore inherently different from each other.

Tidal forests are non-tropical wetlands characterized by woody vegetation and tidal flooding with sufficient frequency to continuously saturate the soil surface (Hackney et al., 2007). In the southeastern United States, these wetlands typically form in two types of riverine geomorphologies: redwater (eutrophic) and blackwater (Doyle et al., 2007). The lower Chowan River is a traditional blackwater tidal forest, it originates on the Coastal Plain with a low river channel gradient, the water has a high dissolved organic carbon content, and exhibits a wide floodplain (Foyle et al., 2007; Kroes et al., 2007; Meyer, 1990). The Tar-Pamlico and Roanoke rivers are considered redwater (eutrophic), they originate in the Piedmont physiographic province, exhibit high sediment loads, and are relatively nutrient rich (Doyle et al., 2007). Tidal forests established near the confluence of saline and freshwater mixing are actively changing.

These fringe tidal forests are subject to salinization from sea level rise, saltwater intrusion during low-flow periods during droughts upstream, and high salinity flushes during storm surge events (Hackney and Avery, 2015; Conner et al., 2007; Day et al., 2007).

When saltwater is not flushed from the system, salts accumulate in soil pore water. Accumulation results in mass mortality of native vegetation and expansion of more salt-tolerant species (Conner at al., 2007). As salt concentrations surpass the threshold of the woody vegetation and tidal forest deteriorate, halophytic species gradually colonize the ecosystem. This ecotone between tidal forest and traditional tidal marshes is known as a 'ghost forest' (Ury et al., 2021; Kirwin and Gedan, 2019; Munns and Tester, 2008). Beyond the species composition, a ghost forest experiences decreased woody biomass production, leading to reduced accretion, elevated sulfate from saltwater influx, and increased methane emissions (Herbert et al., 2015). While the transitory ecosystem progresses toward an herbaceous tidal marsh, it is suspectable to erosion of organic soil material because of anchoring root senescence.

The stable, saline wetland in the estuarine ecosystem is the tidal marsh. Tidal marshes are globally recognized for several ecosystem services which traditionally place them at a higher value compared to other coastal ecosystems due to the ability to buffer storm surge, provide juvenile habitat for aquatic fauna, and demobilize nutrients such as nitrogen (Mitsch et al., 2015; McInnes, 2013; Cahoon and Guntenspergen, 2010). Tidal marshes are the dominant coastal wetland in the APES and concurrently bear the largest proportion of land loss. This loss is due to the exposure of marshes to significant fetch and storm events leading to increased rates of erosion and conversion to open water (Gorczynski et al., 2024; Sapkota, 2021).

For this study, we extended longitudinal transects established in Gorczynski et al. (2024) on the eastern edge of the Albemarle-Pamlico Peninsula to the extent of microtidal influence in

the Chowan, Roanoke, and Tar Rivers. The 12 representative wetland transects, based on salinity levels and mapped soil type, were parsed into representative ecosystems (tidal forest, ghost forest, tidal marsh) with four replicated for each. The transects were extended into the open water with two observations at each site, one representing the ecosystem upon immediate (<5 years) subaerial shoreline submersion and one representing the ecosystem after long-term (>20 years) submersion.

Materials and Methods

Terrestrial Reference Pedons, Salinity Data, and Site Selection

Terrestrial subaerial soil carbon pools, characterization data, and average site water salinity across a gradient of ecosystems (tidal forests, ghost forests, tidal marshes) were obtained from Gorczynski et al. (2024). This dataset and study site locations were used to compare terrestrial and subaqueous soils from nearshore to offshore environments. Subaqueous samples were taken along shore-perpendicular transects to understand how terrestrial soils and associated carbon stocks are changing due to sea level rise, land submergence, and shoreline erosion across a salinity gradient in the Albemarle-Pamlico region (Figure 1.1). The research sites included tidal forests (n = 4), oligohaline degraded forests, or 'ghost forests' (n = 4), and mesohaline tidal marshes (n = 4). Average salinity ranges for ecosystems are tidal forest (0.2 – 1.6 ppt); degraded oligohaline-mesohaline forest, or ghost forest (3.5 – 8.3 ppt), and mesohaline tidal marsh (11.7 – 15.5 ppt).

Subaqueous sites were selected to continue the terrestrial transect conducted by Gorczynski et al. (2024). This approach allowed a terrestrial comparison for the nearshore and offshore cores (Figure 1.2). Nearshore is the term used in this study to describe subaqueous cores

taken as close as reasonably practicable to the current shoreline (mean 15.2 ± 4.4 m from shoreline), in-line with the terrestrial transect; this allows for a space-for-time quantification of the change in soil physical and chemical characteristics upon submersion. Offshore is the term used in this study to describe subaqueous samples taken in-line with the terrestrial transect where a noticeable difference in bathymetry occurs from the nearshore core (mean 150 ± 28.5 m from shoreline). A noticeable difference in bathymetry was defined as an increase in depth to bottom of the water column by approximately 100 cm compared to the nearshore core. In the absence of noticeable difference in bathymetry, the published Soil Survey Geographic Database (SSURGO) lines were used to determine the offshore sampling locations.

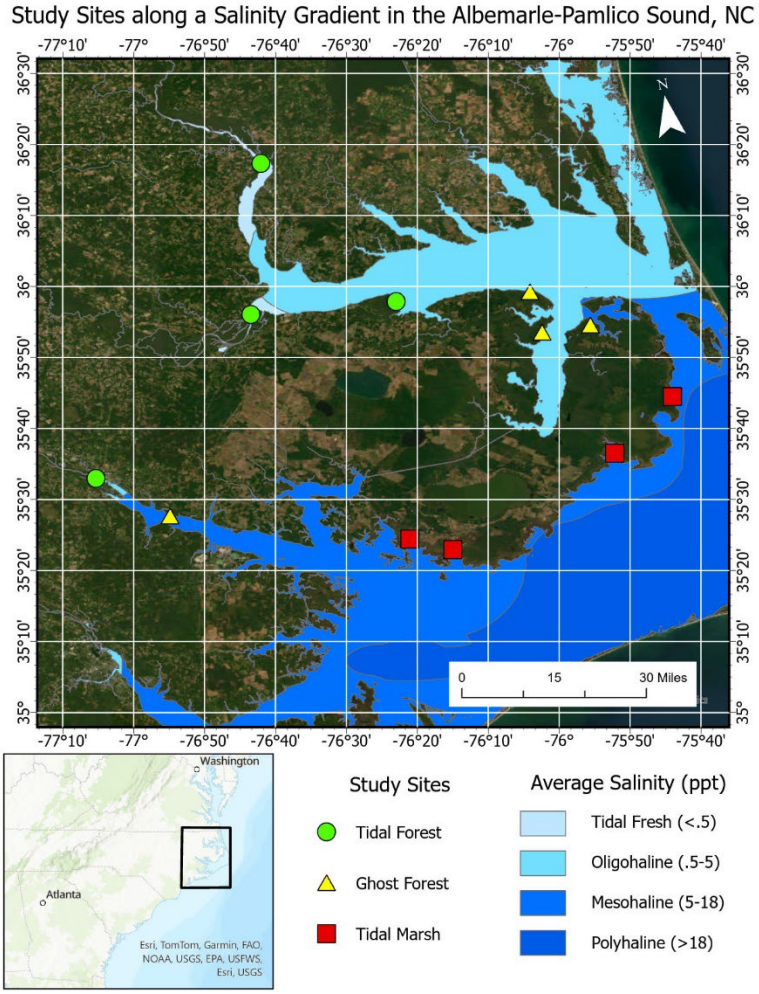

Figure 1.1: Map of study sites representing tidal forested wetlands, ghost forests, and tidal marshes along a salinity gradient (0.2 – 15.5 ppt average water salinity).

The six soil survey areas where this research was conducted were mostly published in 1986, except Hyde (1996) and Washington (1979) counties. These soil survey areas did not receive coastal mapping updates since the original date of publication, an average of 34 years and maximum of 41 years since publication. Use of historical soil survey delineations allowed for an assured location which was submerged for at least 30 years, depending on the county SSURGO publication date. The offshore core provides insight as to what chemical and physical state the submerged or eroded terrestrial soil becomes over an approximately 20-year period, as well as visualizes erosion.

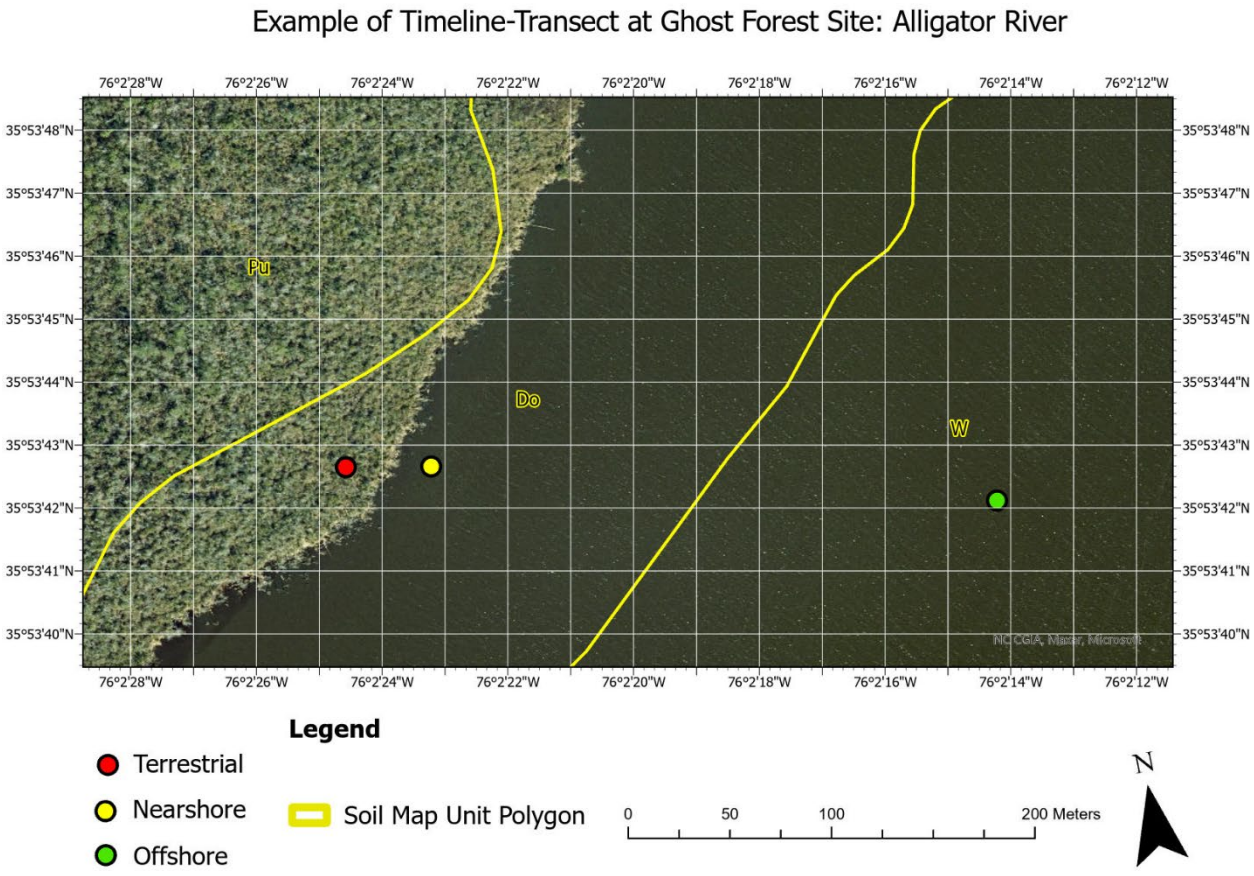

Figure 1.2: Map of the transect performed at designated site Alligator River. The nearshore core was extracted in an area mapped as the Dorovan (Do) soil series in 1986 but has been converted to open water. The offshore core was extracted in an area mapped as Water (W) in 1986, this provides a baseline of the exposure of a submerged soil over a period greater than 20 years.

Field Data Collection

Subaqueous soil sampling occurred in 2020-2021. Sample sites were accessed using a custom-built Clark Boat Company, Inc. 7.3-m pontoon boat designed for subaqueous soil survey. Coring points were chosen in the field using a Garmin GPSMAP 742 Plus and linked real-time sonograph of the subaqueous surface with a Garmin transducer. Subaqueous cores were extracted using a G55H Multiquip Stationary Vibrator Motor and associated flex shaft mounted to a 7.6 cm diameter section of aluminum irrigation pipe with a wall thickness of 0.51 mm. Pipe length was adjusted from site to site based on depth of water and amount of core compaction being experienced. Cores were extracted in accordance with National Soil Survey Handbook Part 656.3 (Soil Science Division Staff, 2017). Some minor deviation from terrestrial transects were necessary due to submerged logs and relict coarse root systems in tidal forests and ghost forests. A total of three cores were taken at all but two of the sites (n = 34). At designated site Palmetto-Peartree, only a nearshore core was taken due to no increase in water depth beyond SSURGO polygons being observed leading to an assumed homogenous soil core between the nearshore and offshore observations. At designated site Chowan River, the depth of the water column was too deep to safely core. Duplicate cores were taken at each nearshore and offshore site; one core was used for description and the other for lab analysis sampling (Soil Survey Staff, 2022a).

Cores were stored at Vernon James Research Center in Plymouth, North Carolina at 4 °C. Soil cores were split with DeWalt 891 metal shears and described according to standard methods for subaqueous soils (Schoeneberger et al., 2012) and classified using the 13th Keys to Soil Taxonomy (Soil Survey Staff, 2022b). Soil horizons with an estimated organic carbon content greater than 12% were described using the von Post humification scale to determine the degree of organic matter decomposition (Von Post and Granlund, 1926).

Laboratory Analysis

Seven sites (7 pedons, 35 horizons) were analyzed by the Kellogg Soil Survey Laboratory in Lincoln, Nebraska according to National Cooperative Soil Survey characterization methods for subaqueous and organic soil materials (USDA 2023; Soil Survey Staff 2022a). The remaining sites (15 pedons, 89 horizons) were analyzed by the NC State University Department of Crop and Soil Sciences using the following methods.

For chemical analysis, 10 cm^3 of soil from each horizon were extracted with a syringe and analyzed for pH using 1:1 (soil : liquid) deionized (DI) water solution and 1:2 calcium chloride ($CaCl_2$) solution. Electrical conductivity (EC) was also analyzed for each horizon using 1:1 and 1:5 DI water solutions (Soil Survey Staff, 2022a). Initial pH and EC measurements were measured with Thermo Scientific Orion Star portable pH/EC meter. Incubation pH (1:1 DI) was measured at room temperature under moist aerobic conditions over 16 weeks to identify sulfidic materials, starting one week after cores were split. Bulk density was measured using the syringe method after oven drying the known volume of 10 cm^3 at 105 °C for 24 hours (USDA, 2023). The texture of mineral horizons was determined using the hydrometer method (Gee and Bauder, 1986). Sandy texture classes were wet sieved to determine sand size distribution and apply texture modifiers (very coarse, coarse, medium, fine, very fine). Total soil carbon and nitrogen (w/w) were measured using the thermal combustion method on a Perkin Elmer 2400 C/N analyzer (Culmo, 1988). Loss on ignition (LOI, %) was determined for both mineral and organic horizons by heating a 2.5 g sample of organic soil material and 5 g sample of mineral material in a muffle furnace at 400 °C for 16 hours (Soil Survey Staff, 2022a).\

Statistical Analysis

All statistical analyses were conducted in R (version 4.3.1, R Core Team 2024). Data visualization and manipulation were performed with ggplot2, dplyr, and plotrix R packages (Wickham, 2016; Wickham et al., 2023; Lemon, 2006). Horizon-scale analysis was conducted on all subaqueous soil core horizons (n = 124) between the ecosystems without differentiating between nearshore and offshore cores, or organic versus mineral, as to increase statistical power. Regressions were used to evaluate relationships between horizon bulk density, soil organic carbon content, and horizon mineral soil content. A one-way ANOVA was used to test the difference in horizon bulk density, soil organic carbon, carbon to nitrogen ratio (C:N), 1:5 EC, 1:1 pH, initial and oxidized pH between ecosystems. Tukey HSD was used for further analysis when ANOVA were significant. Significance level was set to $\alpha = 0.05$ unless otherwise noted.

Pedon-scale analysis was conducted between terrestrial, nearshore, and offshore pedons in each ecosystem at the depths of 50, 100, and 200 cm. Soil sores less than 200 cm in length (n = 6) were excluded from analysis at the 200 cm level comparison to avoid skewing and misrepresentation of data. Weighted pedon averages were calculated for each depth comparison for C:N and 1:5 EC. For mineral and organic horizons, soil C was converted to a mass basis (Mg C ha^{-1}) using bulk density values, horizon thickness (cm) and carbon concentration (Pluske et al., 2020). Horizon carbon stocks were summed together for the total soil C stock to comparable depths of 50, 100, and 200 cm. A two-way 3X3 ANOVA was used to determine significant interaction between terrestrial, nearshore, and offshore pedon weighted averages at 50, 100, and 200 cm and the ecosystem in which they occurred. Tukey HSD was used for further analysis when ANOVA were significant. Significance level was set to $\alpha = 0.05$ unless otherwise noted.

Soil Organic Carbon and Ecosystem Loss Calculations

Horizon carbon stocks were summed together for the total soil C stock to 200 cm. Total terrestrial carbon loss rates for nearshore and offshore pedons were subtracted from the terrestrial pedon carbon stock calculated in Gorczynski et al. (2024) normalized to a depth of 200 cm. Four subaqueous soil cores in tidal forest were less than 200 cm in length because of continuous refusal with the vibracore from buried logs and stumps; these sites were Chowan River (112 cm), Roanoke River (155 cm), Tar River (157 cm), and Bull Neck (132 cm). Two terrestrial soil cores in ghost forest were normalized for the same reason; these were sites Palmetto-Peartree (108 cm) and Goose Creek (150 cm). For data transparency and to issue a conservative estimate, these soil properties were used with the analyzed values only to the depth sampled. For example, Chowan River (112 cm) was still used for terrestrial and nearshore carbon loss comparisons even though the core only went 112 cm deep and the terrestrial site was 200 cm. Therefore, the carbon loss estimates and calculations are conservative in the tidal forest sites; an average carbon loss per ecosystem and by soil core location on the transect were calculated based on the normalized values to 200 cm. The carbon numbers attributed to the 'upland' section of land loss and ecosystem analysis were averaged from the four most prominent mineral upland soil map units being submerged or eroded within North Carolina: Altavista loamy fine sand, 0 to 2 percent slopes; Fork fine sandy loam, 0 to 2 percent slopes, rarely flooded; Yonges loam, 0 to 2 percent slopes, rarely flooded; Hydeland silt loam, 0 to 2 percent slopes, rarely flooded. Mean SOC pool values were drawn from the SoilWeb application which is linked to the Kellog Soil Survey Laboratory database; the representative values for these series are: 60, 90, 160, and 207 Mg C ha $^{-1}$, respectively (University of California, Davis, California Soil Resource Lab, 2019).

The differences in terrestrial and water surface elevations were corrected using LiDAR data from the North Carolina Spatial Data Download Gateway. Difference in surface elevation is important to address as it can lead to misrepresenting the amount of soil lost through submersion and erosion, directly affecting soil C loss (North Carolina Emergency Management, 2016). Soil C losses were averaged by tidal ecosystem and then scaled up for use in total estuary carbon accounting.

GIS Total Land Loss and Terrestrial Carbon Loss Calculations

Landsat images from: 1984, 1990, 1995, 2005, 2011, 2016, and 2020 were extracted from the USGS Earth Explorer interface. The images were taken from May – September to capture peak vegetation. The bands of the satellite images were manipulated to create the greatest contrast between the land and water interface with the most common band setting with Red: Band 1, Green: Band 2, Blue being Band 3 or 4. Once ideal contrast was achieved, a Normalized Difference Vegetation Index (NDVI) was used in ESRI ArcGIS Pro to differentiate between water and land. Manual corrections and corresponding masking of interchangeable raster values were necessary for exposed agricultural land and waterfowl impoundments.

Binary Thresholding is designed for simple, unsupervised classification, but there is inherent difficulty in machine learning between waters stained with dissolved organic material and exposed, organic matter rich agricultural land on the Albemarle-Pamlico Peninsula. The difference in albedo of terrestrial wetlands of the peninsula and that of the Albemarle-Pamlico Estuary water presented a challenge which binary thresholding was unable to overcome and NDVI was used instead because of the greater manipulation available in raster delineation.

NDVI rasters generated from corresponding satellite imagery from years spanning 1984 to 2020 were used to determine the difference between land area using the Clip tool in ESRI

ArcGIS Pro. The amount of land area lost by soil taxonomic classification to the order level was estimated by overlaying the current SSURGO soil map polygon layer with the NDVI raster generated from the 2020 Landsat imagery. The Clip tool was used to calculate the hectarage of each soil series lost as well as its corresponding ecosystem. Based on the assigned ecosystem for the soil map unit (upland, tidal forest, ghost forest, tidal marsh), a total carbon value was assigned to the hectares and summed for the entire peninsula to determine overall area and carbon loss since 1984. Quality control was performed by pinpointing failed NDVI differentiations and recalculating imagery and raster values. When calculating hectares submerged by soil series, any values under one hectare were discarded as to not overestimate the amount of land lost.

Results

Horizon Scale Results

Subaqueous soil horizon properties varied significantly across ecosystem types (Table 1.1). Soil organic carbon (SOC) was significantly higher in tidal forests when compared to ghost forests and tidal marshes environments ($p < 0.001$). Bulk density was significantly higher in ghost forests and tidal marshes environments ($p < 0.001$). C:N ratio was significantly lower in ghost forests when compared to tidal forests ($p = 0.018$), but not in tidal marshes ($p = 0.39$). Horizon 1:5 EC was significantly higher in tidal marshes ($p < 0.001$) when compared to tidal and ghost forests. No significant difference between 1:1 DI pH between the three environments ($p = 0.32$) or delta pH ($p = 0.82$) was detected. Horizon SOC was exponentially related to bulk density ($p < 0.001$, $r^2 = 0.7$) and mineral soil material percent ($p < 0.001$, $r^2 = 0.66$) (Figure 1.3).

Table 1.1: Mean (± SE) subaqueous horizon soil properties compared among ecosystem type. Different letters by column indicate significant differences ($p < 0.05$).

Ecosystem	n	SOC (%)	Bulk Density (g/cm^3)	C:N	EC (1:5 DI)	pH (1:1 DI)	Delta pH (1:1 DI)
Tidal Forests							
Horizons	33	$17.09 \pm 2.74_a$	$0.57 \pm 0.10_a$	$23.42 \pm 1.61_a$	$0.28 \pm 0.03_a$	$5.64 \pm 0.18_a$	$1.23 \pm 0.24_a$
Ghost Forests							
Horizons	42	$2.73 \pm 1.20_b$	$1.27 \pm 0.07_b$	$15.19 \pm 2.28_b$	$0.55 \pm 0.07_a$	$5.67 \pm 0.19_a$	$1.44 \pm 0.23_a$
Tidal Marshes							
Horizons	49	$5.18 \pm 1.50_b$	$1.23 \pm 0.09_b$	$18.69 \pm 1.84_{ab}$	$2.20 \pm 0.24_b$	$5.99 \pm 0.18_a$	$1.39 \pm 0.23_a$

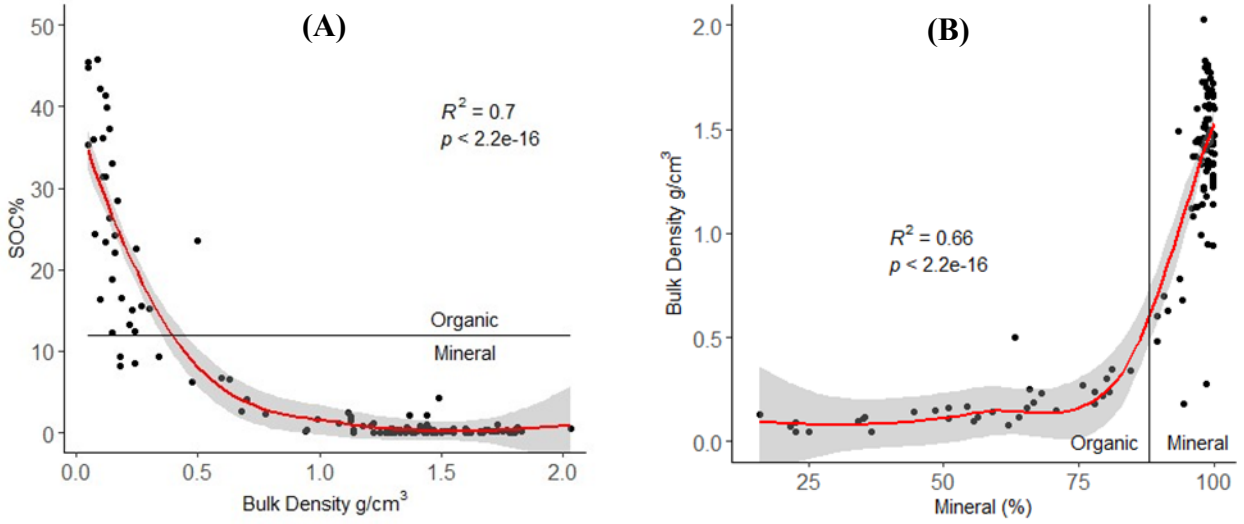

Figure 1.3. (A) Significant exponential regression between horizon bulk density and SOC percent. Organic horizons occur above the 12% SOC solid line and mineral horizons occur below. (B) Significant exponential regression between mineral soil material percent and bulk density. Organic horizons occur below 88% mineral material and mineral horizons occur above. Both regressions were significant at $p < 0.001$. Gray blocks on either side of the regression line represents the 95% confidence interval.

Pedon Scale Results

Two-way ANOVA at 50 cm, 100 cm, and 200 cm revealed significant differences between ecosystems and site locations. Different factors gained and lost significance in the analyses for each depth. In the 50 cm comparison, there were no significant interactions between ecosystems and site locations ($p = 0.66$). Terrestrial sites contained significantly higher SOC ($p = 0.014$) than nearshore and offshore sites. There was no significant difference in SOC between ecosystem types ($p = 0.13$). There was no significant difference in C:N ratio amongst any ecosystem ($p = 0.49$) or site location ($p = 0.06$). Pedon EC 1:5 DI was significantly higher in tidal marsh ecosystems compared to tidal forests and ghost forests ($p < 0.001$), but there was no significant difference between site locations ($p = 0.36$) (Table 1.2).

Table 1.2: Mean (± SE) soil organic carbon stock (Mg ha^{-1}) by depth. Different upper-case letters represent a significant difference between ecosystem and lower-case letter represent a significant difference between terrestrial, nearshore, or offshore by column ($p < 0.05$)

Ecosystem	**50 cm**		**100 cm**		**200 cm**	
Tidal Forests	SOC	n	SOC	n	SOC	n
Terrestrial	$216\pm44_{Aa}$	4	$427\pm60_{Aa}$	4	$924\pm131_{Aa}$	4
Nearshore	$140\pm51_{Ab}$	4	$314\pm87_{Ab}$	4	396_{Ab}	1
Offshore	$73\pm45_{Ab}$	3	$182\pm67_{Ac}$	3	$356\pm61_{Ab}$	2
Ghost Forests						
Terrestrial	$176\pm18_{Aa}$	5	$361\pm35_{Ba}$	5	$610\pm218_{Ba}$	5
Nearshore	$61\pm31_{Ab}$	4	$134\pm85_{Bb}$	4	$159\pm89_{Bb}$	4
Offshore	$44\pm35_{Ab}$	3	$53\pm38_{Bc}$	3	$63\pm40_{Bb}$	3
Tidal Marshes						
Terrestrial	$156\pm26_{Aa}$	4	$307\pm30_{ABa}$	4	$659\pm72_{Ba}$	4
Nearshore	$127\pm9_{Ab}$	4	$294\pm44_{ABb}$	4	$351\pm55_{Bb}$	4
Offshore	$32\pm7_{Ab}$	4	$49\pm10_{ABc}$	4	$69\pm18_{Bb}$	4

In the 100 cm comparison, there was no significant interaction between ecosystems and site locations ($p = 0.08$). There was significantly higher SOC at terrestrial sites ($p = 0.03$) when compared to nearshore and offshore sites; there was also significantly more SOC in nearshore sites when compared to offshore sites ($p = 0.007$). Tidal forests contained significantly more SOC ($p = 0.036$) when compared to ghost forests, but not significantly different than tidal marshes ($p = 0.15$). Offshore sites had significantly lower C:N when compared to nearshore ($p = 0.014$) and terrestrial ($p = 0.045$) sites. There was no significant difference between ecosystem C:N ratios ($p = 0.40$). Tidal marsh pedons had significantly higher EC 1:5 DI ($p < 0.001$) when compared to tidal forest and ghost forest pedons. No significant difference was found between terrestrial, nearshore, and offshore sites for EC 1:5 DI ($p = 0.20$).

In the 200 cm comparison, interaction was significant only between ecosystems and site locations ($p = 0.04$) when comparing EC 1:5; when comparing SOC and C:N the interaction was not significant ($p = 0.24$). When the EC 1:5 interaction was plotted, the means of the ecosystems never crossed. As a result, the cause of this interaction was not investigated further. Tidal forests pedons contained significantly more SOC than other ecosystems ($p < 0.001$) (Figure 1.4). Terrestrial sites contained significantly more SOC than nearshore or offshore sites ($p < 0.001$) and there was not a significant difference between nearshore and offshore sites ($p = 0.054$) (Figure 1.5). When comparing 1:5 EC, tidal marsh ecosystems were significantly higher than other ecosystems ($p < 0.001$). Offshore sites were significantly lower than terrestrial sites ($p = 0.019$) while there was no significant difference between nearshore and terrestrial ($p = 0.25$) and nearshore compared to offshore ($p = 0.45$). There was no significant difference in C:N amongst ecosystems ($p = 0.20$). Offshore sites had significantly lower C:N than nearshore ($p = 0.01$) and terrestrial sites ($p < 0.001$).

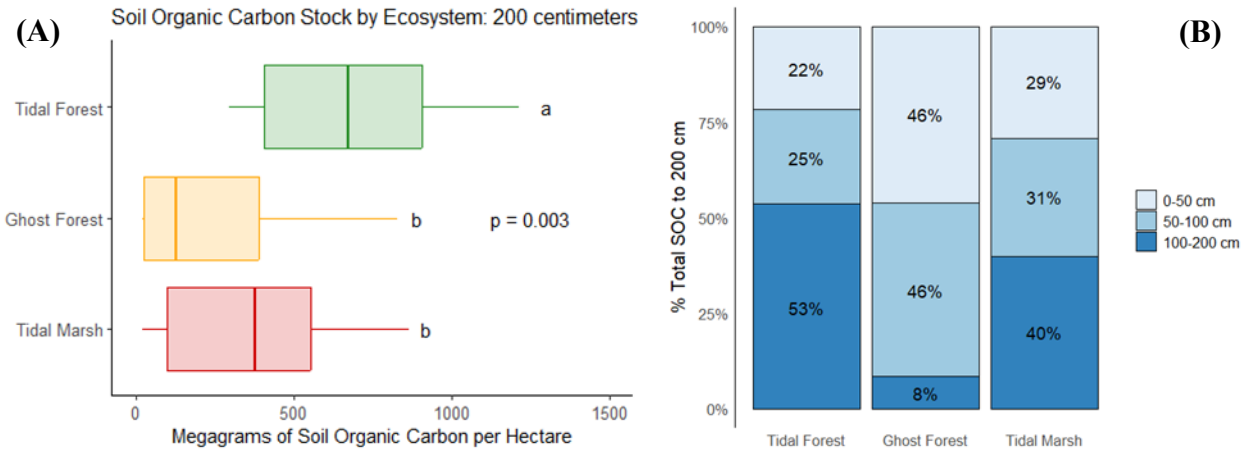

Figure 1.4. (A) Significant difference between SOC stock to 200 cm between tidal forest sites when compared to ghost forests and tidal marshes (B) Total SOC stock contribution in tidal forest (n = 7), ghost forest (n = 9), and tidal marsh (n = 12) by depths of 0-50 cm, 50-100 cm, and 100-200 cm

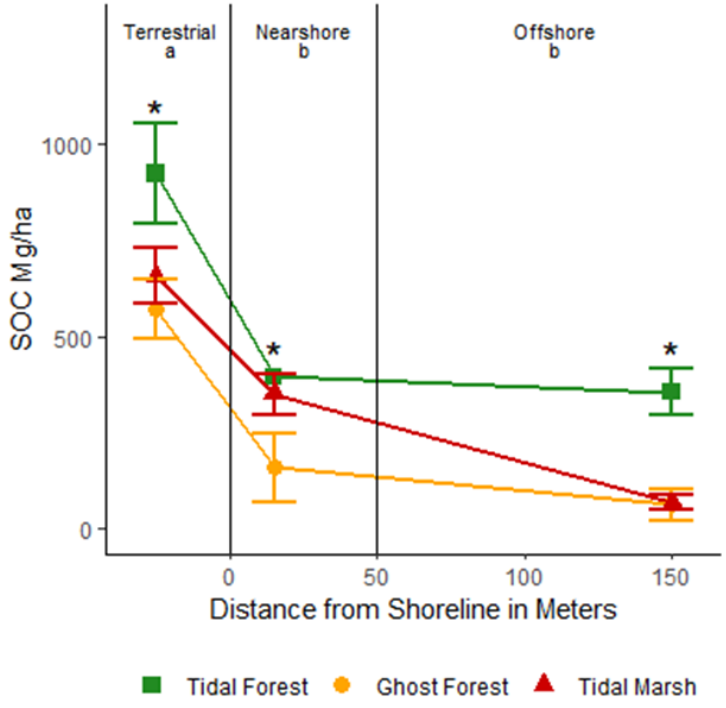

Figure 1.5. SOC stocks in each ecosystem across the transect from terrestrial, nearshore, and then offshore. Significant differences ($p < 0.05$) between terrestrial, nearshore, and offshore locations are indicated by lowercase letters. Significant difference between ecosystems across all sites are indicated by an asterisk above the error bar. This figure only includes terrestrial soil observations and subaqueous soil cores that reach 200 cm, observations that did not reach 200 cm were excluded from this observation to avoid skewing data.

When comparing terrestrial to nearshore net carbon loss (Mg C ha^{-1}): tidal forests lost 420±170 upon submersion, ghost forest lost 446±70, and tidal marsh lost 308±86. No significant difference was found between ecosystem type when comparing terrestrial to nearshore loss ($p = 0.69$). When comparing nearshore to offshore net loss (Mg C ha^{-1}): tidal forests lost 276±22 from nearshore to offshore, ghost forest lost 128±133, and tidal marsh lost 282±59 (Figure 1.6). No significant difference between ecosystem type was apparent when comparing nearshore to offshore loss ($p = 0.38$). Average soil organic material depth lost on submergence in tidal forest is 163±41 cm, 142±23 cm in tidal marsh, and 111±50 cm in ghost forest. There is no significant difference between depth of soil organic material lost between ecosystems ($p = 0.23$), soil organic material is defined as material containing > 12% organic carbon by weight and is commonly referred to as peat. Average soil organic material lost as a percentage compared to terrestrial analogs is 97±7% for ghost forests, 94±12% for tidal marsh, and 82±21% for tidal forests. There was no significant difference between percent of soil organic matter, or peat, depth lost between ecosystems ($p = 0.33$).

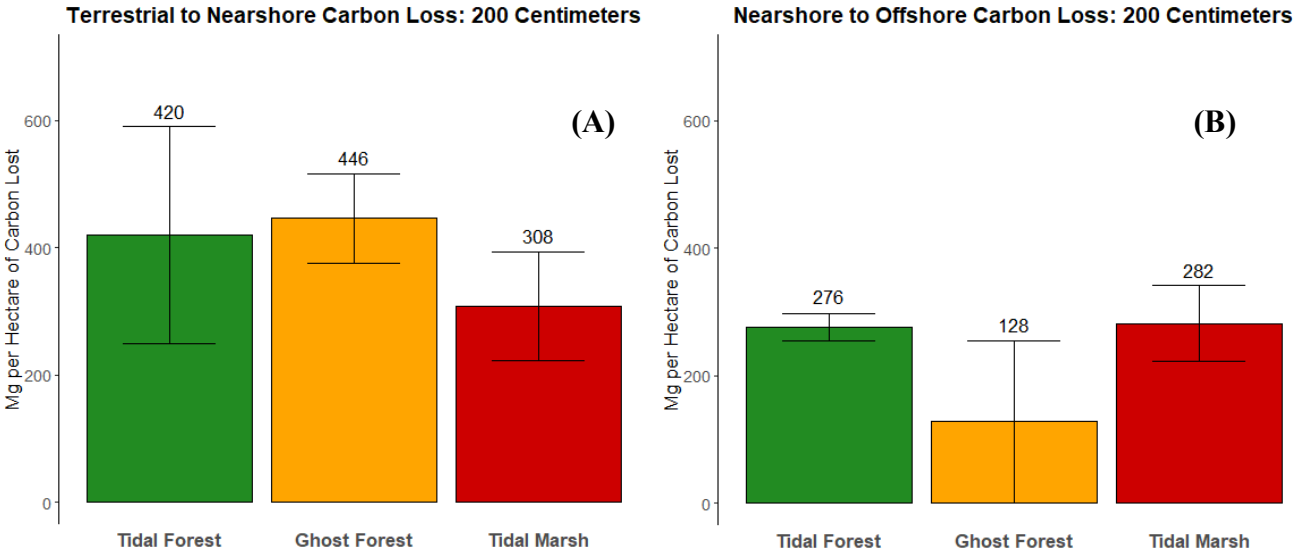

Figure 1.6. (A) Mean terrestrial carbon loss between ecosystem type in terrestrial and nearshore cores **(B)** Mean carbon loss from nearshore to offshore cores

GIS Total Land Loss and Terrestrial Carbon Loss Calculations

From 1984 to 2020, the Albemarle-Pamlico Estuary lost approximately 3,000 hectares of land to shoreline erosion and submersion, a 0.63% loss in land area (Table 1.3).

Table 1.3: Calculated hectares of land lost based on remote sensing and difference in soil map unit polygon area.

Year	Hectares	Hectares Lost	Change (%) from 1984
1984	476,217	-	-
1990	476,047	80	0.02
1995	474,416	1,711	0.36
2005	474,549	1,578*	0.33
2011	474,532	1,595	0.33
2016	474,019	2,107	0.44
2020	473,138	2,833	0.60

* Differences in hectares lost from 1995 to 2005 could be due to storm surge, which lead to large waves or wind set-up. This likely caused some areas to classify as submerged or eroded in 1995 when they were temporarily flooded or ponded.

Based on spatial analysis, 2,833 hectares were submerged from 1984 to 2020; including 2,521 hectares of histosols (Figure 1.7). Of those 2,521 hectares, 1,730 were classified as typic (> 130 cm of organic soil materials) and 791 classified as terric (40-130 cm organic soil materials). Hectares submerged in descending order by ecosystem type were tidal marshes (1,713), ghost forests (883), uplands (204), and tidal forests (33). When scaling the estimates of terrestrial loss of carbon across the study area, tidal marsh ecosystems have lost a projected 1010 Gg C ha^{-1}, ghost forests have lost 478, area with upland soils have lost an estimated 27, and tidal forests have lost 21 (Figure 1.8).

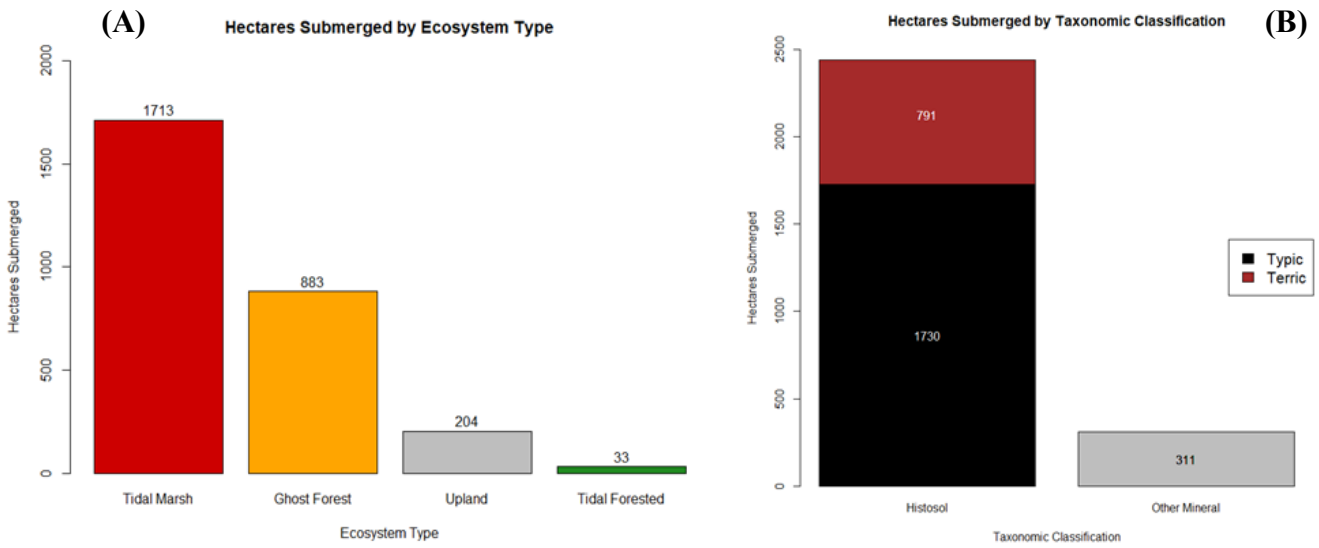

Figure 1.7. (A) the number of hectares submerged or eroded by ecosystem type since 1984. **(B)** hectares lost by soil taxonomic classification since 1984. Histosols are broken into subgroups of Terric and Typic. Other mineral grouping includes Inceptisols, Ultisols, and Alfisols.

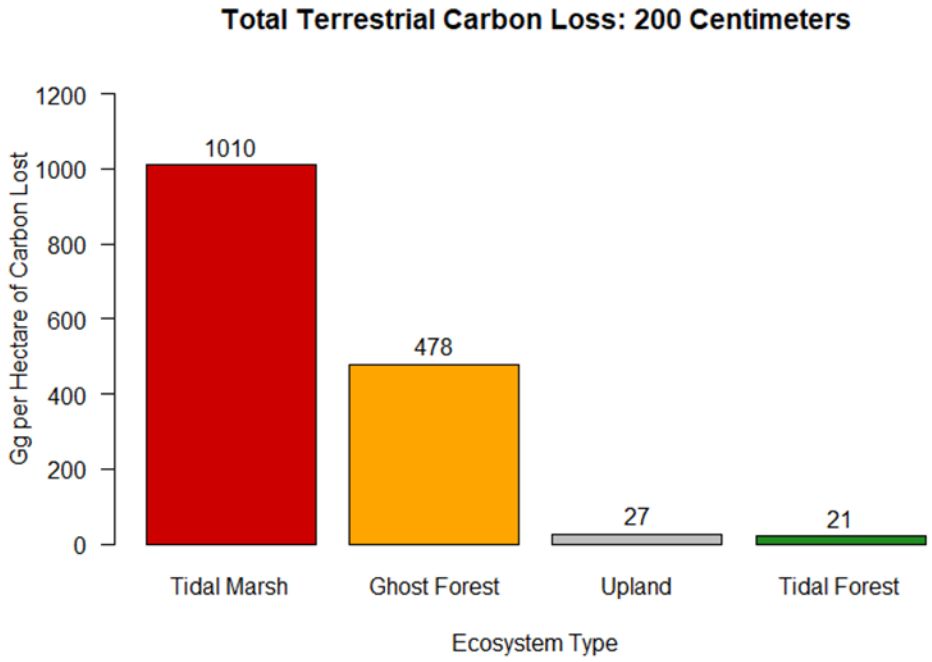

Figure 1.8.
the total carbon lost in gigagrams by ecosystem type within the Albemarle-Pamlico Estuary system.

Discussion

As mean sea level continues to rise, conversion of coastal wetlands to open water will continue regardless of ecosystem salinity, consequently, terrestrial carbon will be mineralized, oxidized, or translocated (Nicholls et al., 2007). Erosion rates will continue to be highest in tidal marshes and ghost forests which are exposed to greater ecological stressors compared to tidal forests (Yao and Liu, 2017a; Williams et al., 1999). There are limited studies using the timeline-transect approach and understanding how baseline soil characteristics and SOC change from the terrestrial pedon, to immediate inundation, and then long-term submersion. Furthermore, there are fewer studies employing the National Cooperative Soil Survey standard to quantify the loss of terrestrial carbon and using historical soil map unit composition to calculate a total loss across an area.

Soil Horizon Characteristics

Over the last three decades, a growing body of work has emerged concerning subaqueous oligohaline and mesohaline areas such as Chincoteague Bay, MD; Banana River Lagoon, FL; and the Lower Chesapeake Bay, VA (Soil Survey Staff, 2024; Soil Survey Staff, 2023; Balduff, 2007). However, a dearth of information exists for subaqueous soils adjacent to upper estuary tidal forests and there is little to compare these soils to in areas with similar environments and erosion rates. We found subaqueous tidal forest soil horizons contained significantly more SOC than both ghost forest and tidal marsh horizons (Table 1.4); this is due to their general protection from wave action; stable accretion rates keeping up with marine transgression, and ultimately considerable soil organic matter accumulation (Anderson and Lockaby, 2007). While not statistically significant, tidal marshes do contain more SOC on average than ghost forest horizons and this can be attributed to several factors: the transitory nature of ghost forest horizons being

exposed to increased salinity and new SOC decomposition pathways, the highly decomposed nature of the existing soil organic matter and its ease of erosion, and the reduction in net primary productivity with changing plant communities (Gorczynski et al., 2024; Ardón et al., 2018; Pierfelice et al., 2017). Ghost forests also occur in areas more exposed to external factors such as fetch, storm surge, and adjacency to anthropogenic ditches that can increase the amount of erosion of surface horizons high in SOC when compared to tidal forests (White et al., 2022; Kirwan and Gedan, 2019). The higher SOC in tidal marshes can be attributed to the persistence of herbaceous vegetation and the surface horizons it produces with high amounts of rhizomes and roots more resistant to wave action (Nyman et al., 2006).

The contrast in soil carbon to nitrogen (C:N) ratios can be explained in similar ways to differences of SOC for different ecosystems. The lower C:N ratios in ghost forests compared to tidal forests can be explained by the higher salinity in these ecosystems; is it documented that an influx of salinity into freshwater ecosystems can release bound ammonium from the cation exchange complex that leads to a lower C:N and higher rates of carbon mineralization (Ardón et al., 2013; Chambers et al., 2013). Tidal forests receive inputs of carbon and nitrogen contingent on the number of allochthonous inputs, this is dependent on the agricultural and urban land density in the watershed (Megonigal and Neubauer, 2019). When compared to other subaqueous datasets, C:N ratio is lower in the APES than other studies in Florida, Maryland, and Virgina. This can be explained by textural differences as well as SOC content in these areas. For example, Florida is significantly higher in sand content of soils when compared to this and other studies, reducing the ability for fine SOC to bind and be retained on the cation exchange complex (Yost and Hartemink, 2019).

The lower bulk density in tidal forest horizons compared to that in other coastal ecosystems is a pattern observed in other studies, albeit not in subaqueous soils (Gorczynski et al., 2024). The pattern of exponentially decreasing bulk density with increased SOC observed in this study is like that observed in other terrestrial and subaqueous environments (Manetta, 2023; Kim, 2022). Bulk density measured in this study compared to others is within standard error and results in similar properties for ghost forests and tidal marshes. There is no comparative data for tidal forests, but compared to terrestrial studies the number is slightly higher (Craft et al., 2022; Gorczynski et al., 2024). This is likely due to the grouping of mineral and organic horizons in past studies, to increase statistical power.

Table 1.4 Comparison of Subaqueous Soil Horizons Characteristics across a Salinity Gradient

System	Salinity	n	SOC (%)	Bulk Density (g cm^{-3})	C:N	EC (1:5) dS m^{-1}	Source
South River, Maryland	Mesohaline	130	1.4	-	16	-	Park (2021)
Lower Chesapeake Bay, Virginia	Mesohaline to Polyhaline	65	1.98	1.19	16.40	2	Soil Survey Staff (2023)
Cape Fear River Estuary, North Carolina	Mesohaline to Polyhaline	68	1.01	1.17	31.5	3.8	Soil Survey Staff (2022c)
Banana River Lagoon, Florida	Polyhaline	107	1.36	1.32	58.8	3	Soil Survey Staff (2024)
Chincoteague Bay, Maryland	Polyhaline	161	1.6	0.98	-	3.69*	Balduff (2007) *n = 166
Albemarle-Pamlico, North Carolina	Mesohaline	49	5.18±1.50	1.23±0.09	18.69±1.84	2.20±0.24	This Study
Albemarle-Pamlico, North Carolina	Oligohaline	42	2.73±1.20	1.27±0.07	15.19±2.28	0.55±0.07	This Study
Albemarle-Pamlico, North Carolina	Tidal Fresh	33	17.09±2.74	0.57±0.10	23.42±1.61	0.28±0.03	This Study

Pedon Level Soil Properties

Pedon level comparison at 50, 100, and 200 cm yielded similar results insofar that terrestrial pedons store significantly more carbon than nearshore subaqueous sites which were recently converted to open water and offshore sites which have been open water for over 20 years. The only instance where this deviated is from the 100 cm analysis where all three sites along the transect were significantly different from each other. The difference is expected with nearshore and offshore soils being subject to wave energy and continual erosion.

When comparing the difference between ecosystems at the 50, 100, and 200 cm level, we found sampling depth is the primary driver for significant differences between ecosystems. At 50 cm, there is no difference between any ecosystem regardless of its location along the terrestrial to offshore subaqueous gradient. When the sampling depth is extended to 200 cm, tidal forests contained significantly more SOC in terrestrial, nearshore, and offshore pedons than did ghost forests and tidal marshes. This observation is pertinent to the question of where the highest SOC stocks are found in each of the three ecosystems. When assessing SOC inventories to a depth of 200 cm: 22% of SOC is in the top 50 cm for tidal forests, 29% for tidal marshes, and 46% for ghost forests. Furthermore, the top 100 cm accounts for 47% of SOC stocks in tidal forests, 60% for tidal marshes, and then 92% for ghost forests. When analyzing the 100-200 cm component of SOC stock contribution, only 8% of ghost forest stock is found at this depth while tidal forest and tidal marsh were 53% and 40%, respectively. This observation further highlights the importance of sampling at depths of 200 cm to encapsulate the SOC storage capacity of different coastal environments. Additionally, Ingram (1987) reported peat depths in excess of 700 cm on the Chowan and Roanoke Rivers, which are considered tidal forests. This observation from Ingram (1987) provides evidence that even a sampling depth of 200 cm may not capture all

Holocene-aged carbon sequestered in the soils of the upper APES. Tidal forests continually exhibit the highest SOC stocks when compared to ghost forests and tidal marshes because of their ecological stability, fluvial influence, and relatively protected positions in geographical areas.

Soil Organic Carbon and Ecosystem Loss

Using remote sensing techniques, with 36 years of satellite imagery, we found the area of interest on the APES has lost 2,833 hectares. Riggs and Ames (2003) used aerial imagery from the 1950s to 1990s to project the amount of hectarage that will be lost annually in northeast North Carolina from sea level rise. These remote sensing observations from Riggs and Ames (2003) were used to calculate shoreline erosion rates at a variety of APES sites over the referenced 30–40-year time period. The average long-term erosion rate was approximately -1.2 m yr^{-1} for the estuary. Riggs and Ames (2003) used the weighted average for all estuarine shoreline erosion measured in northeastern North Carolina, which included the Inner and Outer Pamlico River, Albemarle and Pamlico Sounds, and Back Barrier – North Outer Banks and found net shoreline change to be approximately -0.8 m yr^{-1}. From this data, the total amount of land lost was estimated to be 48 hectares of upland and 100 hectares of wetland for the specific 21 sites studied (Riggs and Ames, 2003). If the average erosion rate was applied to the 2,564 km of estuarine shoreline mapped in Riggs et al. (1978), which is stated to be about 50% of all estuarine shoreline in northeastern North Carolina (Riggs and Ames, 2003), and assuming the remaining 50% of estuarine shoreline is composed of similar ecosystems, then northeast North Carolina shorelines lose about 198 hectares of uplands and 316 hectares of wetlands per year through erosion and submersion. Over 36 years this land loss totals 18,324 hectares, or approximately a six-fold overestimate compared to our observations. The area discussed in Riggs

and Ames (2003) encompassed the barrier islands enclosing the sound which may explain to some degree the large difference in estimates. On the other hand, 9 of the 21 reference sites used by Riggs and Ames (2003) were located on the Albemarle-Pamlico Peninsula and it had one of the highest reported rates of shoreline erosion at approximately -1.2 m yr^{-1} compared to the weighted average of approximately -0.8 m yr^{-1} used. Therefore, the projected erosion rates for the estuarine shorelines put forth in Riggs and Ames (2003) would be even higher than the ones compared here.

There have been several studies on the linear rate of coastline erosion in and around the Albemarle-Pamlico sound (Gorczynski et al., 2024; Eulie et al., 2018; Eulie et al., 2013; Patel, 2010), but few present aerial estimates of land loss on the peninsula as large as those of Riggs and Ames (2003). The way in which our analysis was conducted provides for a more accurate measure with baseline hectares being established through USDA-NRCS soil survey map units. Using the soil survey approach allows a better attribution of land lost by ecosystem based on the soil type mapped there. For example, tidal forest soils are ubiquitously mapped as the Dorovan series in the study area, while tidal marsh is mapped as Currituck, Hobonny, or Longshoal series. Ghost forest attribution can be more difficult because these soils were mapped as Dorovan, Ponzer, or Pungo series, but remote sensing of vegetation and NDVI allowed these soils to be categorized as ghost forest. Most of the hectares submerged in all ecosystems were mapped as Histosols, with 1,730 of the 2,833 hectares (61%) of all submerged lands mapped as Typic Histosols. Typic Histosols must have at least 130 cm of soil with SOC content (percent weight) over 12%. The remaining 311 hectares were other mineral soils (mostly Entisols and Inceptisols) on marine terraces or near extensive erosion that reached the observed upland in the original soil survey areas publication date.

Tidal forest and ghost forest both exhibit similar losses in terrestrial carbon upon immediate conversion to open water in the nearshore core. This is attributed to the highly decomposed nature of the soil organic material and lack of herbaceous root systems and rhizomes to maintain the soil organic material against shear forces of the water column (Brooks et al., 2021; Nyman et al., 2006). The losses experienced in tidal marshes are lower in the conversion to open water because of the more fibrous nature of the soil organic material and higher mineral content in these environments. Tidal marshes are more resistant to erosion than tidal forests or ghost forests because of the adaptive vegetation in these ecosystems and established root/rhizome systems can act as a barrier to reduce the amount of erosion actively occurring (Chen et al., 2018; Baustian et al., 2012; Nyman et al., 2006).

When comparing nearshore to offshore soil carbon loss, tidal forests lost 276 Mg ha^{-1} SOC, but less than the initial conversion to open water (420 Mg ha^{-1}). This difference can be explained by the depth of soil organic material found in these ecosystems and lower wave shear stress at greater water depths (Sui et al., 2024; Ingram 1987). Ghost forests lost the least amount of SOC between nearshore and offshore cores at 126 Mg ha^{-1}, this can be attributed to 92% of SOC stocks in ghost forest ecosystems being in the 0-100 cm section of the pedon and only 8% being in the 100-200 cm section. This would indicate that submerged ghost forest soils lose significance as a SOC sink when converted to open water sites. Tidal marsh sites lose a similar amount of SOC after existing as open water sites for a 20–40-year period (262 Mg ha^{-1}) as when they are initially converted (308 Mg ha^{-1}). This observed change is consistent with the distribution of SOC in the soil profile with 60% being in the 0-100 cm section and 40% being in the 100-200 cm section.

Overall, tidal marsh ecosystems account for the greatest loss of land and terrestrial carbon in the three APES ecosystems observed in this study. Tidal marshes are currently experiencing the brunt of SLR and coincidingly are the greatest contributor of terrestrial carbon loss (Nicholls et al., 2007). Ghost forest terrestrial land area and carbon loss is considerable but will increase significantly with projected accelerated SLR. Upland portions of this analysis were assigned based on the previous mapping when the county soil survey was published, these ecosystems are projected to lose more terrestrial carbon than tidal forests. This assumption based on the observation that the soils used to represent the upland series are still poorly drained or somewhat poorly drained and contain appreciable soil organic carbon as well. Tidal forests had the lowest hectarage of land loss and terrestrial carbon loss. This can be attributed to two things: tidal forests generally convert to ghost forests as salinization occurs before large-scale transition to open water and carbon loss. Additionally, tidal forests are found in the upper APES, farther from the direct effects of sea level rise and tend to have more fluvial influenced hydrology compared to ghost forests and tidal marshes which experience more estuarine tidal regimes (Langston et al., 2017; Day et al., 2007). It is also worth stating again that only one offshore core penetrated to 200 cm in depth in the tidal forest and this study is inherently conservative in the amount of terrestrial SOC estimated to be lost when tidal forests are inundated.

Fate of Lost Terrestrial Carbon

The results of this study beg the question of the fate of the soil carbon that is lost from coastal wetland ecosystems. While it is beyond the initial scope of this study, there is some existing and ongoing research occurring to offer potential answers and pathways to explain the loss of soil carbon. Sapkota and White (2021) found the average age of an intact peat layer in the estuarine bottom mirrored the age of the carbon at similar depths of adjacent terrestrial marshes.

This observation indicates the peat layers above the subaqueous observation were eroded and displaced to a different location. Similarly, they witnessed significant anaerobic microbial activity present at all soil depths in an eroded tidal marsh, which suggests a high potential for carbon to mineralize in the estuary. While Sapkota and White (2021) investigated adjacent deposition of eroding peat, pathways for burial further out in the bay bottom or further transport to ocean are in question. The area studied by Sapkota and White was Barataria Basin, Louisiana, which is not a direct analog to the APES, but shares similarities in that it is a sediment starved tidal estuary. Likewise, Liu et al. (2017a) found that an increase in salinity, as well as variations in local water levels, lead to increased fluxes of climate-relevant greenhouse gases from coastal wetlands like methane (CH_4), carbon dioxide (CO_2), and nitrous oxide (N_2O); these factors will likely increase the breakdown of SOC in submerged soils in ghost forests and eventually tidal forests as saltwater intrusion pushes in the upper reaches of the APES. In the future, more studies are needed to understand the complex carbon dynamics associated with terrestrial soil submersion within coastal estuaries.

Conclusion

Sea-level rise will continue to be a significant driver of ecosystem erosion and submersion, especially in the wind-tide-dominated APES. Understanding which ecosystems are submerging at greater rates and what the associated SOC loss is will allow land managers to make more informed decisions regarding which areas to prioritize for preservation and highlight future areas for conservation practices such as marsh migration corridors, conversion of working lands back to restored states, and appropriate use of financial resources. A soil survey approach to terrestrial land and SOC loss due to sea level rise will be beneficial for better understanding

the fate of coastal wetlands and provide a more holistic understanding of the repercussions associated with climate change. This study illustrated the importance of soil sampling depth, even in subaqueous environments, for generating a better picture of SOC stocks. Future blue carbon inventories would benefit from incorporating historical soil mapping data to create a more realistic interpretation of ecosystem carbon dynamics.

Chapter 2: Lagoonal Soil Accretion and Carbon Sequestration Rates across Longitudinal Salinity Gradients

Introduction

Wetlands occupy 6 to 8 percent of the Earth's surface and provide extensive ecosystem services in the larger terrestrial biome (Mitsch et al., 2014; McInnes, 2013; Mitsch et al., 2013). A subset of global wetlands are in coastal areas. Coastal wetlands play an outsized role with the proven ability to support carbon sequestration, immobilize excess plant nutrients, and mitigate the effects of storm surge (Dixon and Krankina, 1995; Soukup et al., 1994; Wamsley et al., 2010). Coastal wetlands take on different forms dependent on the salinity regime, energy of the system, and climate. Regardless of the type of coastal wetlands, anthropogenic sea level rise (SLR) and intensity of tropical storm systems continues to be an existential threat across the globe (Newton et al., 2020). The estimated rate of SLR in certain areas could lead to a 40-60% loss of coastal wetlands by 2100 (Blankespoor et al., 2014; Nicholls, 2004). The Intergovernmental Panel on Climate Change (IPCC) generated five scenarios to better understand potential SLR based on climate management scenarios (IPCC, 2022). Sweet et al. (2022) further refined this information to generate contiguous and regional ranges for the United States under these five scenarios. Estimated SLR for the contiguous United States is currently projected to be 0.38 m to 0.52 m in 2050 relative to the 2000 mean sea level baseline. When regionalizing these projections, the Southeast United States (considered North Carolina to the Atlantic coast of Florida) could experience 0.28 m to 0.64 m in SLR by 2050 relative to its 2000 baseline mean sea level; at this time the trend is toward a rise of approximately 0.40 m by 2050 (Sweet et al., 2022).

The primary global driver for SLR is the melting of ice sheets and glaciers, as well as thermal expansion of the ocean (Stocker, 2014). Sea level in the Southeast United States is also affected by the Atlantic meridional overturning circulation (AMOC); in this case, the Gulf Stream current (Ezer and Atkinson, 2014; Smeed et al., 2014). A potentially weakened AMOC would further increase in SLR along the southeast coast of the United States (Krasting et al., 2016; Yin et al., 2009). Hence, SLR poses a significant challenge for wetlands in the region, which could be enhanced by other regional factors. Recent studies have shown that SLR can accelerate the rate of sediment accretion and extension of wetlands landward in low-lying areas (Wu et al., 2017; Kirwan et al., 2016). However, direct and secondary, negative effects such as saltwater intrusion, coastal wetland submergence or 'drowning', and complete ecological shifts typically occur simultaneously or shortly thereafter (Pierfelice et al., 2017; Craft, 2012; Kearney et al., 2002).

The Southeast United States contains a diverse suite of coastal ecosystems and estuarine entities (Stedman and Dahl, 2008). One of the most important estuarine and wetland systems in the Southeast United States is the Albemarle-Pamlico Estuary System (APES). The APES is the second largest estuary in the United States and largest in the Southeast region, spanning a large section of North Carolina and Southern Virginia (Giese et al., 1985). The APES exhibits coastal wetlands with a salinity gradient from tidal fresh to polyhaline moving from west (inland) to east toward the Atlantic Occean and a barrier island system known as the Outer Banks. The APES is a flooded river valley, like the Chesapeake Bay. However, the APES is also a restricted lagoonal system due to tidal restriction through the Outer Banks inlets (Riggs and Ames, 2003). This leads to tides being dominantly wind-driven instead of astronomically controlled, although astronomic tides do play a larger role closer to inlets on the far eastern side of the Pamlico Sound (Luettich

et al., 2002). Due to its proximity to inlets, the south side of Pamlico Sound has higher salinity (Eulie, 2014) than other parts of the APES. In contrast, the Albemarle Sound on the north side is less saline because of its distance from tidal inlets and seasonal freshwater flow from the Chowan and Roanoke Rivers (Giese et al., 1985). The dominant forms of coastal wetlands in the APES are tidal forests, ghost forests, and tidal marshes. While extensive studies on the response of tidal marshes to SLR are available, limited data exists on how tidal forests and ghost forests respond to SLR within the restricted lagoonal system (Cassalho et al., 2021; Lagomasino et al., 2013; Kemp et al., 2009). With the risk of SLR and the known importance of coastal wetlands for climate mitigation and ecosystem services, studies are beginning to focus on how these ecosystems' respond to this external pressure through increased sediment accretion and subsequently carbon sequestration (Gorczynski et al., 2024; Gunderson et al., 2021).

Sediment accretion is defined as the net positive balance between deposition and removal processes in a certain environment (Hatton et al., 1983). Accretion as a process is vital for coastal wetlands to maintain elevation and negate ongoing and future SLR. The process occurs by different pathways depending on the system in question; a typical example is the deposition of sediment occurring on a riverine floodplain. A reduction of energy in flow allows for suspended sediment to settle from the water column onto the soil surface and the sediment remains *in situ* after the water has receded (Nicholas and Walling, 1998; Middleton, 1993). A similar scenario occurs in in tidal marsh wetlands as tidal currents flood and ebb. During the ingoing (flood) tide, suspended sediment is carried over the marsh surface, where it may be trapped by vegetation and contribute to the accretion and elevation (Bost et al., 2024; Möller et al., 2014; Temmerman et al., 2004; Morris et al., 2002). Sediment accretion can also occur locally through net primary production (NPP) of the ecosystem in question through the

deposition of perennial or annual plant detritus produced from vegetative cycles (Temmerman et al., 2003). These various processes play an important role in sediment accretion and the ability of coastal wetlands to maintain higher with SLR. In the event coastal wetlands are unable to keep pace with SLR, the ecosystems will submerge and 'drown,' a process where the level of soil saturation and inundation becomes detrimental to the primary productivity of the ecosystem in question (Mariotti, 2020; Wasson et al., 2019; Crosby et al., 2016). The ability of coastal wetlands to accrete sediment is paramount to survival in the face of climate change.

An ecosystem service that may occur simultaneously with sediment accretion is carbon sequestration, but they are not synonymous. Depending on the source of sediment and NPP of the ecosystem, it is not uncommon for comparative ecosystems to have similar accretion rates, but significantly different carbon sequestration rates (Gunderson et al., 2021; Krauss et al., 2018; Craft, 2012). Carbon sequestration is touted as one of the primary services wetlands provide. It can occur through autochthonous or allochthonous means, as with sediment accretion. Ecosystems such as tidal marshes significantly influenced by astronomic tides that regularly receive sediment from external sources may have lower carbon sequestration rates than a low gradient, blackwater river tidal forest because the source of the sediment is dominantly composed of mineral particles instead of sequestration being driven by NPP (Hupp et al., 2019; Marion et al., 2009; Temmerman et al., 2003). To date, very few studies have coupled wetland accretion rates and SOC sequestration across salinity gradients in lagoonal systems.

There are several established methods for measuring accretion and subsequent sequestration across varying timescales. Radiocarbon (^{14}C) dating provides a broad overview of rates in an environment, this method covers tens of thousands of years and is reliably used across several fields of study; it typically relies on dating of more recalcitrant material such as bone,

charcoal, and some types of wood (Hajdas et al., 2021; Kulp, 1952). ^{210}Pb and ^{137}Cs isotopic sediment dating is often used for more recent estimates of sediment accumulation, usually on the scale of 100 to 150 years before present (Hunter et al., 2023; Appleby and Oldfield, 1992). For decadal measurements, rod-surface-elevation tables (RSET) are becoming more commonplace; accomplished by implementing a mechanical leveling device to rod benchmarks to measure change in elevation throughout a soil profile (Cahoon et al., 2002). Finally, and perhaps the most cost-effective method for short-term measurements of accretion are marker horizons; this consists of spreading a layer of material (typically feldspar) over the surface for which one is interested in measuring sedimentation rates and returning at certain intervals of time to take a core or use a measuring stick to quantify accretion. All these methods have limitations and advantages, but all provide an avenue for measuring sediment accumulation rates over time.

For this study, we extracted ^{210}Pb and ^{14}C samples from sites and transects established in Gorczynski et al. (2024) on the eastern edge of the Albemarle-Pamlico Peninsula to the extent of microtidal influence in the Chowan, Roanoke, and Tar Rivers. These 12 sites represent the tidal forest, ghost forest, and tidal marsh wetlands which exist across a salinity gradient. Each ecosystem type has different hydrology, vegetative communities, and dominant sources and drivers of sediment accretion and carbon sequestration. All three ecosystem types were sampled for ^{210}Pb and ^{14}C in this study. We hypothesize that progressive salinization of tidal forest and then ghost forest will lead to significant decrease in sediment accretion and carbon sequestration rates when compared to tidal marsh environments; this is due to the vegetative shift which will occur, causing a decrease in net primary productivity and further vulnerability to sea level rise. Therefore, the goal of this research is to understand how ecosystems across a salinity gradient are

deviating from historic sediment accretion and carbon sequestration rates in the modern era of accelerated sea level rise.

Area of Interest

The Albemarle-Pamlico Estuarine System (APES) is the second largest estuary in the United States, containing 607,028 hectares of estuarine water that is the ultimate destination of over 14,484 kilometers of freshwater rivers (Riggs and Ames, 2003). The APES consists of three dominant types of coastal wetlands: tidal forests, ghost forests, and tidal marshes. Each coastal wetland is influenced by different hydrologic regimes, vegetative communities, sources of sediment; therefore, the ecosystems are all inherently different from each other.

Tidal forests are located at the interface freshwater river systems and saline estuarine waters. Long-term average salinity is usually less than 0.5 ppt (Conner et al., 2007). Tidal forests occur on the west side of the APES, with the most extensive stands in the Albemarle Sound. These ecosystems are dominated by hardwood tree species, such as *Taxodium distichum* (Bald cypress) and *Nyssa Aquatica* (Water tupelo) (Gorczynski et al., 2024). Tidal forest hydrology is influenced primarily by riverine discharge and to a minor extent by astronomical or wind tides and salinity rarely exceeds the tolerance threshold of freshwater wetland tree species (Conner et al., 2007). Sediment accretion in tidal forests is due to a mix of allochthonous and autochthonous inputs. Allochthonous inputs are dictated by weather; a year with heavy rainfall in an agricultural or urban watershed may lead to an increase in sediment accretion downstream as the floodplain widens and energy decreases (Hupp et al., 2019). In contrast, a year with low rainfall and irregular inundations with saltwater may lead to reduced sediment deposition and lower vegetative production in a tidal forest (Conner et al., 2007). Southeast tidal forests have the

lowest riverine discharge and influence in October which creates conditions for potential saltwater intrusion into these environments (Conner et al., 2007). If the saline water is not flushed from the system, the non-halophytic tree species become stressed and will ultimately senesce. This increase in salinity and reduction in freshwater riverine influence can lead to the formation of degraded, oligohaline forests (Ury et al., 2021; Kirwan and Gedan, 2019).

Degraded tidal forests are commonly referred to as 'ghost forests.' This moniker is derived from the extensive stands of deceased snags and salt-affected non-halophytic tree species distributed throughout the landscape (Kirwan and Gedan, 2019). Ghost forests occur widely throughout the APES and other Southeast region estuaries. These ecosystems display a significant decrease in NPP with the influx of saline water and vegetative community shifts (Pierfelice et al., 2017). Due to SLR, the increase in saltwater in these areas irreversibly changes the ecosystem and leads to the conversion of stressed tidal forests towards herbaceous, halophytic tidal marshes (Ury et al., 2021; Ardón et al., 2016). Ghost forests contain few live tree species with limited levels of salt tolerance such as *Pinus taeda* (Loblolly pine) but are otherwise dominated by salt tolerant understory plants like *Cladium jamaicense* (sawgrass) or invasive species like *Phragmites australis* (Gorczynski et al., 2024). Deposition of allochthonous sediment in these environments is dependent on their proximity to fluvial and estuarine sediment sources. In some studies, ghost forests became stable tidal marshes in approximately 50 years, depending on the level of saltwater intrusion and stability of the environment (Langston et al., 2017). Ghost forest accretion rates are largely due to allochthonous inputs as the result of the reduction in NPP experienced from saltwater intrusion (Gorczynski et al., 2024; Pierfelice et al., 2017; Craft, 2012). Active erosion occurring at the shoreline could lead to suspension and deposition of sediment, but it depends on factors such as tidal level or exposure (Hopkinson et

al., 2018). The initial dieback of tidal forest vegetation often leaves the soils rich in organic material exposed to aggressive and significant erosion as the transition to tidal marsh begins (Riggs and Ames, 2003).

Tidal marshes in the APES are concentrated along the eastern and southern edge of the system, which experience mesohaline/polyhaline salinity (5-23 ppt) (Jia and Li., 2012). Pamlico Sound contains more acres of tidal marsh than the Albemarle Sound because of the proximity and number of tidal inlets such as the Oregon, Ocracoke, and Hatteras (Giese et al., 1985). These tidal inlets promote a higher salinity and more influence from astronomical tides; therefore, tidal marsh generally experience more astronomic tidal influence than tidal forests and ghost forests (Riggs and Ames, 2003). Unlike in tidal forests and to an extent in ghost forests, tidal marsh hydrology is dominated by tidal exchange with negligible influence from fluvial systems (Giese et al., 1985). Tidal marsh accretion is controlled by a mix of internal and external factors; the APES is a sediment starved system because of the restriction of astronomic tides by the Outer Banks. Likewise, much of the sediment entering the Albemarle-Pamlico through riverine sources is deposited along the broad floodplains of tidal forests before it reaches further into the estuary (Hupp et al., 2019; Giese et al., 1985). Furthermore, Marsh drowning is rarely observed in the APES due to sustained levels of water on the surface of tidal marshes from tidal inundation being restricted by the Outer Banks (Riggs and Ames 2003). Erosion of marsh edges are common, with the phenomenon of calving occurring. Some sediment is eroded, suspended, and redeposited on marsh edges in the APES, but the extent of this process is not well understood locally. (Lagomasino et al., 2013). Tidal marshes in the APES are dominated by *Juncus roemerianus* (Black needle rush), *Spartina alterniflora* (Smooth cordgrass), and *Spartina cynosuroides* (Big cordgrass) (Gorczynski et al., 2024).

Materials and Methods

Bulk density, ^{210}Pb, and ^{14}C samples were taken within a 1-meter radius of the original pedon location in Gorczynski et al. (2024). This dataset was chosen because of an identical ecosystem salinity gradient sampling regimen implemented in Chapter I of this analysis, accessibility to sites, and applicability of soil carbon data to this study's analysis of carbon sequestration rates via ^{210}Pb and ^{14}C. This choice permitted a system to understand how terrestrial soils and associated carbon stocks accrete and sequester organic carbon in response to sea level rise.

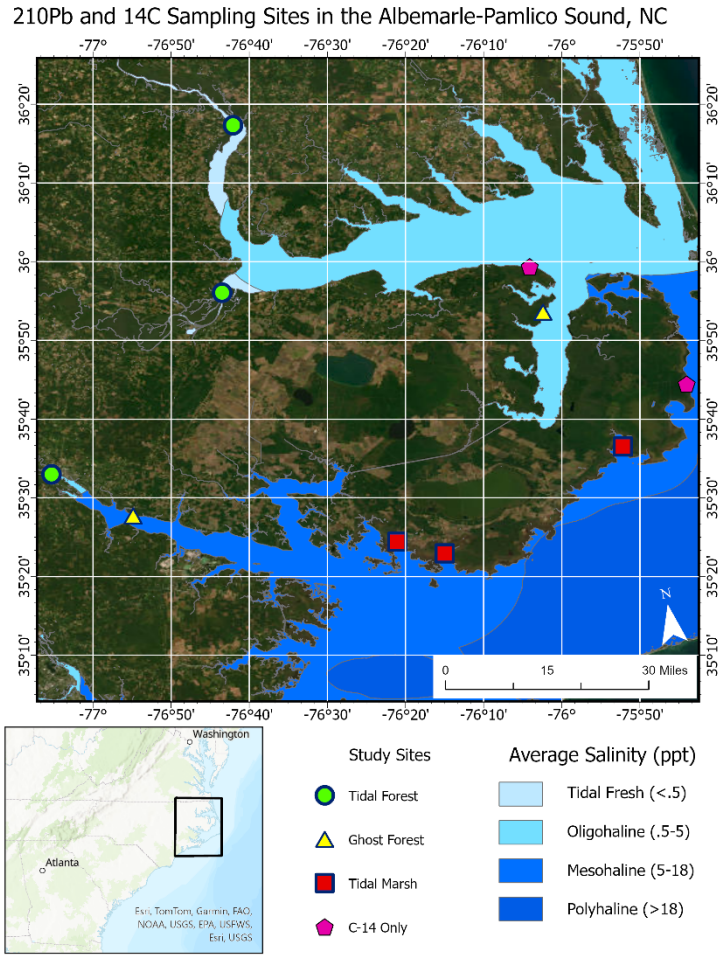

Figure 2.1. Map of ^{210}Pb and ^{14}C sampling sites representing tidal forests, ghost forests, and tidal marshes along a salinity gradient (0.15-15.47 ppt average water salinity). Areas denoted with a pink pentagon were sampled for only ^{14}C while all other sites were sampled for both.

The selected sites for ^{210}Pb and ^{14}C included three tidal forests, two ghost forests, and three tidal marshes (Figure 2.1). Two sites were samples only for ^{14}C analysis: Point Peter (tidal marsh) and Palmetto-Peartree (ghost forest). Average salinity ranges for the ecosystems are tidal forest (0.15-1.6 ppt); ghost forest (3.5-8.3 ppt) and tidal marsh (11.7-15.5 ppt).

Field Data Collection

Field soil core sampling for ^{210}Pb occurred in Spring of 2021. Study points were located using a handheld Garmin GPSMAP 78s. A fixed total sampling depth of 50 cm was implemented with a Macauley peat sampler; the upper 30 cm was sampled in 2 cm increments for radiometric dating. ^{222}Rn reference samples were collected at 5 cm intervals for the remaining 20 cm (i.e., 30-35 cm, 35-40 cm, etc.). This sampling regimen was implemented at three points within a meter of the original Gorczynski et al., (2024) sites where each depth was homogenized for analysis while the 5 cm increments were sampled two times and homogenized. Samples were stored on ice for transit to the laboratory.

^{14}C samples were extracted with a Macauley peat sampler during the summer of 2020. These were extracted from sites referenced in Gorczynski et al. (2024) and within the 1-meter radius of the ^{210}Pb samples. Congruent with Gorczynski et al. (2024) methods, as a soil was sampled and described, any charcoal and wood buried deeper than 100 cm was taken for dating; average depth of ^{14}C samples were 154 ± 10 cm. Two ghost forest sites were sampled at less than 100 cm due to shallow peat depths at these locations, these were the Palmetto-Peartree (82 cm) and Goose Creek (96 cm) sites. Ecosystem distribution of ^{14}C samples consisted of tidal forests (n = 6), ghost forests (n = 4), and tidal marshes (n = 5). Multiple ^{14}C samples were retrieved from some pedons at different depths, these were from tidal forest site Chowan (n = 3), ghost forest site Alligator River (n = 2), and tidal marsh site Longshoal (n = 2). The average vertical

difference between sampling depth in the singular, representative pedon from Gorczynski et al., (2024) at these three locations was 48 ± 4 cm. Once collected, samples were placed in a separate bag with the labeled depth at which they were sampled. All samples were put on ice for transit to the laboratory and frozen upon arrival.

Laboratory Analysis

The bulk density was calculated by taking the known volume of homogenized samples from each depth and weighing them after drying at 105 °C for 24 hours (Soil Survey Staff, 2022a). The volume was calculated using the following volumetric formulas: (a) is the 2 cm increment calculations, (b) is the 5 cm increment calculations where *v* is the volume, *r* is the radius of the Macauley peat sampler, and *h* is the length of the sample.

$$v = \frac{1}{2}\pi r^2 h$$

(a) $v = \frac{1}{2}\pi(2.6)^2(2) = 21.24\ cm^3 * 3$

(b) $v = \frac{1}{2}\pi(2.6)^2(5) = 53.09\ cm^3 * 2$

After bulk density was calculated, the samples were ground with a mortar and pestle, processed with a No. 10 (< 2.0 mm) sieve, and 10 g of soil were placed into plastic bags and double-sealed for shipping. Samples were sent to Core Scientific International (Winnipeg, Canada) for alpha spectroscopic analysis of radioisotopic ^{210}Pb activity for each depth increment sampled. Radon analysis via ionization chamber detection at the 45-50 cm incremental depths at sites Alligator River, Juniper Bay, Roanoke River, and Tar River were also conducted to understand the difference in supported and unsupported ^{210}Pb in the soil (Core Scientific International, 2023).

Radiocarbon dating was performed on 16 samples by DirectAMS Radiocarbon Dating Service (Bothell, Washington, USA). Wood and charcoal samples were thawed, weighed, and any adhering soil or roots were removed with tweezers. Samples were wrapped in aluminum foil, placed on a labeled plastic bag, boxed, and shipped to DirectAMS for analysis by a National Electrostatics Corporation Pelletron 500 kV AMS. Before analysis, an acid-base-acid treatment was conducted (DirectAMS, 2023).

Accretion Rate and Carbon Sequestration Rate Calculations

^{210}Pb activity data from Core Scientific International was converted to becquerel per square meter using the following formula: any risk of compaction was accounted for by multiplying Bq g^{-1} to the measured bulk density (ρ_b):

$$(210_{Po} - Rn_{222}) * \frac{1}{60} \rightarrow \frac{Bq}{g} * \rho_b \rightarrow (\frac{Bq}{cm^3} * \frac{1}{2}(or\ \frac{1}{5})) * \frac{1}{0.0001} = Unsupported\ 210_{Pb}\ \frac{Bq}{m^2}$$

The Constant Rate of Supply method described in Appleby and Oldfield (1978) was used to determine age:

$$t = \frac{1}{\lambda} ln \frac{I_t}{I_i}$$

Where t is the age of the layer, I_t is the total of unsupported ^{210}Pb (Bq m^{-2}), I_i is the inventory of unsupported ^{210}Pb below the layer (Bq m^{-2}), and λ is the ^{210}Pb decay constant (0.0311). The 0-2 cm depth was discarded from analysis because of mixing in the surface. The depth at which the sample was taken then divided by the measured age to determine the accretion rate in cm yr^{-1}. The Constant-Initial-Concentration (CIC) method proved unsuitable in this case because of unsteady rates in mineral and organic matter input, common within wetland systems (Appleby et al., 1988).

Each fixed sampled depth was assigned an estimated carbon content (w/w) based on the corresponding horizon analysis and soil description in Gorczynski et al. (2024). The accretion

rate, carbon content, and bulk density were used to determine carbon sequestration rate for each depth (kg C m^{-2} yr^{-1}) and an average sequestration rate for the site:

$$r(x) * C\left(\frac{w}{w}\right) * P_b * 10 = r(C_x)$$

Where $r(x)$ is the calculated constant rate of supply accretion, $C(\frac{w}{w})$ is the measured organic carbon percent of the soil by weight, and P_b is the measured bulk density of the soil; 10 is used as a conversion factor to kg C m^{-2} yr^{-1} (Manetta, 2023; Kim, 2022; Craft, 2012).

^{14}C age was determined by taking the uncalibrated radiocarbon age before present (1950) provided by DirectAMS and using the CALIB program (CALIB rev. 8; Stuiver and Reimer, 1993) to calibrate the data to years since 0 A.D. Simple year and depth comparisons were then made to calculate accretion rates; long-term carbon sequestration for ^{14}C samples was calculated using the bulk density and SOC data collected in Gorczynski et al. (2024). Two samples were removed from statistical analysis due inexplicably high accretion rates; these were tidal forest site Chowan (0.283 cm yr^{-1}) and ghost forest site Palmetto Peartree (0.441 cm yr^{-1}). It was determined the Chowan sample was contaminated because it followed a non-monotonical pattern when compared to other ^{14}C samples in the same profile. It was deduced the Palmetto-Peartree sample contained live root contamination at its relatively shallow sampled depth (82 cm). This reduced the total number of ^{14}C samples by ecosystem to tidal forest (n = 5), ghost forest (n = 3), and tidal marsh (n = 5).

Sea Level Rise, Accretion Rate Scenarios, and Regional Accretion Comparisons

Projected regional sea level rise (SLR) estimates were taken from the NOAA 2022 Sea Level Rise Technical Reports (Sweet et al., 2022). Two SLR projections for Intermediate and Intermediate-High scenarios in the Southeast United States were selected for 2050 and 2100. The average SLR expected in these scenarios were compared to the mean, calculated accretion rates

for each ecosystem from the ^{210}Pb portion of this study. Projected SLR from the 2000 baseline sea levels in Sweet et al. (2022) were corrected with an appropriate decrease to more accurately reflect the anticipated SLR from time of measurement in 2021 to the comparison dates in 2050 and 2100. For example, if a uniform rate of SLR was assumed from 2000 to 2050 for a tidal increase in MSL of 0.36 m, 21 years or 42% of this rise would already have occurred by 2021 and the subsequent 0.21 m left or 58% of SLR would occur from 2021 to 2050 using this projection.

Three scenarios for sediment accretion were evaluated based on trends in SLR and the ^{210}Pb data. The distinct periods of accretion over the past 171 years were: (1) 1850 – 1970 where SLR is first recorded in the area and steady; (2) 1970 – 2006 when accretion rates were elevated during a period of more rapid SLR in the study area; (3) 2006 – 2021 in the present period of increasingly accelerated local SLR. These scenarios are based on data from this study where three clear windows of accretion are observed across the ecosystems in question, with supporting regional and global observations from Hamlington et al. (2024), Kopp et al. (2015) and Riggs and Ames (2003). For example, based on the derived age of the 2 or 5 cm slices in tidal forest ^{210}Pb samples, we found the depths and accretion rates between 10 and 22 cm correlated to the 1970 – 2006 period. Likewise, the average age and accretion rate from 2 to 10 cm correlated to the 2006 – 2021 period; anything below 22 cm was attributed to the 1850 – 1970 accretion rates. 1850 was chosen as the start date for these accretion scenarios because the average age of the ^{210}Pb material at 50 cm in each ecosystem was approximately 165 to 175 years old.

Regional accretion comparison data were selected based on their proximity to the area of interest (Gunderson et al., 2021; Lagomasino et al., 2013; Ingram, 1987). Comparative

ecosystem accretion data were from adjacent states including Georgia, Maryland, and South Carolina (Craft, 2023; Ensign et al., 2014; Noe et al., 2016; Craft, 2012).

Comparative and Statistical Analysis

Statistical analyses were conducted in R (version 4.3.1, R Core Team, 2024). Data visualization and manipulation were performed with the ggplot2, dplyr, and plotrix R packages (Wickham et al., 2023; Wickham, 2016; Lemon, 2006). A one-way ANOVA was used to test significant differences between ecosystems regarding sediment accretion rate, overall age, carbon sequestration rate, bulk density, carbon content, and mineral content. Tukey HSD was used for post-hoc analysis when ANOVA was significant ($\alpha = 0.05$).

To reflect long-term accretion and carbon sequestration rates, ^{14}C was corrected to only represent the rates measured deeper than 50 cm in the profile. This was done by subtracting the calibrated age (from 0 A.D.) of the ^{14}C sampled from the average age of each ecosystem in the ^{210}Pb cores. For example, the average age at the bottom of a ^{210}Pb core for a tidal forest was 172 years. 172 years would be subtracted from the calibrated age of the ^{14}C sample; additionally, the depth of the sample would be adjusted to ensure the time-depth relationship-maintained integrity. This was conducted by subtracting 50 cm -the deepest depth of the ^{210}Pb core- from the depth of the ^{14}C sample. Hence long-term accretion and sequestration rates at depths not influenced by current (0-50 cm) rates were established. A one-way ANOVA was used to test significant differences between ecosystems regarding ^{14}C derived age, depth, accretion rate, and sequestration rate. Tukey HSD was used for post-hoc analysis when ANOVA was significant ($\alpha = 0.05$). A Welch two sample t-test was used to determine if there was a significant difference between the average of the long-term ^{14}C accretion rates and short-term ^{210}Pb accretion rates; a

Welch two sample t-test was also used to compare the long-term ^{14}C carbon sequestration rates and short-term ^{210}Pb carbon sequestration rates.

A one-way ANOVA was used to determine any significant differences between rates in the delineated accretion scenarios for each ecosystem in the 1850 – 1970, 1970 – 2006, and 2006 – 2021 timeframes. Tukey HSD was used for post-hoc analysis when ANOVA was significant ($\alpha = 0.05$).

Results

Short-term ^{210}Pb Accretion and Carbon Sequestration Rates

^{210}Pb accretion rates and associated soil characteristics vary significantly across the ecosystem gradient (Table 2.1). Tidal forests had significantly higher accretion rates than ghost forests ($p = 0.048$) but were not significantly different from tidal marshes ($p = 0.65$); tidal marshes did not accrete at significantly more rapid rates than ghost forests ($p = 0.28$) in the observed period. Tidal forests sequestered significantly more carbon than ghost forests and tidal marshes ($p < 0.001$) and ghost forests sequestered more carbon than tidal marshes ($p = 0.01$). SOC content was significantly higher in ghost forests when compared to tidal forests ($p = 0.01$) and tidal marshes ($p < 0.001$); furthermore, tidal forests contained significantly more mineral material than ghost forests ($p < 0.001$). Ghost forests had significantly lower bulk densities than tidal forests and tidal marshes ($p < 0.001$), while there was no difference between tidal forest and tidal marsh bulk densities ($p = 0.05$). Finally, there was no significant difference between the age of the soil profiles in the top 50 cm of the three ecosystems ($p = 0.97$).

Table 2.1: Mean (± SE) current ^{210}Pb whole core accretion and sequestration rates and associated properties. Different letters by column indicate significant differences. *n = 3; **n=2

Ecosystem	n	Accretion Rate (cm yr^{-1})	Sequestration Rate (kg C yr^{-1} m^{-2})	SOC (%)	Mineral (%)	Bulk Density (g cm^{-3})	Age (years) since 2021 A.D.
Tidal Forest	17	$0.49\pm0.04_a$	$0.18\pm0.02_a$	$18\pm0.01_a$	$59.3\pm1.6_a$	$0.26\pm0.02_a$	$172\pm18_a$*
Ghost Forest	17	$0.38\pm0.02_b$	$0.12\pm0.004_b$	$25\pm0.02_b$	$45.8\pm2.2_b$	$0.14\pm0.003_b$	$169\pm26_a$**
Tidal Marsh	17	$0.42\pm0.03_{ab}$	$0.08\pm0.003_c$	$11\pm0.005_c$	$73.7\pm1.0_c$	$0.22\pm0.01_a$	$166\pm7_a$*

Long-term ^{14}C Accretion and Carbon Sequestration Rates

When comparing ^{14}C accretion and sequestration rates, few significant differences were found (Table 2.2). Accretion rates were significantly lower in tidal marsh when compared to tidal forest ($p = 0.048$) and ghost forest ($p = 0.038$). There was no significant difference between tidal forest and ghost forest accretion rates ($p = 0.86$). There was no significant difference between the sequestration rates between ecosystems ($p = 0.151$). No significant difference was observed between depth ($p = 0.62$) or age ($p = 0.16$ for the ecosystems in question either.

Table 2.2: Mean (± SE) long-term ^{14}C accretion and sequestration rates and associated properties. Different letters by column indicate significant differences

Ecosystem	n	Accretion Rate (cm yr^{-1})	Sequestration Rate (kg C yr^{-1} m^{-2})	Depth (cm)	Age (Years) since 0 A.D.
Tidal Forest	5	$0.12\pm0.01_a$	$0.05\pm0.01_a$	$170\pm16_a$	$1266\pm212_a$
Ghost Forest	3	$0.13\pm0.02_a$	$0.05\pm0.02_a$	$144\pm22_a$	$873\pm69_a$
Tidal Marsh	5	$0.07\pm0.01_b$	$0.03\pm0.01_a$	$156\pm9_a$	$1745\pm299_a$

Comparison of Long-term (^{14}C) and Short-term (^{210}Pb) Accretion and Carbon Sequestration

The Welch Two Sample t-test performed between the short-term ^{210}Pb, and long-term ^{14}C accretion and sequestration rates found significant differences. Average accretion rates were significantly different ($p < 0.001$) with a t-value of 14.89. Average sequestration rates were also significantly different ($p < 0.001$) with a t-value of 8.05. Figure 2.2(A) shows the difference between the current and historic accretion rates while Figure 2.2(b) exhibits the trends in carbon sequestration over time.

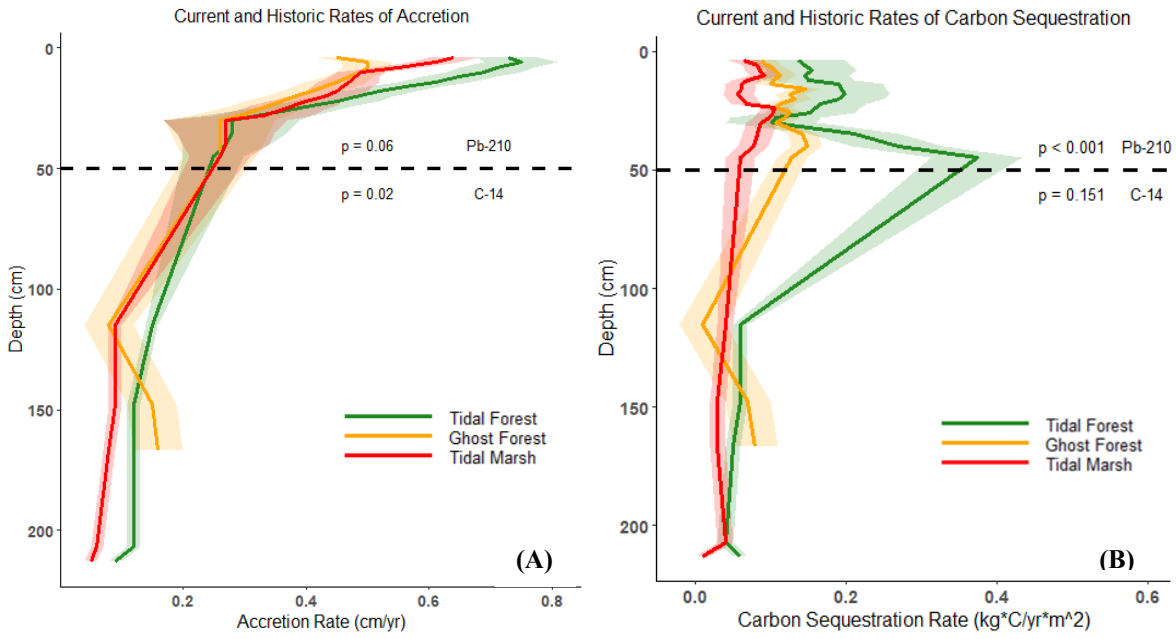

Figure 2.2: **(A)** current (above 50 cm) and historic soil accretion rates (below 50 cm). **(B)** current (above 50 cm) and historic carbon sequestration rates (below 50 cm). Significance values are for differences within the individual datasets of Pb-210 and C-14 and not between them

Sea Level Rise and Accretion Rate Scenarios

Three specific intervals of accretion were identified based on data analysis and time correlation of the ^{210}Pb data. These were 1850-1970, 1970-2006, 2006-2021 (Table 2.3). All three time periods were found to be significantly different in tidal forest environments ($p < 0.001$). The tidal forest accretion rate from 2006-2021 was significantly higher than 1850-1970 and 1970-2006 ($p < 0.001$). The accretion rate from 1850-1970 was significantly lower than 1970-2006 and 2006-2021 ($p < 0.001$). When analyzing the ghost forest ecosystem, accretion rates from 1850-1970 were significantly lower than both 1970-2006 ($p < 0.001$) and 2006-2021 ($p = 0.0014$). There was no significant difference between 1970-2006 and 2006-2021 ($p = 0.80$) in ghost forest accretion. When comparing tidal marsh accretion rates, 2006-2021 were significantly higher than 1850-1970 and 1970-2006 ($p < 0.001$). 1850-1970 accretion rates were significantly lower than 2006-2021 accretion rates as well ($p < 0.001$). Table 2.3 reviews the means and standard errors.

Table 2.3. Mean (± SE) of distinct accretion windows. Different letters by column indicate significant differences. *n = 4 **n=14 ***n=16

	N	Tidal Forest	Ghost Forest	Tidal Marsh
2006-2021	9	$0.73 \pm 0.03_a$	$0.48 \pm 0.02_a$*	$0.60 \pm 0.03_a$
1970-2006	21	$0.57 \pm 0.02_b$	$0.45 \pm 0.03_a$**	$0.45 \pm 0.01_b$
1850-1970	21	$0.31 \pm 0.01_c$	$0.29 \pm 0.02_b$***	$0.31 \pm 0.01_c$

Measured accretion rates can be compared with projected Intermediate and Intermediate-High SLR scenarios for the Southeast United States to evaluate net ecosystem submersion rates (Sweet et al., 2022; Table 2.4). There is no scenario calculated in which accretion rates exceed or keep pace with regional SLR projections.

Table 2.4. Simple difference (delta) between measured accretion rates (cm yr^{-1}) by ecosystem with overall mean accretion rate from 1850-2021 and most recent accretion rates from 2006-2021 paired with projected SLR in Intermediate and Intermediate-High from Sweet et al (2022)

	1850 – 2021			2006 – 2021		
	Tidal Forest	Ghost Forest	Tidal Marsh	Tidal Forest	Ghost Forest	Tidal Marsh
Intermediate 2050	-0.25	-0.36	-0.32	-0.01	-0.26	-0.14
Intermediate-High 2050	-0.39	-0.50	-0.46	-0.15	-0.40	-0.28
Intermediate 2100	-0.62	-0.73	-0.69	-0.38	-0.63	-0.51
Intermediate High 2100	-1.12	-1.23	-1.19	-0.88	-1.13	-1.01

Figure 2.3 accentuates this point. With an estimated increase of 20% on 2006 – 2021 accretion rates in 2050 and a 40% increase in 2100. None of the ecosystems keep pace with SLR.

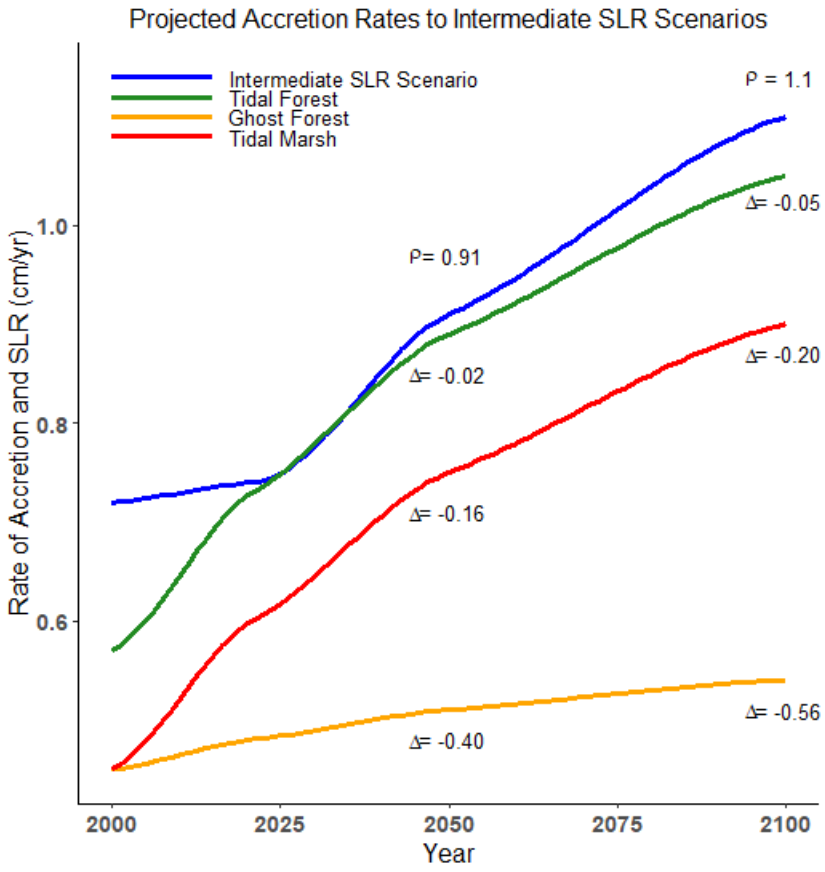

Figure 2.3. differences in projected accretion rates over time by ecosystems under the Intermediate SLR scenario. The Δ indicates the calculated difference between the estimated rate of accretion by ecosystem and ρ, the projected rate of SLR.

Discussion

Sea level rise is a continuous threat to all Southeast coastal ecosystems (Figures 2.4-6), regardless of the vegetative composition and location on the landscape (Ury et al., 2021; Short et al., 2016; Conner et al., 2007). Accretion rates are a direct connection and indicator we can use to assess the viability and long-term survivability of these vital ecosystems. A foundational set of studies exist in the Mid-Atlantic and Southeast United States to understand how tidal forests, ghost forests, and tidal marshes are responding to SLR (Craft, 2022; Noe et al., 2016; Ensign et al., 2014). A growing body of work exists showing that most coastal wetlands in the Southeast United States are struggling to maintain accretion rates which equal or outpace projected SLR. Without direct anthropogenic intervention such as thin-layer deposition, creation of living shorelines features, and hard shoreline features, these crucial, ecosystems will be submerged or eroded in the coming decades (Garcia et al., 2018; Bilkovic et al., 2016; Ford et al., 1999).

Figure 2.4. A photo of the site Tar River, a typical tidal forested wetland with *Nyssa aquatica* dominant and positive soil water potential.

Figure 2.5. A photo of the site Goose Creek, an advanced stage ghost forest site with *Spartina cynosuroides and Juncus roemerianus.* Remnant Bald cypress (*Taxodium distichum)* roots and knees are visible along the shoreline.

Figure 2.6. A photo of the site Swanquarter. A stable, mesohaline microtidal marsh. The higher salinity areas are dominated by *Spartina patens* with decreasing salinity from the marsh edge leading to an increase in *Juncus roemerianus.*

Short-term ^{210}Pb Accretion and Carbon Sequestration Rates

Significant differences were identified in accretion rates between tidal forests and ghost forests based on whole core analysis, where accretion and carbon sequestration rates were averaged for all depths from 0 – 50 cm. Tidal forests and tidal marshes exhibited higher accretion rates than ghost forests. This can be attributed to the decrease in net primary productivity which occurs in ghost forests as they transition from tidal forests and to tidal marshes (Gorczynski et al., 2024; Martinez and Ardón, 2021; Krauss et al., 2018; Pierfelice et al., 2017). This trend of ghost forests, or degraded oligohaline forests, exhibiting the lowest rate of accretion is not universally observed in other regional studies (Table 2.5).

Table 2.5. Comparison of mean (± SE) regional accretion rates across a salinity gradient of ecosystems (cm yr^{-1}).

Area of Interest	Tidal Forest	Ghost Forest	Tidal Marshes	Source
Savannah River, Georgia	0.60	1.91	1.52	Ensign et al., 2014
Waccamaw River, South Carolina	0.74	0.75	1.14	
Sapelo Island, Georgia	-	-	0.29	Craft 2022
Ogeechee River, Georgia	0.23	-	-	Craft 2012
Altamaha River, Georgia	0.25	-	-	
Satilla River, Georgia	0.19	-	-	
South Newport River, Georgia	-	0.22	-	
Waccamaw River, South Carolina	0.35	0.21	0.17	Noe et al., 2016
Chesapeake Bay, Maryland	-	-	0.63	Palinkas and Koch, 2012
Albemarle Sound, North Carolina	0.18	0.35	0.18	Gunderson et al., 2021
Pamlico Sound, North Carolina	-	0.35	0.31	Lagomasino et al., 2013
Albemarle-Pamlico, North Carolina	0.56	-	0.37	Moorman et al., 2024
Median of Comparison Studies	0.39±0.08	0.35±0.27	0.34±0.18	Synthesis of Above Referenced Studies
Albemarle-Pamlico, North Carolina	0.49±0.04	0.38±0.02	0.42±0.03	This Study

An explanation for the differences observed in whole core accretion between ecosystems in this study could be regional variation. Gunderson et al. (2021) and Lagomasino et al. (2013), who studied the APES and the adjacent area, observed similar accretion rates to this study in

ghost forests and tidal marshes, but not in tidal forests. The different results can be attributed to the fact that in Gunderson et al. (2021) the tidal forest sites were generally farther inland from the marsh than in this study. The design of Gunderson et al., (2021) encompassed a dynamic lateral transect of tidal marsh, onto a transitional ghost forest, and the freshwater forested wetland beyond. The tidal forest sites analyzed in our study were located 20 m from the edge of the shoreline and closer to the freshwater river tributaries into the sound and thus were directly influenced by alluvial sediment deposition, especially near the Roanoke and Tar Rivers. The transects in Gunderson et al. (2021) were as much as 1500 to 8000 m inland and the associated accretion rates were likely controlled primarily by autochthonous, organic inputs than the tidal forest sites in this study. The tidal forest studied in Ensign et al. (2014), Noe et al. (2016), and Moorman et al. (2024) are more similar in accretion rate and site proximity to fluvial deposition to those investigated here. The Surface Elevation Table (SET) in Moorman et al. (2024) on the Roanoke River is close in proximity to the Roanoke River site in this study.

The differences in tidal forest accretion rates observed in Craft (2012) are slightly more difficult to explain. The Satilla River is a blackwater river originating in the Atlantic Coastal Plain with a low sediment load (Marton et al., 2012; Stanley and Hobbie, 1976). The Altamaha and Ogeechee Rivers studied by Craft (2012) originate in the Piedmont and would likely carry an appreciable sediment load from the mineral rich headwaters (Giese et al., 1985). The differences in net accretion rates amongst these studies could be attributed to differences in site location, sediment loads, and watershed land use over time. Extensive land clearing for agriculture and timber harvesting occurred in the Coastal Plain of the Southeast United States in the mid-1800s and early 1900s, declining in the region on the mid-20th century with the mechanization of agriculture, consolidation of farm ownership, and abandonment of less productive lands (Craft,

2012; Craft and Casey, 2000; Trimble, 1974; Happ, 1945). Another, effect which may explain the generally higher accretion rates in all ecosystems from this study is the severity of hurricane impacts in the coastal plain of North Carolina over the past 100 years compared to in Georgia and other neighboring states (Paerl et al., 2019; Konrad and Perry, 2010; NWS, 2010). These storm events mobilize sediment higher in the watershed which can ultimately be deposited in coastal estuaries as water energy dissipates (Benninger et al., 2008; Cahoon, 2006; Cahoon et al., 1995). In addition, the APES is enclosed by the Outer Banks barrier island systems with few major inlets, in essence acting as a sediment retention basin compared to the direct outfalls of the rivers into the Atlantic Ocean (Craft, 2012; Riggs and Ames, 2003).

Generally, the accretion rates observed in other studies for ghost forests agree with those presented in this study, specifically Gunderson et al. (2021) and Lagomasino et al. (2013) which were conducted in the Albemarle and Pamlico estuaries, respectively. Ghost forests observed in the referenced studies were closer to the shoreline and subject to similar factors as those in this one, including prolonged influx and exposure to saltwater and associated chloride concentrations (Ury et al., 2021; Kirwan and Gedan, 2019). However, net accretion rates in Ensign et al. (2014) are significantly higher than those measured in this study and in others. A possible explanation of this trend is the increase in tide-dominant sediment transport occurring at the estuarine interface and a shift toward halophytic, herbaceous vegetation led to surface roughening allowing for a higher rate of capture for sediments mobilized in tidal fluctuations seen on the Savannah and Waccamaw River sites (Ensign et al. 2014; Pasternack and Brush, 2002).

The median values of tidal marsh accretion in cited literature are within the standard error values observed in this study. The values presented in Ensign et al. (2014) are 2.5 to 3 times higher than those observed in the APES; this can be explained by the dominance of astronomic

tides and higher sediment loads in the lower estuary of the Waccamaw and Savannah Rivers. This leads to a new inland movement of sediment from the lower estuary to the upper estuary (Meade, 1969). Tidal marshes in the APES are sediment starved and largely exist in a tidally restricted, wind-driven setting (Riggs and Ames, 2003). This leads to suspension and redeposition of existing sediments with few additions. Additional sediment inputs usually occur during large storm events during which sediment is introduced from the upper reaches of the river basins. Thus, much of the accretion in the tidal marshes of the APES is local and derived from occasional storm events and *in situ* net primary productivity (NPP) (Eulie et al., 2017; Giese et al., 1985; Bellis et al., 1975).

Our study found tidal forests sequester significantly more carbon than tidal marshes and ghost forests., Interestingly, however, ghost forest soils have the highest organic C content of all ecosystems. The most straightforward explanation is that these ghost forests are formed as inland peat swamps, or pocosins, with no active, consistent form of sedimentation. These prior environments would be little influenced by mineral input and their recalcitrant organic matter, rich in lignin, which is readily preserve. Due to the long-term erosion of the shoreline and the recent saltwater intrusion, there has been a shift in ecosystem characteristics (Kalu et al., 2025; Pierfelice et al., 2017; Richardson, 1983). Previous studies in ghost forests have also shown that the conversion to more halophytic vegetation types and loss in NPP in these ecosystems decreases their potential to sequester carbon (Gorczynski et al., 2024; Mazhar et al., 2022; Smart et al., 2020; Herbert et al., 2015).

Significant differences in organic soil material mineral content are observed in each ecosystem (Gorczynski et al., 2024). Tidal marshes exhibited the highest mineral content of the three ecosystems with approximately 15% more than tidal forest and 30% higher than ghost

forest. Tidal marshes in the APES generally experience disturbance during storm events leading to wave-driven erosion; this reduced the ecosystems' ability to accumulate more organic rich soil material (Gorczynski et al., 2024; Riggs and Ames, 2003; Bellis et al., 1975). Alternatively, the significance of carbon sequestration in tidal forests can be attributed to the associated river basins. The Tar and Roanoke River tidal forest sites experience regular sediment supply from higher in the basin since both systems originate in the Piedmont (Giese et al., 1985). A comparison of regional carbon sequestration rates is presented in Table 2.6.

Table 2.6. Comparison of mean (± SE) carbon sequestration rates across a salinity gradient of ecosystems (kg C yr^{-1} m^{-2}).

Area of Interest	Tidal Forest	Ghost Forest	Tidal Marsh	Source
Ogeechee River, Georgia	0.09			Craft 2012
Altamaha River, Georgia	0.08			
Satilla River, Georgia	0.06			
South Newport River, Georgia		0.09		
Bull Neck, North Carolina	0.14	0.43		Gunderson et al. 2021
Pledger Harbor, North Carolina	0.05	0.03	0.09	
Brier Hall, North Carolina	0.09	0.18	0.05	
Point Peter, North Carolina	0.12	0.14	0.12	
Carteret County, North Carolina			0.11±0.01	Bost et al., 2024
New Hanover County, North Carolina			0.08±0.01	
Cape Fear River, North Carolina			0.03±0.01	Weston et al. 2023
York River, Virginia			0.08±0.02	
James River, Virginia			0.16±0.01	
Median of Comparison Studies	0.09±0.01	0.14±0.07	0.09±0.01	Synthesis of Above Referenced Studies
Albemarle-Pamlico, North Carolina	0.18±0.02	0.12±0.004	0.08±0.003	This Study

In comparison to other regional studies, the tidal forests in this study have higher carbon sequestration rates than all other regional examples. A factor not discussed thus far is hummock versus hollow microtopography which exists in tidal forests. Hummocks are characterized as existing above the higher-water mark and hollows existing below mean low water (Courtwright and Findley, 2011; Duberstein and Conner, 2009). Ensign et al. (2014) reported accretion rates in hollows were significantly higher than those of hummocks. This trend could explain the elevated

levels of accretion and sequestration reported in this study. While we did not separate or characterize the difference between hummocks and hollows at tidal forest sites; site selection in tidal forest falls to the same bias in traditional soil survey: the desire to leave an appreciable distance from a tree to avoid striking a root. The microtopography of the tidal forest sites in this study would likely be categorized as hollows and would have comparably higher carbon sequestration rates than hummocks.

The ghost forest carbon sequestration rates measured in this study are slightly lower than those observed regionally but fall within the range of reported values. The regional comparison which stands out is Bull Neck in Gunderson et al. (2021); while not sampled in this portion the study, previous work performed in Gorczynski et al. (2024) informs the following observation: Bull Neck occurs in an area of elevated fetch for the Albemarle Sound, existing on an exposed east-facing platform where the sound narrows from approximately 16 kilometer to 10 kilometers. The site characterized as transition, or ghost forest, in Gunderson et al. (2021) sits approximately at sea level in an anthropogenic ditch experiencing saltwater intrusion that is 40 meters wide. It is possible this site's comparatively high sequestration rate could be due to deposition of remobilized, eroded soil organic and mineral material at this site during wind-driven floods.

Tidal marsh carbon sequestration rates fell within the range reported by other regional studies. The James River (Weston et al., 2023) tidal marsh's higher sequestration rate could be attributed to its location near the terminus of the river into the Chesapeake Bay. Based on historical soil survey map units and polygons, significant erosion occurred at this site, which could lead to the redeposition of suspended sediment from the actively eroding marsh edge (French, 2006). Another possible explanation is the proximity of the junction of the James River with Chesapeake Bay where significant tidal exchange occurs, leading to larger amounts of

mineral sediment and organic matter being trapped at this site (Marion et al., 2009; Temmerman et al., 2003). Ultimately, the driving factor leading carbon sequestration in any of these coastal wetland environments is the stability of the hydrologic regimen and vegetative communities coupled with allochthonous mineral inputs through fluvial or tidal interaction (Riggs and Ames, 2003; Wells and Kim, 1989).

Long-term ^{14}C Accretion and Carbon Sequestration Rates

The long-term ^{14}C accretion rates observed in this study were largely similar in age and depth; furthermore, the C sequestration rate was similar across all sites. The only significant difference emerged in accretion rate, where long term tidal marsh accretion rates were significantly lower than those observed in tidal forest and ghost forest. Another observation is the difference in age between the sites. While not significantly different ($p = 0.162$); tidal marsh ^{14}C samples were on average 600 to 700 years older than those from the other two environments. One explanation is that rapid erosion at some of the tidal marsh sites could be exposing older material. Freshwater forested wetland settings were converted to tidal marsh in the 1970 – 2006 period; these forested wetlands would have been accreting at a slow rate and their soils would contain old organic material (Moorman et al., 2024; Gunderson et al., 2021). There are also historical records indicating a significant extent of low-lying tidal marsh extended from the southern edge of Roanoke Island to the mainland on the eastern side of the Dare County Peninsula, known as the Croatan Narrows (Tise and Crow, 2017), as late as 1866. Therefore, some of the areas analyzed as tidal marsh in this study could have resembled more like a 'high marsh' prior to 1970. The volatility of inlet formation and overwash within the Outer Banks may have also played a role in the lower historic accretion rates observed in tidal marshes. Depending on width of the inlets and proximity to land, it is reasonable to believe that accretion in adjacent

coastal wetlands would have been lower with inlets being further away and narrower; countering, if the inlets were closer and there was greater tidal influence, more sediment inputs could be expected (Riggs and Ames, 2003; Giese et al., 1985). It is also worth acknowledging the accretion date between tidal forest and ghost forest is alike, save a greater standard error in ghost forest rates of accretion and carbon sequestration. This increased standard error suggests that variation in time and speed at which ghost forest undergo the ecotonal shift to a brackish-saline environment. Some ghost forest environments began undergoing the shift from a tidal forest 40 years ago and are failing to reach a level of stability in the environment to counteract SLR through net accretion; while other sites began the shift as recently as a decade ago depending on the locale in question (Ury et al., 2021; Kirwan and Gedan, 2019). Schieder (2017) reported the Longshoal River in North Carolina is experiencing a forest retreat rate of 4.5 m yr^{-1}. Overall tidal forest had the greatest level of stability based on historic ^{14}C accretion rates and standard error, this is due to the consistence in their freshwater regime, general protection from saltwater intrusion in the APES, and fluvially derived inputs (Hupp et al., 2015; Conner et al., 2007; Riggs and Ames, 2003).

A comparison of regional ^{14}C accretion rates is shown in Table 2.7, the most important comparison is data extracted from Ingram (1987) which was collected from the area of interest for this study. The average sampled depth in Ingram (1987) was 404 ± 209 cm, so the environment sampled was not attributed to tidal forest, ghost forest, or tidal marsh. Furthermore, the average age across all sites was 5379 ± 2647 years before present (1950), compared to the overall average age in this study of 1327 ± 501 years A.D. A second study conducted in the eastern section of the Albemarle Sound, was Aguilos et al. (2021). The long-term accretion rates measured by Aguilos et al. (2021) are over two times higher than what was observed in this

study; however, their study focused on a tidal forest adjacent to a ghost forest on the northern edge of Alligator River National Wildlife Refuge which was hydrologically disconnected by an access road and drainage ditch to the typical waterflow regime of Albemarle Sound. Their study design was implemented as a localized approach to understand the difference in accretion rates between two ecosystems with similar histories up to the point of anthropogenic ditching. Potential explanations for the comparatively high accretion rates observed in that study were significant mineral deposition from reconfiguring the local hydrology on the ghost forest side and, conversely, lowering the seasonal high-water table on the tidal forest side, increasing oxidation of SOC, and reducing overall accretion rates.

Table 2.7. Comparison of mean (± SE) historic accretion (cm yr^{-1}) and carbon sequestration rates across a salinity gradient of ecosystems (kg C yr^{-1} m^{-2}). *Age reported in years BP (1950) while our data is reported in years since 0 A.D.

Area of Interest	Ecosystem	Age	Accretion Rate	C Sequestration Rate	Source
Albemarle Sound	Tidal and Ghost Forest	1223±135*	0.26±0.05	-	Aguilos et al. 2021
Albemarle-Pamlico Estuary System	Mixed	5379±2647*	0.09±0.05	-	Ingram 1987
Albemarle-Pamlico Estuary System	Tidal Forest	1082±334	0.12±0.01	0.05±0.01	This Study
	Ghost Forest	1155±500	0.12±0.04	0.05±0.03	
	Tidal Marsh	1745±669	0.07±0.01	0.03±0.01	

Comparison of ^{14}C and ^{210}Pb Accretion and Carbon Sequestration Rates

Based on comparison of ^{14}C and ^{210}Pb accretion rates, the results of this study point to a statistically significant difference between the accretion rates prior to 1850 (^{14}C) and those in the last 170 years (^{210}Pb). This is reinforced by other studies which observed increased net rates of accretion and carbon sequestration since the mid-19th century (Weston et al., 2023; Kirwan and Mudd, 2012). Ecosystems are responding to SLR, where it is ecologically possible to do so (Kirwan and Megonigal, 2013; Kolker et al., 2010). Tidal forests and tidal marshes are exhibiting trends of increased accretion rates, but only tidal forests display increased rates of carbon

sequestration in this study. An increase in tidal marsh net accretion was observed in this study but also decline in net SOC sequestration over time. This change is likely driven by an increase in allochthonous mineral sediment from storm events on the eroding edges of the marshes and subsequent mineral material being redeposited (Carey et al., 2017; Mudd et al., 2009). Tidal forests also receive periodic influx of sediment, but largely from flooding events higher in the river basin (Noe and Hupp, 2005; Hupp, 2000). A significant peak in carbon sequestration in the tidal forests of this study exists at the bottom of the ^{210}Pb cores, approximately 170 years ago (Figure 2.2). One explanation for this is the Great Hurricane of 1846, which would have been at or around this time based on calculated ages in tidal forest cores (Hudgins, 2007). This storm struck the Florida Keys and then moved into Central North Carolina where the Tar and Roanoke Rivers basins would be impacted (Cerrito et al., 2022). Estimates from Cerrito et al. (2022) on the Great Hurricane of 1846, also known as the Great Havana Hurricane of 1846, indicate it was still a hurricane as it entered eastern North Carolina and roughly following the interface of the Coastal Plain and Piedmont of the state, gradually weakening to a tropical storm. Coupling this with the knowledge of historical agricultural practices and land clearing, it is likely a significant amount of sediment was mobilized and eventually captured in the alluvial tidal forests of the APES (Hupp, 2000; Mead et al., 1990; Trimble, 1974). Cerrito et al. (2022) also reports an economic loss of approximately $100 billion in damage from this hurricane. This figure would be greater than Hurricane Hazel (1954) which is consistently referred to as the most destructive hurricane in coastal North Carolina history (Barnes, 2013; Hudgins, 2007; Hardy and Carney, 1962).

In more recent times, an increase in tidal forest net accretion and carbon sequestration rates may be enhanced by hurricanes including Floyd, Matthew, and the 1940 South Carolina

Hurricane which caused significant rainfall, flooding, and erosion in the Roanoke and Tar Rivers basins (Musset et al., 2017; Hudgins, 2007; Leece et al., 2004). Hurricanes and tropical storms of significant disruption and destruction have been recorded since the 16th century on the eastern edge of the APES (Hudgins, 2007). The Outer Banks restriction of lunar enhance storm-surge may offer some protection to tidal forests from extensive hurricane-associated saltwater intrusion (Riggs and Ames, 2003; Giese et al, 1985). Saltwater intrusion during hurricanes, tropical storms, and droughts significantly impact tidal forests in other areas (Yu et al., 2019; Liu et al., 2017b; Craft, 2012). Therefore, hurricanes and weaker tropical storm events play an outsized role on coastal wetlands in this region, especially during the historic era of exploitative timber harvesting and land clearing practices in the piedmont and coastal plain of North Carolina.

Sea Level Rise, Accretion Rates, and Regional Accretion Comparisons

We identified three distinct rates of net accretion for each ecosystem from 1850 – 2021 in this study (Table 2.3). We found when comparing the time intervals of 1850 – 1970, 1970 – 2006, and 2006 – 20212 that there were significant differences within the ecosystems. Statistically different rates of accretion during these periods occurred in tidal forests and tidal marshes, likely a response to accelerating SLR over time. However, within the ghost forests the accretion rate in 1970 – 2006 and 2006 – 2021 were not significantly different. This observation is consistent with previous analysis and projections of ghost forests losing NPP and their ability to accrete during the transition from a freshwater to a brackish or a saline ecosystem (Kirwan and Gedan, 2019). This characteristic of ghost forests is concerning regionally because they comprise significant areas of the coastal wetlands in the APES and are projected to spread over time with accelerated SLR (Ury et al., 2021). The timeframe for ghost forests to become stable tidal marshes via marsh migration is not entirely clear, and is dependent on salinity influx, and

resiliency (Fagherazzi et al., 2019; Wasson et al., 2013). Preliminary results from this study indicate rapid erosion of ghost forests may ultimately hinder the ability of tidal marsh to establish and mitigate further effects of SLR in the western area of the APES.

While promising, the rapid increase in tidal forest accretion rates in the short-term (^{210}Pb) does not account for the inevitable increase in salinity which will occur in these environments. Tidal forests subject to continued saltwater intrusion, droughts, and subsequent reduction in NPP will become ghost forests and ecosystem accretion and carbon sequestration rates will decrease (Kirwan and Gedan, 2019). Current climate change research suggests increased severity of droughts and SLR will act as compound stressors on these environments (IPCC, 2022). Furthermore, establishing marsh migration corridors receives significant academic attention, but tidal forest displacement has had far less study (Schieder, 2017; Kirwan et al., 2016). The localized increase in tidal forest accretion rates offer promise for keeping pace with projected sea level rise to a certain degree, but incorporating risks, threats, and potential outcomes are required to understand how these ecosystems will respond.

Utilizing the three scenarios of accretion identified and placing them against the projections of relative SLR from Sweet et al. (2022) for 2050 and 2100 shows the extent to which all coastal wetlands will likely submerge in the future. While tidal forest and tidal marsh accretion rates from 2006 – 2021 are more than double those calculated from 1850 – 1970, the current rates are not enough to maintain elevation and outpace SLR. All projections utilized will not be enough to outpace projected relative SLR of 0.36 m in 2050 and 1.1 m in 2100 from Sweet et al. (2022) in the Southeast United States, let alone the Intermediate-High scenario of 0.43 m in 2050 and 1.6 m in 2100. Therefore, all ecosystems across the salinity gradient which

exists in the APES are at risk of submersion and erosion based on the scenarios put forth and analysis conducted.

Conclusion

The results from this research provide long-term and short-term accretion and carbon sequestration rates for coastal wetlands across a salinity gradient. Our results suggest tidal forest ecosystems are the closest to maintaining elevation with projected SLR, while ghost forests are at the greatest risk of being submerged over the next 75 years. Concurrently, tidal forests are sequestering the most carbon of the ecosystems studied, potentially tied to the frequency and strength of hurricanes in the APES which provide large supplies of alluvial sediment to these areas of the estuary. Finally, three clear time periods of accretion rates have emerged over the past 150 years as the coastal wetlands contend with SLR. These findings should be used to re-evaluate which ecosystems are most at risk over the next century from climate change and how they are naturally adapting to compound stressors. Understanding how accretion rates are increasing in these ecosystems or being surpassed by SLR, will allow for more informed land use and management decisions in the coming years.

REFERENCES

Aguilos, M., Brown, C., Minick, K., Fischer, M., Ile, O. J., Hardesty, D., ... & King, J. (2021). Millennial-scale carbon storage in natural pine forests of the north carolina lower coastal plain: Effects of artificial drainage in a time of rapid sea level rise. *Land*, *10*(12), 1294.

Appleby, P. G., & Oldfield, F. (1992). Applications of lead-210 to sedimentation studies. In *Uranium-series disequilibrium: applications to earth, marine, and environmental sciences. 2. ed*.

Appleby, P. G., Nolan, P. J., Oldfield, F., Richardson, N., & Higgitt, S. R. (1988). 210Pb dating of lake sediments and ombrotrophic peats by gamma essay. *Science of the total environment*, *69*, 157-177.

Appleby, P. G., & Oldfield, F. (1978). The calculation of lead-210 dates assuming a constant rate of supply of unsupported 210Pb to the sediment. *Catena*, *5*(1), 1-8.

Ardón, M., Helton, A. M., & Bernhardt, E. S. (2018). Salinity effects on greenhouse gas emissions from wetland soils are contingent upon hydrologic setting: a microcosm experiment. Biogeochemistry, 140, 217-232.

Ardón, M., Morse, J. L., Colman, B. P., & Bernhardt, E. S. (2013). Drought-induced saltwater incursion leads to increased wetland nitrogen export. Global change biology, 19(10), 2976-2985.

Arrhenius, S. (1896). XXXI. On the influence of carbonic acid in the air upon the temperature of the ground. The London, Edinburgh, and Dublin Philosophical Magazine and Journal of Science, 41(251), 237-276.

Balduff, D. M. (2007). Pedogenesis, inventory, and utilization of subaqueous soils in Chincoteague Bay, Maryland. University of Maryland, College Park.

Barnes, J. (2013). *North Carolina's hurricane history: Updated with a decade of new storms from Isabel to Sandy*. UNC Press Books.

Baustian, J. J., Mendelssohn, I. A., & Hester, M. W. (2012). Vegetation's importance in regulating surface elevation in a coastal salt marsh facing elevated rates of sea level rise. Global Change Biology, 18(11), 3377-3382.

Bellis Jr, V. J., O'Connor, M. P., & Riggs, S. R. (1975). Estuarine Shoreline Erosion in The Albemarle-Pamlico Region Of North Carolina.

Benninger, L. K., Alperin, M. J., Wells, J. T., Ream, B. J., Muñoz, P., Nie, Y., ... & Lafond, S. (2008). *Impact of Hurricane Floyd on sediment deposition, erosion, and benthic nutrient fluxes in Pamlico Sound, North Carolina*. Water Resources Research Institute of the University of North Carolina.

Bilkovic, D. M., Mitchell, M., Mason, P., & Duhring, K. (2016). The role of living shorelines as estuarine habitat conservation strategies. *Coastal Management*, *44*(3), 161-174.

Blankespoor, B., Dasgupta, S., & Laplante, B. (2014). Sea-level rise and coastal wetlands. *Ambio*, *43*, 996-1005.

Bost, M. C., Rodriguez, A. B., & McKee, B. A. (2024). Impact of land-use change on salt marsh accretion. *Estuarine, Coastal and Shelf Science*, *299*, 108693.

Brooks, H., Möller, I., Carr, S., Chirol, C., Christie, E., Evans, B., Spencer, K.L., Spencer, T., & Royse, K. (2021). Resistance of salt marsh substrates to near-instantaneous hydrodynamic forcing. Earth Surface Processes and Landforms, 46(1), 67-88.

Cahoon, D. R., & Guntenspergen, G. R. (2010). Climate change, sea-level rise, and coastal wetlands. National Wetlands Newsletter, 32(1), 8-12.

Cahoon, D. R. (2006). A review of major storm impacts on coastal wetland elevations. *Estuaries and coasts*, *29*, 889-898.

Cahoon, D. R., Lynch, J. C., Perez, B. C., Segura, B., Holland, R. D., Stelly, C., ... & Hensel, P. (2002). High-precision measurements of wetland sediment elevation: II. The rod surface elevation table. *Journal of Sedimentary Research*, *72*(5), 734-739.

Cahoon, D. R., Reed, D. J., Day Jr, J. W., Steyer, G. D., Boumans, R. M., Lynch, J. C., ... & Latif, N. (1995). The influence of Hurricane Andrew on sediment distribution in Louisiana coastal marshes. *Journal of Coastal Research*, 280-294.

CALIB rev. 8; Stuiver, M., and Reimer, P.J., 1993, Radiocarbon, 35, 215-230.

Camelo, J., Mayo, T. L., & Gutmann, E. D. (2020). Projected climate change impacts on hurricane storm surge inundation in the coastal United States. Frontiers in Built Environment, 6, 588049.

Carey, J. C., Moran, S. B., Kelly, R. P., Kolker, A. S., & Fulweiler, R. W. (2017). The declining role of organic matter in New England salt marshes. *Estuaries and Coasts*, *40*, 626-639.

Cassalho, F., Miesse, T. W., de Lima, A. D. S., Khalid, A., Ferreira, C. M., & Sutton-Grier, A. E. (2021). Coastal wetlands exposure to storm surge and waves in the Albemarle-Pamlico estuarine system during extreme events. *Wetlands*, *41*(4), 49.

Cerrito, E. L., Mock, C. J., & Collins, J. M. (2022). The Great Havana Hurricane of 1846: a reconstruction of the storm's track, intensity, and impacts. *Annals of the American Association of Geographers*, *111*(6), 1585-1601.

Chambers, L. G., Osborne, T. Z., & Reddy, K. R. (2013). Effect of salinity-altering pulsing events on soil organic carbon loss along an intertidal wetland gradient: a laboratory experiment. *Biogeochemistry*, *115*, 363-383.

Chen, Y., Li, Y., Thompson, C., Wang, X., Cai, T., & Chang, Y. (2018). Differential sediment trapping abilities of mangrove and saltmarsh vegetation in a subtropical estuary. Geomorphology, 318, 270-282.

Conner, W.H., Krauss, K.W., Doyle, T.W. (2007). Ecology of Tidal Freshwater Forests in Coastal Deltaic Louisiana and Northeastern South Carolina. In: Ecology of Tidal Freshwater Forested Wetlands of the Southeastern United States. Springer, Dordrecht. https://doi.org/10.1007/978-1-4020-5095-4_9

Core Scientific International. (2023). Alpha Spectroscopy Services (*Geochronology and Paleolimnology Services).* Core Scientific International.

Courtwright, J., & Findlay, S. E. (2011). Effects of microtopography on hydrology, physiochemistry, and vegetation in a tidal swamp of the Hudson River. *Wetlands*, *31*, 239-249.

Cowart, L., Corbett, D. R., & Walsh, J. P. (2011). Shoreline change along sheltered coastlines: Insights from the Neuse River Estuary, NC, USA. Remote Sensing, 3(7), 1516-1534.

Craft, C. (2023). Tidal marsh restoration on Sapelo Island: A legacy of RJ Reynolds, Jr., Eugene Odum and the University of Georgia Marine Institute. *Ecological Engineering*, *187*, 106875.

Craft, C. B., Li, S., & Xie, T. (2022). From the headwaters to the sea: The role of riparian, alluvial, and tidal wetlands to filter nutrients and ameliorate eutrophication. River, 1(2), 133-141.

Craft, C.B. (2012), Tidal freshwater forest accretion does not keep pace with sea level rise. Glob Change Biol, 18: 3615-3623. https://doi-org.prox.lib.ncsu.edu/10.1111/gcb.12009

Craft, C. B., & Casey, W. P. (2000). Sediment and nutrient accumulation in floodplain and depressional freshwater wetlands of Georgia, USA. *Wetlands*, *20*(2), 323-332.

Crosby, S. C., Sax, D. F., Palmer, M. E., Booth, H. S., Deegan, L. A., Bertness, M. D., & Leslie, H. M. (2016). Salt marsh persistence is threatened by predicted sea-level rise. *Estuarine, Coastal and Shelf Science*, *181*, 93-99.

Culmo, F. C. (1988). Principle of operation—The Perkin-Elmer pe 2400 CHN elemental analyzer. Perkin Elmer Corp., Norwalk, CT.

Day, R.H., Williams, T.M., Swarzenski, C.M. (2007). Hydrology of Tidal Freshwater Forested Wetlands of the Southeastern United States. In: Ecology of Tidal Freshwater Forested

Wetlands of the Southeastern United States. Springer, Dordrecht. https://doi.org/10.1007/978-1-4020-5095-4_2

DeLaune, R. D., & White, J. R. (2012). Will coastal wetlands continue to sequester carbon in response to an increase in global sea level?: a case study of the rapidly subsiding Mississippi river deltaic plain. Climatic Change, 110, 297-314.

DirectAMS. (2023). AMS Measurement *(Process Measurement – NEC Pelletron 500 kV AMS)*. https://www.directams.com/measurement.

Dixon, R. K., & Krankina, O. N. (1995). Can the terrestrial biosphere be managed to conserve and sequester carbon?. In *Carbon Sequestration in the Biosphere: Processes and Prospects* (pp. 153-179). Berlin, Heidelberg: Springer Berlin Heidelberg.

Doyle, T.W., O'Neil, C.P., Melder, M.P., From, A.S., Palta, M.M. (2007). Tidal Freshwater Swamps of the Southeastern United States: Effects of Land Use, Hurricanes, Sea-level Rise, and Climate Change. In: Ecology of Tidal Freshwater Forested Wetlands of the Southeastern United States. Springer, Dordrecht. https://doi.org/10.1007/978-1-4020-5095-4_1

Duberstein, J. A., & Conner, W. H. (2009). Use of hummocks and hollows by trees in tidal freshwater forested wetlands along the Savannah River. *Forest Ecology and Management*, *258*(7), 1613-1618.

Ensign, S.H., Hupp, C.R., Noe, G.B. *et al.* Sediment Accretion in Tidal Freshwater Forests and Oligohaline Marshes of the Waccamaw and Savannah Rivers, USA. *Estuaries and Coasts* **37**, 1107–1119 (2014). https://doi.org/10.1007/s12237-013-9744-7

Eulie, D. O., Corbett, D. R., & Walsh, J. P. (2018). Shoreline erosion and decadal sediment accumulation in the Tar-Pamlico estuary, North Carolina, USA: A source-to-sink analysis. Estuarine, Coastal and Shelf Science, 202, 246-258.

Eulie, D. O., Walsh, J. P., Corbett, D. R., & Mulligan, R. P. (2017). Temporal and spatial dynamics of estuarine shoreline change in the Albemarle-Pamlico estuarine system, North Carolina, USA. *Estuaries and Coasts*, *40*, 741-757.

Eulie, D. O. (2014). *Examination of estuarine sediment dynamics: Insights from the large, shallow, Albemarle-Pamlico Estuarine System, NC, USA*. East Carolina University.

Eulie, D. O., Walsh, J. P., & Corbett, D. R. (2013). High-resolution analysis of shoreline change and application of balloon-based aerial photography, Albemarle-Pamlico Estuarine System, North Carolina, USA. Limnology and Oceanography: Methods, 11(4), 151-160.

Ezer, T., & Atkinson, L. P. (2014). Accelerated flooding along the US East Coast: On the impact of sea-level rise, tides, storms, the Gulf Stream, and the North Atlantic Oscillations. *Earth's Future*, *2*(8), 362-382.

Fairbridge, R. W. (1980). The estuary: its definition and geodynamic cycle. *Chemistry and biochemistry of estuaries*, 1-35.

Fagherazzi, S., Anisfeld, S. C., Blum, L. K., Long, E. V., Feagin, R. A., Fernandes, A., ... & Williams, K. (2019). Sea level rise and the dynamics of the marsh-upland boundary. *Frontiers in environmental science*, *7*, 25.

Fest, B. J., Swearer, S. E., & Arndt, S. K. (2022). A review of sediment carbon sampling methods in mangroves and their broader impacts on stock estimates for blue carbon ecosystems. *Science of the Total Environment*, *816*, 151618.

Ford, M. A., Cahoon, D. R., & Lynch, J. C. (1999). Restoring marsh elevation in a rapidly subsiding salt marsh by thin-layer deposition of dredged material. *Ecological Engineering*, *12*(3-4), 189-205.

Garner, G., Hermans, T. H., Kopp, R., Slangen, A., Edwards, T., Levermann, A., ... & Pearson, B. (2022). IPCC AR6 WGI Relative Sea Level Projection Distributions without Background Component.

Gee, G. W., & Bauder, J. W. (1986). Particle-size analysis. *Methods of soil analysis: Part 1 Physical and mineralogical methods*, *5*, 383-411.

Giese, G. L., Wilder, H. B., & Parker, G. G. (1985). Hydrology of major estuaries and sounds of North Carolina (Vol. 2221). US Government Printing Office.

Google Earth Pro 7.3. (1985-2021), Satellite. Data SIO, NOAA, U.S. Navy, NGA, GEBCO. (16 October 2021)

Gorczynski, L. E., Wilson, A. R., Odhiambo, B. K., & Ricker, M. C. (2024). Coastal Forest Change and Shoreline Erosion across a Salinity Gradient in a Micro-Tidal Estuary System. Forests, 15(6), 1069.

Gracia, A., Rangel-Buitrago, N., Oakley, J. A., & Williams, A. T. (2018). Use of ecosystems in coastal erosion management. *Ocean & coastal management*, *156*, 277-289.

Gundersen, G., Corbett, D.R., Long, A. *et al.* Long-Term Sediment, Carbon, and Nitrogen Accumulation Rates in Coastal Wetlands Impacted by Sea Level Rise. *Estuaries and Coasts* **44**, 2142–2158 (2021). https://doi.org/10.1007/s12237-021-00928-z

Hackney, C. T., & Avery, G. B. (2015). Tidal wetland community response to varying levels of flooding by saline water. Wetlands, 35, 227-236.

Hackney, C.T., Avery, G.B., Leonard, L.A., Posey, M., Alphin, T. (2007). Biological, Chemical, and Physical Characteristics of Tidal Freshwater Swamp Forests of the Lower Cape Fear River/Estuary, North Carolina. In: Ecology of Tidal Freshwater Forested Wetlands of the

Southeastern United States. Springer, Dordrecht. https://doi.org/10.1007/978-1-4020-5095-4_8

Hajdas, I., Ascough, P., Garnett, M. H., Fallon, S. J., Pearson, C. L., Quarta, G., ... & Yoneda, M. (2021). Radiocarbon dating. *Nature Reviews Methods Primers*, *1*(1), 62.

Hamlington, B. D., Bellas-Manley, A., Willis, J. K., Fournier, S., Vinogradova, N., Nerem, R. S., ... & Kopp, R. (2024). The rate of global sea level rise doubled during the past three decades. *Communications Earth & Environment*, *5*(1), 601.

Happ, S. C. (1945). Sedimentation in South Carolina piedmont valleys. *American Journal of Science*, *243*(3), 113-126.

Hatton, R. S., DeLaune, R. D., & Patrick Jr, W. H. (1983). Sedimentation, accretion, and subsidence in marshes of Barataria Basin, Louisiana 1. *Limnology and Oceanography*, *28*(3), 494-502.

Herbert, E. R., Boon, P., Burgin, A. J., Neubauer, S. C., Franklin, R. B., Ardón, M., ... & Gell, P. (2015). A global perspective on wetland salinization: ecological consequences of a growing threat to freshwater wetlands. Ecosphere, 6(10), 1-43.

Hoegh-Guldberg, O., Mumby, P. J., Hooten, A. J., Steneck, R. S., Greenfield, P., Gomez, E., ... & Hatziolos, M. E. (2007). Coral reefs under rapid climate change and ocean acidification. science, 318(5857), 1737-1742.

Hopkinson, C. S., Morris, J. T., Fagherazzi, S., Wollheim, W. M., & Raymond, P. A. (2018). Lateral marsh edge erosion as a source of sediments for vertical marsh accretion. *Journal of Geophysical Research: Biogeosciences*, *123*(8), 2444-2465.

Hudgins, J. E. (2007). Tropical cyclones affecting North Carolina since 1586: an historical perspective.

Hunter, H. N., Gowing, C. J. B., Marriott, A. L., Lacey, J. H., Dowell, S., & Watts, M. J. (2023). Developments in Pb-210 methodologies to provide chronologies for environmental change. *Environmental Geochemistry and Health*, *45*(4), 1173-1181.

Hupp, C. R., Kroes, D. E., Noe, G. B., Schenk, E. R., & Day, R. H. (2019). Sediment trapping and carbon sequestration in floodplains of the lower Atchafalaya Basin, LA: Allochthonous versus autochthonous carbon sources. *Journal of Geophysical Research: Biogeosciences*, *124*(3), 663-677.

Hupp, C. R., Schenk, E. R., Kroes, D. E., Willard, D. A., Townsend, P. A., & Peet, R. K. (2015). Patterns of floodplain sediment deposition along the regulated lower Roanoke River, North Carolina: Annual, decadal, centennial scales. *Geomorphology*, *228*, 666-680.

Hupp, C. R. (2000). Hydrology, geomorphology and vegetation of Coastal Plain rivers in the

south-eastern USA. *Hydrological processes*, *14*(16-17), 2991-3010.

Ingram, R.L. (1987). Peat Deposits of North Carolina. Bulletin 88. United States.

Jia, P., & Li, M. (2012). Circulation dynamics and salt balance in a lagoonal estuary. *Journal of Geophysical Research: Oceans*, *117*(C1).

Kalu, S., Ricker, M. C., Janson, J., Nordlund, D., & Li, H. (2025). Destabilization of Soil Carbon After Saltwater Intrusion in Coastal Agricultural Soils. *Environmental Science & Technology*.

Kearney, M. S., Rogers, A. S., Townshend, J. R., Rizzo, E., Stutzer, D., Stevenson, J. C., & Sundborg, K. (2002). Landsat imagery shows decline of coastal marshes in Chesapeake and Delaware Bays. *Eos, Transactions American Geophysical Union*, *83*(16), 173-178.

Kemp, A. C., Horton, B. P., & Culver, S. J. (2009). Distribution of modern salt-marsh foraminifera in the Albemarle–Pamlico estuarine system of North Carolina, USA: Implications for sea-level research. *Marine Micropaleontology*, *72*(3-4), 222-238.

Kim, J. D. S. (2022). Distribution and Variability of Carbon Stocks in Mid-Atlantic Tidal Marsh Soils (Master's thesis, University of Maryland, College Park).

Kirwan, M. L., & Gedan, K. B. (2019). Sea-level driven land conversion and the formation of ghost forests. *Nature Climate Change*, *9*(6), 450-457.

Kirwan, M. L., Walters, D. C., Reay, W. G., & Carr, J. A. (2016). Sea level driven marsh expansion in a coupled model of marsh erosion and migration. *Geophysical Research Letters*, *43*(9), 4366-4373.

Kirwan, M. L., & Megonigal, J. P. (2013). Tidal wetland stability in the face of human impacts and sea-level rise. *Nature*, *504*(7478), 53-60.

Kirwan, M. L., & Mudd, S. M. (2012). Response of salt-marsh carbon accumulation to climate change. *Nature*, *489*(7417), 550-553.

Kolker, A. S., Kirwan, M. L., Goodbred, S. L., & Cochran, J. K. (2010). Global climate changes recorded in coastal wetland sediments: Empirical observations linked to theoretical predictions. *Geophysical Research Letters*, *37*(14).

Konrad, C. E., & Perry, L. B. (2010). Relationships between tropical cyclones and heavy rainfall in the Carolina region of the USA. *International Journal of Climatology: A Journal of the Royal Meteorological Society*, *30*(4), 522-534.

Kopp, R. E., Hay, C. C., Little, C. M., & Mitrovica, J. X. (2015). Geographic variability of sea-level change. *Current Climate Change Reports*, *1*, 192-204.

Krauss, K. W., Noe, G. B., Duberstein, J. A., Conner, W. H., Stagg, C. L., Cormier, N., ... & Whitbeck, J. L. (2018). The role of the upper tidal estuary in wetland blue carbon storage and flux. Global Biogeochemical Cycles, 32(5), 817-839.

Krasting, J. P., Dunne, J. P., Stouffer, R. J., & Hallberg, R. W. (2016). Enhanced Atlantic sea-level rise relative to the Pacific under high carbon emission rates. *Nature Geoscience*, *9*(3), 210-214.

Kroes, D.E., Hupp, C.R., Noe, G.B. (2007). Sediment, Nutrient, and Vegetation Trends Along the Tidal, Forested Pocomoke River, Maryland. In: Ecology of Tidal Freshwater Forested Wetlands of the Southeastern United States. Springer, Dordrecht. https://doi.org/10.1007/978-1-4020-5095-4_5

Kulp, J. L. (1952). The carbon 14 method of age determination. *The Scientific Monthly*, *75*(5), 259-267.

Lagomasino, D., Corbett, D.R. & Walsh, J.P. Influence of Wind-Driven Inundation and Coastal Geomorphology on Sedimentation in Two Microtidal Marshes, Pamlico River Estuary, NC. *Estuaries and Coasts* **36**, 1165–1180 (2013). https://doi-org.prox.lib.ncsu.edu/10.1007/s12237-013-9625-0

Langston, A. K., Kaplan, D. A., & Putz, F. E. (2017). A casualty of climate change? Loss of freshwater forest islands on Florida's Gulf Coast. Global Change Biology, 23(12), 5383-5397.

Lecce, S. A., Pease, P. P., Gares, P. A., & Rigsby, C. A. (2004). Floodplain sedimentation during an extreme flood: the 1999 flood on the Tar River, eastern North Carolina. *Physical Geography*, *25*(4), 334-346.

Lemon, J. (2006). Plotrix: a package in the red light district of R. R-News 6 (4): 8–12. URL https://cran. r-project. org/doc/Rnews/Rnews_2006-4. pdf.

Liu, X., Ruecker, A., Song, B., Xing, J., Conner, W. H., & Chow, A. T. (2017a). Effects of salinity and wet–dry treatments on C and N dynamics in coastal-forested wetland soils: Implications of sea level rise. Soil Biology and Biochemistry, 112, 56-67.

Liu, X., Conner, W. H., Song, B., & Jayakaran, A. D. (2017b). Forest composition and growth in a freshwater forested wetland community across a salinity gradient in South Carolina, USA. *Forest Ecology and Management*, *389*, 211-219.

Lovelock, C. E., & Duarte, C. M. (2019). Dimensions of blue carbon and emerging perspectives. *Biology letters*, *15*(3), 20180781.

Luettich Jr, R. A., Carr, S. D., Reynolds-Fleming, J. V., Fulcher, C. W., & McNinch, J. E. (2002). Semi-diurnal seiching in a shallow, micro-tidal lagoonal estuary. Continental Shelf Research, 22(11-13), 1669-1681.

MacKenzie, A. B., Hardie, S. M. L., Farmer, J. G., Eades, L. J., & Pulford, I. D. (2011). Analytical and sampling constraints in 210Pb dating. *Science of the Total Environment*, *409*(7), 1298-1304.

Manetta, J. V. (2023). Distribution and Variability of Blue Carbon in Tidal Marsh Soils of Southern New England. University of Rhode Island.

Marion, C., Anthony, E. J., & Trentesaux, A. (2009). Short-term (≤ 2 yrs) estuarine mudflat and saltmarsh sedimentation: High-resolution data from ultrasonic altimetry, rod surface-elevation table, and filter traps. *Estuarine, Coastal and Shelf Science*, *83*(4), 475-484.

Mariotti, G. (2020). Beyond marsh drowning: The many faces of marsh loss (and gain). *Advances in Water Resources*, *144*, 103710.

Martinez, M., & Ardón, M. (2021). Drivers of greenhouse gas emissions from standing dead trees in ghost forests. *Biogeochemistry*, *154*(3), 471-488.

Marton, J. M., Herbert, E. R., & Craft, C. B. (2012). Effects of salinity on denitrification and greenhouse gas production from laboratory-incubated tidal forest soils. *Wetlands*, *32*, 347-357.

Mcleod, E., Chmura, G. L., Bouillon, S., Salm, R., Björk, M., Duarte, C. M., ... & Silliman, B. R. (2011). A blueprint for blue carbon: toward an improved understanding of the role of vegetated coastal habitats in sequestering CO2. Frontiers in Ecology and the Environment, 9(10), 552-560.

McInnes, R. J. (2013). Recognizing ecosystem services from wetlands of international importance: an example from Sussex, UK. *Wetlands*, *33*(6), 1001-1017.

Meade, R. H., Yuzyk, T. R., & Day, T. J. (1990). Movement and storage of sediment in rivers of the United States and Canada.

Meade, R. H. (1969). Landward transport of bottom sediments in estuaries of the Atlantic coastal plain. *Journal of Sedimentary Research*, *39*(1), 222-234.

Megonigal, J. P., & Neubauer, S. C. (2019). Biogeochemistry of tidal freshwater wetlands. In *Coastal wetlands* (pp. 641-683). Elsevier.

Meyer, J. L. (1990). A blackwater perspective on riverine ecosystems. *BioScience*, *40*(9), 643-651.

Michener, W. K., Blood, E. R., Bildstein, K. L., Brinson, M. M., & Gardner, L. R. (1997). Climate change, hurricanes and tropical storms, and rising sea level in coastal wetlands. *Ecological applications*, *7*(3), 770-801.

Middleton, G. V. (1993). Sediment deposition from turbidity currents. *Annual Review Of Earth And Planetary Sciences, Volume 21, pp. 89-114.*, *21*, 89-114.

Mitchell, J. F. (1989). The "greenhouse" effect and climate change. *Reviews of Geophysics*, *27*(1), 115-139.

Mitsch, W. J., Bernal, B., & Hernandez, M. E. (2015). Ecosystem services of wetlands. *International Journal of Biodiversity Science, Ecosystem Services & Management*, *11*(1), 1-4.

Mitsch, W. J., Bernal, B., Nahlik, A. M., Mander, Ü., Zhang, L., Anderson, C. J., ... & Brix, H. (2013). Wetlands, carbon, and climate change. *Landscape ecology*, *28*, 583-597.

Möller, I., Kudella, M., Rupprecht, F., Spencer, T., Paul, M., Van Wesenbeeck, B. K., ... & Schimmels, S. (2014). Wave attenuation over coastal salt marshes under storm surge conditions. *Nature Geoscience*, *7*(10), 727-731.

Montzka, S. A., Dlugokencky, E. J., & Butler, J. H. (2011). Non-CO2 greenhouse gases and climate change. *Nature*, *476*(7358), 43-50.

Moorman, M., Tsai, E., Marain, D., Ladin, Z. (2024). USFWS, Southeast Region Surface Elevation Table and Marker Horizon Data Analysis, 2012-2024. Atlanta, GA. <https://iris.fws.gov/APPS/ServCat/DownloadFile/254962>

Morris, J. T., Sundareshwar, P. V., Nietch, C. T., Kjerfve, B., & Cahoon, D. R. (2002). Responses of coastal wetlands to rising sea level. *Ecology*, *83*(10), 2869-2877.

Mudd, S. M., Howell, S. M., & Morris, J. T. (2009). Impact of dynamic feedbacks between sedimentation, sea-level rise, and biomass production on near-surface marsh stratigraphy and carbon accumulation. *Estuarine, Coastal and Shelf Science*, *82*(3), 377-389.

Munns, R., & Tester, M. (2008). Mechanisms of salinity tolerance. *Annu. Rev. Plant Biol.*, *59*(1), 651-681.

Musser, J. W., Watson, K. M., & Gotvald, A. J. (2017). *Characterization of peak streamflows and flood inundation at selected areas in North Carolina following Hurricane Matthew, October 2016* (No. 2017-1047). US Geological Survey.

National Weather Service. (2010). *Tropical Cyclone Climatology*. National Hurricane Center and Central Pacific Hurricane Center. https://www.nhc.noaa.gov/climo/#:~:text=Atlantic%20and%20Eastern%20Pacific%20Hurricane,Sea%2C%20and%20Gulf%20of%20America.

Newton, A., Icely, J., Cristina, S., Perillo, G. M., Turner, R. E., Ashan, D., ... & Kuenzer, C. (2020). Anthropogenic, direct pressures on coastal wetlands. *Frontiers in Ecology and*

Evolution, *8*, 144.

Nicholas, A. P., & Walling, D. E. (1998). Numerical modelling of floodplain hydraulics and suspended sediment transport and deposition. *Hydrological Processes*, *12*(8), 1339-1355.

Nicholls, R. J., Wong, P. P., Burkett, V., Codignotto, J. O., Hay, J., Roger, F., ... & Woodroffe, C. D. (2007). Coastal systems and low-lying areas.

Nicholls, R. J. (2004). Coastal flooding and wetland loss in the 21st century: changes under the SRES climate and socio-economic scenarios. *Global environmental change*, *14*(1), 69-86.

Noe, G.B., Hupp, C.R., Bernhardt, C.E. *et al.* Contemporary Deposition and Long-Term Accumulation of Sediment and Nutrients by Tidal Freshwater Forested Wetlands Impacted by Sea Level Rise. *Estuaries and Coasts* **39**, 1006–1019 (2016). https://doi.org/10.1007/s12237-016-0066-4

Noe, G. B., & Hupp, C. R. (2005). Carbon, nitrogen, and phosphorus accumulation in floodplains of Atlantic Coastal Plain rivers, USA. *Ecological Applications*, *15*(4), 1178-1190.

North Carolina Emergency Management. (2016). *North Carolina Spatial Data Download.* https://sdd.nc.gov/DataDownload.aspx

Nyman, J. A., Walters, R. J., Delaune, R. D., & Patrick Jr, W. H. (2006). Marsh vertical accretion via vegetative growth. *Estuarine, Coastal and Shelf Science*, *69*(3-4), 370-380.

Refuge marsh fire all but extinguished after burning 85 acres. The Outer Banks Voice. (2015, May 20). https://www.outerbanksvoice.com/2015/05/20/refuge-marsh-fire-all-but-extinguished-after-burning-85-acres/

Paerl, H. W., Hall, N. S., Hounshell, A. G., Luettich Jr, R. A., Rossignol, K. L., Osburn, C. L., & Bales, J. (2019). Recent increase in catastrophic tropical cyclone flooding in coastal North Carolina, USA: Long-term observations suggest a regime shift. *Scientific reports*, *9*(1), 10620.

Palinkas, C.M., Koch, E.W. Sediment Accumulation Rates and Submersed Aquatic Vegetation (SAV) Distributions in the Mesohaline Chesapeake Bay, USA. *Estuaries and Coasts* **35**, 1416–1431 (2012). https://doi-org.prox.lib.ncsu.edu/10.1007/s12237-012-9542-7

Pasternack, G. B., & Brush, G. S. (2002). Biogeomorphic controls on sedimentation and substrate on a vegetated tidal freshwater delta in upper Chesapeake Bay. *Geomorphology*, *43*(3-4), 293-311.

Patel, M. (2010). Estuarine Shoreline Change: An Analysis of Hyde County, North Carolina.

Park, C. E. (2021). Subaqueous Soils of South River, Maryland: Soil-Landscape Model Evaluation (Master's thesis, University of Maryland, College Park).

Perillo, G. M. (1995). Definitions and geomorphologic classifications of estuaries. In *Developments in sedimentology* (Vol. 53, pp. 17-47). Elsevier.

Pierfelice, K. N., Graeme Lockaby, B., Krauss, K. W., Conner, W. H., Noe, G. B., & Ricker, M. C. (2017). Salinity influences on aboveground and belowground net primary productivity in tidal wetlands. *Journal of Hydrologic Engineering*, *22*(1), D5015002.

Pluske, W., Murphy, D., & Sheppard, J. (2020). Total Organic Carbon. Department of Agriculture and Food, The State of Western Australia. Retrieved from http://soilquality.org.au/factsheets/organic-carbon

Pörtner, H. O., Roberts, D. C., Adams, H., Adelekan, I., Adler, C., Adrian, R., ... & Zaiton Ibrahim, Z. (2022). IPCC. Technical summary. *Climate change*, 37-118.

Pritchard, D. W. (1967). What is an estuary: physical viewpoint. American Association for the Advancement of Science.

R Core Team (2024). _R: A Language and Environment for Statistical Computing_. R Foundation for Statistical Computing, Vienna, Austria. <https://www.R-project.org/>.

Richardson, C. J. (1983). Pocosins: vanishing wastelands or valuable wetlands?. *Bioscience*, *33*(10), 626-633.

Riggs, S. R., & Ames, D. V. (2003). Drowning the North Carolina coast: sea-level rise and estuarine dynamics.

Riggs, S.R., O'Connor, M.P., and Bellis, V.J. (1978). Estuarine shoreline erosion in North Carolina: Univ. of North Carolina Sea Grant College, Raleigh, NC, Five-part poster series.

Sapkota, Y. (2021). *Soil Organic Matter Accretion, Complexity, and Degradation in Eroding Coastal Wetlands*. Louisiana State University and Agricultural & Mechanical College.

Sapkota, Y., & White, J. R. (2021). Long-term fate of rapidly eroding carbon stock soil profiles in coastal wetlands. *Science of the Total Environment*, *753*, 141913.

Scenarios, E. (2000). IPCC Special Report. *Cambridge Univ, Cambridge*.

Schieder, N. W. *Reconstructing coastal forest retreat and marsh migration response to historical sea level rise*. MSc thesis, College of William and Mary, Virginia Institute of Marine Science (2017).

Schoeneberger, P. J., Wysocki, D. A., & Benham, E. C. (Eds.). (2012). *Field book for describing and sampling soils*. Government Printing Office.

Short, A. D. (2012). Coastal processes and beaches, Nature Education Knowledge. *Tersedia pada: https://www. nature. com/scitable/knowledge/library/coastal-processes-and-beaches-26276621/(Diakses: 18 Januari 2022)*.

Short, F. T., Kosten, S., Morgan, P. A., Malone, S., & Moore, G. E. (2016). Impacts of climate change on submerged and emergent wetland plants. *Aquatic Botany*, *135*, 3-17.

Sierra, C. A., Hoyt, A. M., He, Y., & Trumbore, S. E. (2018). Soil organic matter persistence as a stochastic process: Age and transit time distributions of carbon in soils. *Global Biogeochemical Cycles*, *32*(10), 1574-1588.

Smart, L. S., Taillie, P. J., Poulter, B., Vukomanovic, J., Singh, K. K., Swenson, J. J., ... & Meentemeyer, R. K. (2020). Aboveground carbon loss associated with the spread of ghost forests as sea levels rise. *Environmental Research Letters*, *15*(10), 104028.

Smeed, D. A., McCarthy, G., Cunningham, S. A., Frajka-Williams, E., Rayner, D., Johns, W. E., ... & Bryden, H. L. (2013). Observed decline of the Atlantic Meridional Overturning Circulation 2004 to 2012. *Ocean Science Discussions*, *10*(5).

Soil Survey Staff, Natural Resources Conservation Service, United States Department of Agriculture. (2024) *Coastal Zone Soil Survey of Banana River Lagoon*. Data available upon request (andrew.wilson@usda.gov)

Soil Survey Staff, Natural Resources Conservation Service, United States Department of Agriculture. (2023) *Coastal Zone Soil Survey of the Lower Chesapeake Bay.* Data available upon request (andrew.wilson@usda.gov)

Soil Survey Staff. (2022a). Kellogg Soil Survey Laboratory methods manual. Soil Survey Investigations Report No. 42, Version 6.0. U.S. Department of Agriculture, Natural Resources Conservation Service. Washington, DC: U.S. Government Printing Office

Soil Survey Staff (2022b). Keys to Soil Taxonomy (13th ed.). Washington, DC: U.S. Government Printing Office

Soil Survey Staff, Natural Resources Conservation Service, United States Department of Agriculture. (2022c) *Coastal Zone Soil Survey of Cape Fear River*. Data available upon request (andrew.wilson@usda.gov)

Soil Science Division Staff. 2017. Soil survey manual. C. Ditzler, K. Scheffe, and H.C. Monger (eds.). USDA Handbook 18. Government Printing Office, Washington, D.C.

Stanley, D. W., & Hobbie, J. E. (1976). *Nitrogen recycling in the Chowan River*. Water

Resources Research Institute of the University of North Carolina.

Stedman, S. M., & Dahl, T. E. (2008). Status and trends of wetlands in the coastal watersheds of the eastern United States, 1998 to 2004.

Stocker, T. (Ed.). (2014). *Climate change 2013: the physical science basis: Working Group I contribution to the Fifth assessment report of the Intergovernmental Panel on Climate Change*. Cambridge university press.

Sui, T., Yang, M., Peng, L., Chen, J., Zhang, C., & Zheng, J. (2024). Wave-induced residual response and liquefaction of a nonhomogeneous layered seabed. *Frontiers in Marine Science*, *11*, 1360641.

Sweet, W. V., Hamlington, B. D., Kopp, R. E., Weaver, C. P., Barnard, P. L., Bekaert, D., ... & Zuzak, C. (2022). Global and Regional Sea Level Rise Scenarios for the United States: Updated Mean Projections and Extreme Weather Level Probabilities along US Coastlines.

Temmerman, S., Govers, G., Wartel, S., & Meire, P. (2004). Modelling estuarine variations in tidal marsh sedimentation: response to changing sea level and suspended sediment concentrations. *Marine Geology*, *212*(1-4), 1-19.

Temmerman, S., Govers, G., Wartel, S., & Meire, P. (2003). Spatial and temporal factors controlling short-term sedimentation in a salt and freshwater tidal marsh, Scheldt estuary, Belgium, SW Netherlands. *Earth Surface Processes and Landforms: The Journal of the British Geomorphological Research Group*, *28*(7), 739-755.

Tise, L. E., & Crow, J. J. (Eds.). (2017). *New Voyages to Carolina: Reinterpreting North Carolina History*. UNC Press Books.

Thomas, S. (2014). Blue carbon: Knowledge gaps, critical issues, and novel approaches. *Ecological Economics*, *107*, 22-38.

Thrush, S. F., Townsend, M., Hewitt, J. E., Davies, K., Lohrer, A. M., Lundquist, C., ... & Dymond, J. (2013). The many uses and values of estuarine ecosystems. *Ecosystem services in New Zealand–conditions and trends. Manaaki Whenua Press, Lincoln, New Zealand*, 226-237.

Trimble, S. W. (1974). Man-induced soil erosion on the southern Piedmont. *Soil Conservation Society of America*.

U.S. Department of Agriculture, Natural Resources Conservation Services. (2023) National soil survey handbook (656.2), title 430-VI. https://www.nrcs.usda.gov/resources/guides-and-instructions/national-soil-survey-handbook

University of California, Davis, California Soil Resource Lab; University of California, Division

of Agriculture and Natural Resources; Natural Resources Conservation Service (2019). SoilWeb. University of California; USDA-NRCS. Dataset. https://hdl.handle.net/10113/AA23078

Ury, E. A., Yang, X., Wright, J. P., & Bernhardt, E. S. (2021). Rapid deforestation of a coastal landscape driven by sea-level rise and extreme events. *Ecological applications*, *31*(5), e02339.

Von Post, L. & Granlund, E. (1926). Peat resources in southern Sweden – Sveriges geologiska undersökning, Yearbook

Wamsley, T. V., Cialone, M. A., Smith, J. M., Atkinson, J. H., & Rosati, J. D. (2010). The potential of wetlands in reducing storm surge. *Ocean Engineering*, *37*(1), 59-68.

Wasson, K., Ganju, N. K., Defne, Z., Endris, C., Elsey-Quirk, T., Thorne, K. M., ... & Raposa, K. B. (2019). Understanding tidal marsh trajectories: evaluation of multiple indicators of marsh persistence. *Environmental Research Letters*, *14*(12), 124073.

Wasson, K., Woolfolk, A., & Fresquez, C. (2013). Ecotones as indicators of changing environmental conditions: rapid migration of salt marsh–upland boundaries. *Estuaries and Coasts*, *36*, 654-664.

Wells, J. T., & Kim, S. Y. (1989). Sedimentation in the Albemarle—Pamlico lagoonal system: synthesis and hypotheses. *Marine Geology*, *88*(3-4), 263-284.

Weston, N. B., Rodriguez, E., Donnelly, B., Solohin, E., Jezycki, K., Demberger, S., ... & Craft, C. B. (2023). Recent acceleration of wetland accretion and carbon accumulation along the US East Coast. *Earth's Future*, *11*(3), e2022EF003037.

White Jr, E. E., Ury, E. A., Bernhardt, E. S., & Yang, X. (2022). Climate change driving widespread loss of coastal forested wetlands throughout the North American coastal plain. *Ecosystems*, *25*(4), 812-827.

Wickham H, François R, Henry L, Müller K, Vaughan D (2023). dplyr: A Grammar of Data Manipulation. R package version 1.1.4, <https://CRAN.R-project.org/package=dplyr>

Wickham, H. (2016). Toolbox. *ggplot2: Elegant Graphics for Data Analysis*, 33-74.

Williams, K., Ewel, K.C., Stumpf, R.P., Putz, F.E. and Workman, T.W. (1999), Sea-Level Rise and Coastal Forest Retreat on the West Coast of Florida, USA. Ecology, 80: 2045-2063. https://doi.org/10.1890/0012-9658(1999)080[2045:SLRACF]2.0.CO;2

Wu, W., Biber, P., & Bethel, M. (2017). Thresholds of sea-level rise rate and sea-level rise acceleration rate in a vulnerable coastal wetland. *Ecology and Evolution*, *7*(24), 10890-10903.

Yao, Q., & Liu, K. B. (2017). Dynamics of marsh-mangrove ecotone since the mid-Holocene: A palynological study of mangrove encroachment and sea level rise in the Shark River Estuary, Florida. *PloS one*, *12*(3), e0173670.

Yin, J., Schlesinger, M. E., & Stouffer, R. J. (2009). Model projections of rapid sea-level rise on the northeast coast of the United States. *Nature Geoscience*, *2*(4), 262-266.

Yost, J. L., & Hartemink, A. E. (2019). Soil organic carbon in sandy soils: A review. *Advances in agronomy*, *158*, 217-310.

Young, M. A., Macreadie, P. I., Duncan, C., Carnell, P. E., Nicholson, E., Serrano, O., ... & Ierodiaconou, D. (2018). Optimal soil carbon sampling designs to achieve cost-effectiveness: a case study in blue carbon ecosystems. *Biology letters*, *14*(9), 20180416.

Yu, M., Rivera-Ocasio, E., Heartsill-Scalley, T., Davila-Casanova, D., Rios-López, N., & Gao, Q. (2019). Landscape-level consequences of rising sea-level on coastal wetlands: saltwater intrusion drives displacement and mortality in the twenty-first century. *Wetlands*, *39*(6), 1343-1355.

Zhong, C., Li, T., Bi, R., Sanganyado, E., Huang, J., Jiang, S., ... & Du, H. (2023). A systematic overview, trends and global perspectives on blue carbon: A bibliometric study (2003–2021). *Ecological Indicators*, *148*, 110063.

APPENDICES

Appendix A – Decadal Land Loss Rates

Methods

Average decadal rate of land loss was calculated at each research site using the earliest discernable satellite imagery available on Google Earth and then measuring the distance from the initial shoreline to the next time frame (Google Earth Pro 7.3, 2021). All sites were measured over five chronological satellite images, except for Roanoke River. Roanoke River was only measured four times from 1994 – 2021 due to a background measurement not being discernable in the mid-1980s. This is due to the low-resolution satellite imagery available. Decadal values were then averaged based on each ecosystem type across the Albemarle-Pamlico peninsula. Designated site Point Peter was removed from statistical analysis because it was an outlier among the dataset and skewed the standard deviation.

Results

Based on remote sensing, tidal forest shoreline changed -0.9±0.3 m yr^{-1}; ghost forest changed -1.3±0.6 m yr^{-1}; and tidal marshes changed -2.2±2.9 m yr^{-1}. When removing designated site Point Peter which exhibited an outlier shoreline change rate of -6.6 m yr^{-1}, the tidal marsh shoreline change rate becomes -0.7±0.3 m yr^{-1}. There was no significant difference between shoreline change rate and ecosystem ($p = 0.28$). There was no significant difference between total change rate and ecosystem ($p = 0.25$) with tidal forest averaging -32±15 m, ghost forest averaging -44±24 m, and tidal marsh averaging -19±11 m. The rolling decadal average is reported below.

Table A1. Comparison of decadal average shoreline erosion rates (m yr^{-1}) between ecosystems.

Decade	Tidal Forest	Ghost Forest	Tidal Marsh
1985 to 1995	-1.0±0.9	-2.1±0.8	-1.4±0.5
1996 to 2005	-0.6±0.2	-1.4±0.8	-0.6±0.6
2006 to 2015	-0.9±0.3	-0.9±0.6	-0.7±0.5
2016 to 2021	-1.0±0.6	-0.7±0.6	-0.1±0.1

Discussion

Measurements of shoreline change are a simple, common form of analysis conducted to analyze and quantify the amount of shoreline change which is occurring at the land-water interface. We found there were no significant differences between ecosystems when comparing shoreline change rates over an approximate 35–40-year range; even when Point Peter was included in statistical analysis. Point Peter experienced greater than eight times the next tidal marsh site (Juniper Bay) total land loss: 238 meters compared to 29 meters over the same period of 1985 to 2020. This can be attributed to two primary drivers: the site is approximately 19 km due west of the Oregon Inlet and an 85-acre pear fire in 2015 reduced the cohesion and stressed the ecosystem further (Outer Banks Voice, 2015). Our shoreline change rate observation at Point Peter is larger than what was observed by others at -6.6±1.8 m yr^{-1}; Riggs and Ames (2003) recorded its average shoreline change rate to be -2.2 to 2.5 m yr^{-1} from 1969 to 2000. Table X compares shoreline change rates observed in this study and other in North Carolina.

Table A2. Comparisons of regional shoreline change rates (m yr^{-1})

Study	Tidal Forest	Ghost Forest	Tidal Marsh	Source
Albemarle-Pamlico Sound	-0.7	-	-0.9	Riggs and Ames 2003
Neuse River Estuary	-0.5	-0.5	-0.5*	Cowart et al. 2011 *Study grouped all wetlands as one type
Tar-Pamlico Sub-Estuary	-0.5±0.9	-0.5±0.9	-0.5±0.9	Eulie et al. 2018 *Study grouped all shorelines as one type
Albemarle-Pamlico Sound	0.26	-0.65	-1.6	Gorczynski et al., 2024
Albemarle-Pamlico Sound	-0.9±0.3	-1.3±0.6	-0.7±0.3	This Study

Appendix B – Pedon versus Depth Comparison Statistics

Table B1: Mean (± SE) weighted pedon soil properties compared among site and sampling location to a depth of 50 cm. Different letters by column indicate significant differences ($p < 0.05$).

Ecosystem	N	SOC (Mg/ha)	**C:N**	**EC (1:5 DI)**
Tidal Forest				
Terrestrial	4	$216\pm44_{a}$	$20\pm4_{a}$	$0.06\pm0.01_{a}$
Nearshore	4	$140\pm51_{b}$	$21\pm5_{a}$	$0.15\pm0.06_{a}$
Offshore	3	$73\pm45_{b}$	$16\pm6_{a}$	$0.15\pm0.03_{a}$
Ghost Forest				
Terrestrial	5	$176\pm18_{a}$	$20\pm3_{a}$	$0.87\pm0.29_{a}$
Nearshore	4	$61\pm31_{b}$	$21\pm8_{a}$	$0.62\pm0.16_{a}$
Offshore	3	$44\pm35_{b}$	$11\pm4_{a}$	$0.67\pm0.38_{a}$
Tidal Marsh				
Terrestrial	4	$156\pm26_{a}$	$20\pm2_{a}$	$4.33\pm1.05_{b}$
Nearshore	4	$127\pm9_{b}$	$29\pm5_{a}$	$3.64\pm1.23_{b}$
Offshore	4	$32\pm7_{b}$	$15\pm1_{a}$	$1.83\pm0.47_{b}$

Table B2: Mean (± SE) weighted pedon soil properties compared among site and sampling location to a depth of 100 cm. Different letters by column indicate significant differences ($p < 0.05$).

Ecosystem	N	SOC (Mg/ha)	**C:N**	**EC (1:5 DI)**
Tidal Forest				
Terrestrial	4	$427\pm60_{d}$	$21\pm3_{a}$	$0.08\pm0.02_{a}$
Nearshore	4	$314\pm87_{e}$	$23\pm4_{a}$	$0.15\pm0.06_{a}$
Offshore	3	$182\pm67_{f}$	$21\pm4_{b}$	$0.15\pm0.06_{a}$
Ghost Forest				
Terrestrial	5	$361\pm35_{a}$	$24\pm3_{a}$	$0.86\pm0.28_{a}$
Nearshore	4	$134\pm85_{b}$	$18\pm3_{a}$	$0.55\pm0.16_{a}$
Offshore	3	$53\pm38_{c}$	$11\pm3_{b}$	$0.56\pm0.33_{a}$
Tidal Marsh				
Terrestrial	4	$307\pm30_{ad}$	$21\pm2_{a}$	$4.76\pm1.03_{b}$
Nearshore	4	$294\pm44_{be}$	$31\pm5_{a}$	$3.36\pm1.15_{b}$
Offshore	4	$49\pm10_{cf}$	$13\pm1_{b}$	$1.60\pm0.42_{b}$

Table B3: Mean (± SE) weighted pedon soil properties compared among site and sampling location to a depth of 200 cm. Different letters by column indicate significant differences ($p < 0.05$).

Ecosystem	N	SOC (Mg/ha)	**C:N**	**EC (1:5 DI)**
Tidal Forest				
Terrestrial	4	$924 \pm 131_{ac}$	$23 \pm 3_{ac}$	$0.10 \pm 0.03_{ac}$
Nearshore	1	396_{ad}	22_{ac}	0.14_{ad}
Offshore	2	$356 \pm 61_{ae}$	$18 \pm 4_{bc}$	$0.17 \pm 0.08_{ad}$
Ghost Forest				
Terrestrial	2	$635 \pm 194_{bc}$	$27 \pm 8_{ad}$	$0.54 \pm 0.25_{ac}$
Nearshore	4	$159 \pm 89_{bd}$	$14 \pm 3_{ad}$	$0.53 \pm 0.20_{ad}$
Offshore	3	$63 \pm 40_{be}$	$8 \pm 2_{bd}$	$0.53 \pm 0.35_{ad}$
Tidal Marsh				
Terrestrial	4	$659 \pm 72_{bc}$	$25 \pm 3_{adc}$	$4.67 \pm 0.90_{bc}$
Nearshore	4	$351 \pm 55_{bd}$	$24 \pm 3_{adc}$	$2.78 \pm 0.89_{bd}$
Offshore	4	$69 \pm 18_{be}$	$11 \pm 0_{bdc}$	$1.42 \pm 0.26_{bd}$

Appendix C – Supplementary Accretion Data

Table C1. Tidal forest supplementary accretion data and sites for ^{210}Pb

Site	Depth (cm)	Oven Dry Bulk Density (g cm^{-3})	Total ^{210}Pb Activity (dpm g^{-1})	Measurement Error	Radon Measured (dpm g^{-1})
Chowan River, NC 36.2888800, -76.7010800	0 – 2	0.07	12.1	0.44	-
	2 – 4	0.1	11.43	0.43	-
	4 – 6	0.1	11.1	0.42	-
	6 – 8	0.11	10.71	0.41	-
	8 – 10	0.09	9.67	0.39	-
	10 – 12	0.11	11.47	0.48	-
	12 – 14	0.12	8.39	0.37	-
	14 – 16	0.14	7.85	0.36	-
	16 – 18	0.14	7.3	0.34	-
	18 – 20	0.16	6.7	0.33	-
	20 – 22	0.13	5.93	0.31	-
	22 – 24	0.14	5.51	0.3	-
	24 – 26	0.14	4.92	0.28	-
	26 – 28	0.14	5.26	0.33	-
	28 – 30	0.16	3.62	0.24	-
	30 – 35	0.22	2.86	0.22	-
	35 – 40	0.25	2.51	0.2	-
	40 – 45	0.26	2.1	0.19	-
	45 – 50	0.24	1.87	0.18	-
Roanoke River, NC 35.9341600, -76.7245100	0 – 2	0.12	12.02	0.44	-
	2 – 4	0.15	11.74	0.43	-
	4 – 6	0.16	11.25	0.43	-
	6 – 8	0.18	10.87	0.42	-
	8 – 10	0.19	10	0.4	-
	10 – 12	0.2	9.47	0.39	-
	12 – 14	0.3	8.62	0.37	-
	14 – 16	0.32	8.03	0.36	-
	16 – 18	0.37	7.38	0.34	-
	18 – 20	0.37	6.63	0.33	-
	20 – 22	0.37	6.07	0.31	-
	22 – 24	0.38	5.51	0.3	-
	24 – 26	0.43	5.14	0.29	-
	26 – 28	0.3	4.67	0.27	-
	28 – 30	0.32	4.19	0.26	-
	30 – 35	0.38	3.44	0.24	-
	35 – 40	0.55	2.85	0.22	-
	40 – 45	0.52	2.44	0.2	-
	45 – 50	0.44	1.84	0.18	1.05±0.13
Tar River, NC 35.5495900,	0 – 2	0.11	12.04	0.44	-
	2 – 4	0.13	11.82	0.44	-
	4 – 6	0.15	11.33	0.43	-
	6 – 8	0.19	10.89	0.42	-
	8 – 10	0.2	10.11	0.4	-
	10 – 12	0.22	9.5	0.39	-
	12 – 14	0.2	8.78	0.37	-
	14 – 16	0.23	8.05	0.36	-

-77.0885700	16 – 18	0.23	7.46	0.35	-
	18 – 20	0.25	6.68	0.33	-
	20 – 22	0.22	6.16	0.32	-
	22 – 24	0.26	5.58	0.3	-
	24 – 26	0.3	5.18	0.29	-
	26 – 28	0.31	4.55	0.27	-
	28 – 30	0.16	4.16	0.26	-
	30 – 35	0.17	3.39	0.24	-
	35 – 40	0.19	2.83	0.22	-
	40 – 45	0.12	2.38	0.2	-
	45 – 50	0.12	1.8	0.18	1.02±0.15

Table C2. Ghost forest supplementary accretion data and sites for ^{210}Pb

	Depth (cm)	Oven Dry Bulk Density (g cm^{-3})	Total ^{210}Pb Activity (dpm g^{-1})	Measurement Error	Radon Measured (dpm g^{-1})
Alligator River, NC 35.8951800, -76.04010600	0 – 2	0.18	11.79	0.43	-
	2 – 4	0.13	11.24	0.43	-
	4 – 6	0.12	10.98	0.42	-
	6 – 8	0.19	10.52	0.41	-
	8 – 10	0.19	9.54	0.39	-
	10 – 12	0.17	11.33	0.47	-
	12 – 14	0.17	8.28	0.37	-
	14 – 16	0.15	7.84	0.36	-
	16 – 18	0.15	6.96	0.33	-
	18 – 20	0.13	6.48	0.32	-
	20 – 22	0.12	5.94	0.31	-
	22 – 24	0.12	5.4	0.3	-
	24 – 26	0.1	4.78	0.28	-
	26 – 28	0.1	5.4	0.33	-
	28 – 30	0.08	3.58	0.24	-
	30 – 35	0.1	2.93	0.22	-
	35 – 40	0.08	2.57	0.21	-
	40 – 45	0.06	2.14	0.19	-
	45 – 50	0.1	1.92	0.18	0.98±0.15
Goose Creek, NC 35.4639400, -76.9145800	0 – 2	0.11	12.04	0.44	-
	2 – 4	0.11	11.58	0.43	-
	4 – 6	0.11	11.22	0.43	-
	6 – 8	0.09	10.78	0.42	-
	8 – 10	0.11	9.81	0.4	-
	10 – 12	0.11	9.19	0.38	-
	12 – 14	0.11	8.59	0.37	-
	14 – 16	0.15	8.01	0.36	-
	16 – 18	0.13	7.34	0.34	-
	18 – 20	0.16	6.77	0.33	-
	20 – 22	0.14	5.84	0.31	-
	22 – 24	0.15	5.55	0.3	-
	24 – 26	0.12	4.75	0.28	-
	26 – 28	0.13	4.1	0.26	-
	28 – 30	0.15	3.58	0.24	-
	30 – 35	0.21	2.93	0.22	-
	35 – 40	0.24	2.46	0.2	-

	40 – 45	0.25	2.02	0.18	-
	45 – 50	0.24	1.86	0.18	-

Table C3. Tidal marsh supplementary accretion data and sites for ^{210}Pb

Site	Depth (cm)	Oven Dry Bulk Density (g cm^{-3})	Total ^{210}Pb Activity (dpm g^{-1})	Measurement Error	Radon Measured (dpm g^{-1})
Juniper Bay, NC 35.3823900, -76.2497800	0 – 2	0.09	12.22	0.44	-
	2 – 4	0.8	11.76	0.43	-
	4 – 6	0.1	11.44	0.43	-
	6 – 8	0.14	10.97	0.42	-
	8 – 10	0.24	9.98	0.4	-
	10 – 12	0.15	9.38	0.39	-
	12 – 14	0.1	8.82	0.38	-
	14 – 16	0.12	8.14	0.36	-
	16 – 18	0.13	7.44	0.35	-
	18 – 20	0.16	6.71	0.33	-
	20 – 22	0.16	6.04	0.31	-
	22 – 24	0.11	5.7	0.3	-
	24 – 26	0.13	5.11	0.29	-
	26 – 28	0.18	4.89	0.28	-
	28 – 30	0.13	4.45	0.27	-
	30 – 35	0.24	3.51	0.24	-
	35 – 40	0.24	3.08	0.22	-
	40 – 45	0.21	2.57	0.21	-
	45 – 50	0.24	2.03	0.18	1.12±0.14
Longshoal, NC 35.6087200, -75.8696200	0 – 2	0.24	12.13	0.44	-
	2 – 4	0.28	11.83	0.44	-
	4 – 6	0.31	11.33	0.43	-
	6 – 8	0.46	10.93	0.42	-
	8 – 10	0.44	10.09	0.4	-
	10 – 12	0.46	9.48	0.39	-
	12 – 14	0.52	8.89	0.38	-
	14 – 16	0.37	8.22	0.37	-
	16 – 18	0.35	7.42	0.35	-
	18 – 20	0.41	6.77	0.33	-
	20 – 22	0.41	6.2	0.32	-
	22 – 24	0.38	5.63	0.3	-
	24 – 26	0.41	5.17	0.29	-
	26 – 28	0.42	4.86	0.28	-
	28 – 30	0.42	4.34	0.27	-
	30 – 35	0.27	3.46	0.24	-
	35 – 40	0.27	2.88	0.22	-
	40 – 45	0.21	2.49	0.2	-
	45 – 50	0.23	2.03	0.18	-
	0 – 2	0.08	12.1	0.44	-
	2 – 4	0.1	11.73	0.43	-
	4 – 6	0.18	11.27	0.43	-
	6 – 8	0.11	10.81	0.42	-
	8 – 10	0.1	10.03	0.4	-
	10 – 12	0.08	9.43	0.39	-

Swanquarter, NC 35.4070600, -76.3509500	12 – 14	0.08	8.64	0.37	-
	14 – 16	0.11	8.14	0.36	-
	16 – 18	0.09	7.29	0.34	-
	18 – 20	0.09	6.61	0.33	-
	20 – 22	0.15	5.88	0.31	-
	22 – 24	0.11	5.47	0.3	-
	24 – 26	0.1	5.11	0.29	-
	26 – 28	0.08	4.41	0.27	-
	28 – 30	0.2	3.76	0.25	-
	30 – 35	0.2	3.18	0.23	-
	35 – 40	0.15	2.72	0.21	-
	40 – 45	0.17	2.02	0.18	-
	45 – 50	0.16	1.68	0.17	-

Table C4. C-14 supplementary accretion data for all ecosystems

Site	Latitude, Longitude	Ecosystem	Horizon	Depth (cm)	Uncalibrated Radiocarbon Age Before Present (1950)	Error	Calibrated Year (AD)
Chowan A	36.2888800, -76.7010800	Tidal Forest	Oa3	115	522	30	1415
Chowan B		Tidal Forest	Oa5	207	1580	25	485
Chowan C		Tidal Forest	Oa4	171	519	28	1416
Point Peter A	35.7416000, -75.7337500	Tidal Marsh	3Bhse & 2Oase4	159	1801	30	30
Roanoke A	35.9341600, -76.7245100	Tidal Forest	Oa3	148	1047	20	1006
Longshoal A	35.6087200, -75.8696200	Tidal Marsh	3Oase2	138	1205	20	829
Longshoal B		Tidal Marsh	4Cg	191	2776	23	-921
Swanquarter A	35.4070600, -76.3509500	Tidal Marsh	2Oase1	138	1204	22	830
Tar River A	35.5495900, -77.0885700	Tidal Forest	O'a	167	1176	20	849
Bull Neck A	35.9798000, -76.0431000	Tidal Forest	Oase2	213	1994	23	19
Alligator River A	35.8951800, -76.04010600	Ghost Forest	Oase3	146	838	21	1217
Alligator River B		Ghost Forest	Oase4	191	1075	21	979
Palmetto Peartree Two A	35.9899100, -76.0691200	Ghost Forest	3Cg1	82	100	20	1835
Juniper Bay A	35.3823900, -76.2497800	Tidal Marsh	2Oase2	152	1416	23	628
Goose Creek A	35.4639400, -76.9145800	Ghost Forest	2Oase	96	784	27	1248

Appendix D – Supplementary Subaqueous Data

The following pedon descriptions can be accessed through the National Soil Information System database (NASIS) by entering the associated pedon identification number listed below, maintained by the USDA-NRCS:

https://nasis.sc.egov.usda.gov/NasisReportsWebSite/limsreport.aspx?report_name=WEB-Masterlist_SUB_pedon_site_description_usepedonid

Table D1. Supplementary information for subaqueous soils

Site	Ecosystem	Pedon Identification Number	Latitude, Longitude
Brier Hall – Nearshore	Ghost Forest	S2020NC055005	35.9123000, -75.926000
Brier Hall – Offshore	Ghost Forest	S2020NC055006	35.9125000, -75.9261000
Bull Neck – Nearshore	Tidal Forest	S2020NC187001	35.9646000, -76.3830000
Bull Neck – Offshore	Tidal Forest	S2020NC187002	35.9660000, -76.3814000
Chowan – Nearshore	Tidal Forest	S2021NC091001	36.28940000, -76.7007000
Palmetto – Peartree – Nearshore	Ghost Forest	S2020NC177003	35.9902000, -76.0685000
Roanoke River – Nearshore	Tidal Forest	S2020NC015001	35.9349330, -76.7253500
Roanoke River – Offshore	Tidal Forest	S2020NC015002	35.9382670, -76.7294000
Alligator River – Nearshore	Ghost Forest	S2020NC177001	35.8951833, -76.0397833
Alligator River – Offshore	Ghost Forest	S2020NC177002	35.8950330, -76.0372830
Swanquarter – Nearshore	Tidal Marsh	S2020NC095003	35.4071500, -76.4006830
Swanquarter – Offshore	Tidal Marsh	S2020NC095004	35.4074330, -76.3499500
Longshoal – Nearshore	Tidal Marsh	S2020NC055003	35.6083330, -75.8695500
Longshoal – Offshore	Tidal Marsh	S2020NC055004	35.6075560, -75.8710560
Point Peter – Nearshore	Tidal Marsh	S2020NC055001	35.7417830, - 75.7334670
Point Peter – Offshore	Tidal Marsh	S2020NC055002	35.7433170, -75.7306170
Tar River – Nearshore	Tidal Forest	S2020NC013001	35.5499000, -77.0888333
Tar River – Offshore	Tidal Forest	S2020NC013002	35.5502667, -77.089033
Goose Creek – Nearshore	Ghost Forest	S2020NC013004	35.4634667, -76.9146500
Goose Creek – Offshore	Ghost Forest	S2020NC013003	35.4622167, -76.9152167

Juniper Bay – Nearshore	Tidal Marsh	S2020NC095001	35.3826333, -76.2498167
Juniper Bay – Offshore	Tidal Marsh	S2020NC095002	35.3830833, -76.2502667

Appendix E – BACON Analysis of Accretion Rates Including ^{210}Pb and ^{14}C

Blaauw, M., Christen, J.A., 2011. Flexible paleoclimate age-depth models using an autoregressive gamma process. *Bayesian Analysis* 6, 457-474

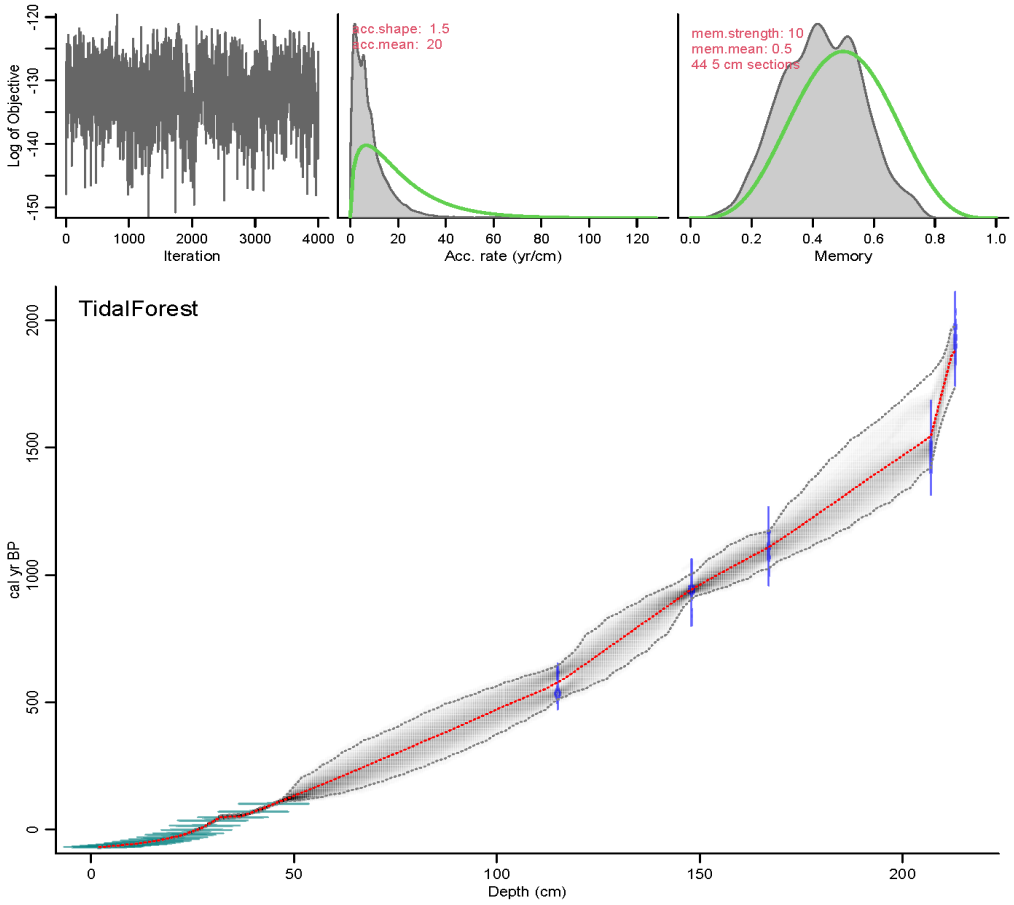

Figure E1. Figure generated using BACON program in R to compare ^{210}Pb and ^{14}C data without using bulk density in Tidal Forest

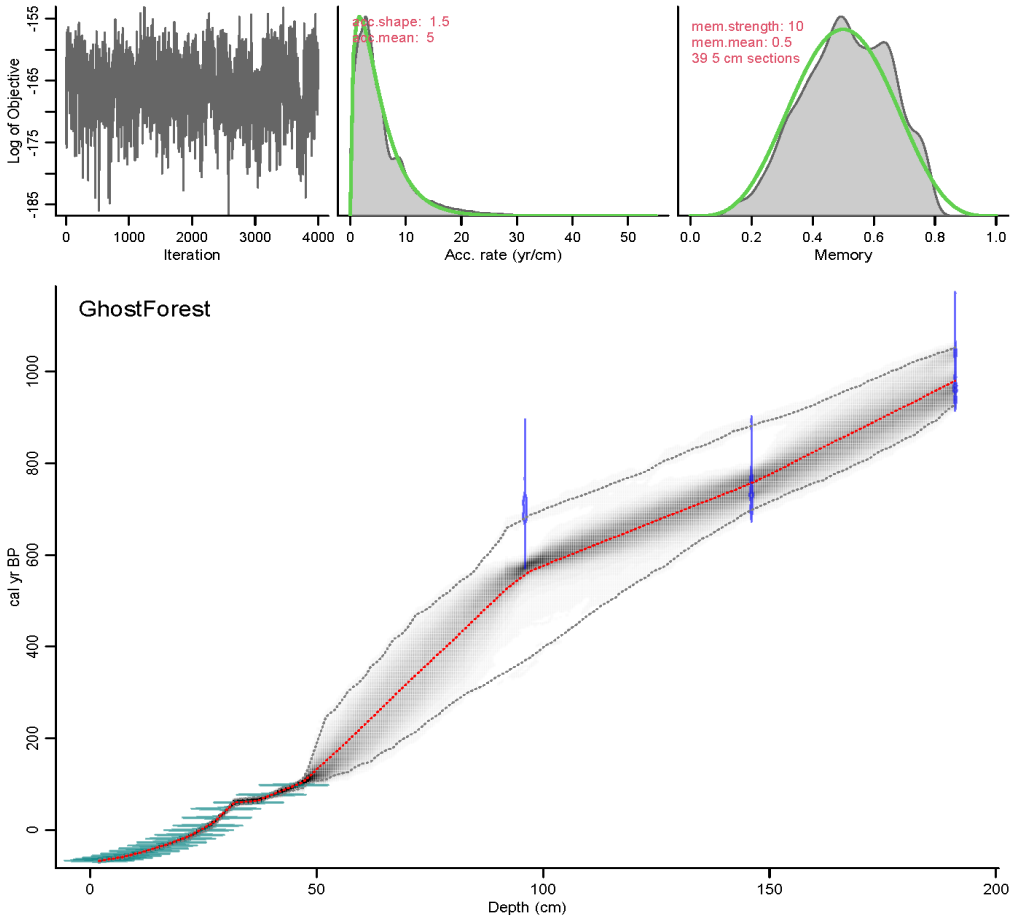

Figure E2. Figure generated using BACON program in R to compare ^{210}Pb and ^{14}C data without using bulk density in Ghost Forest

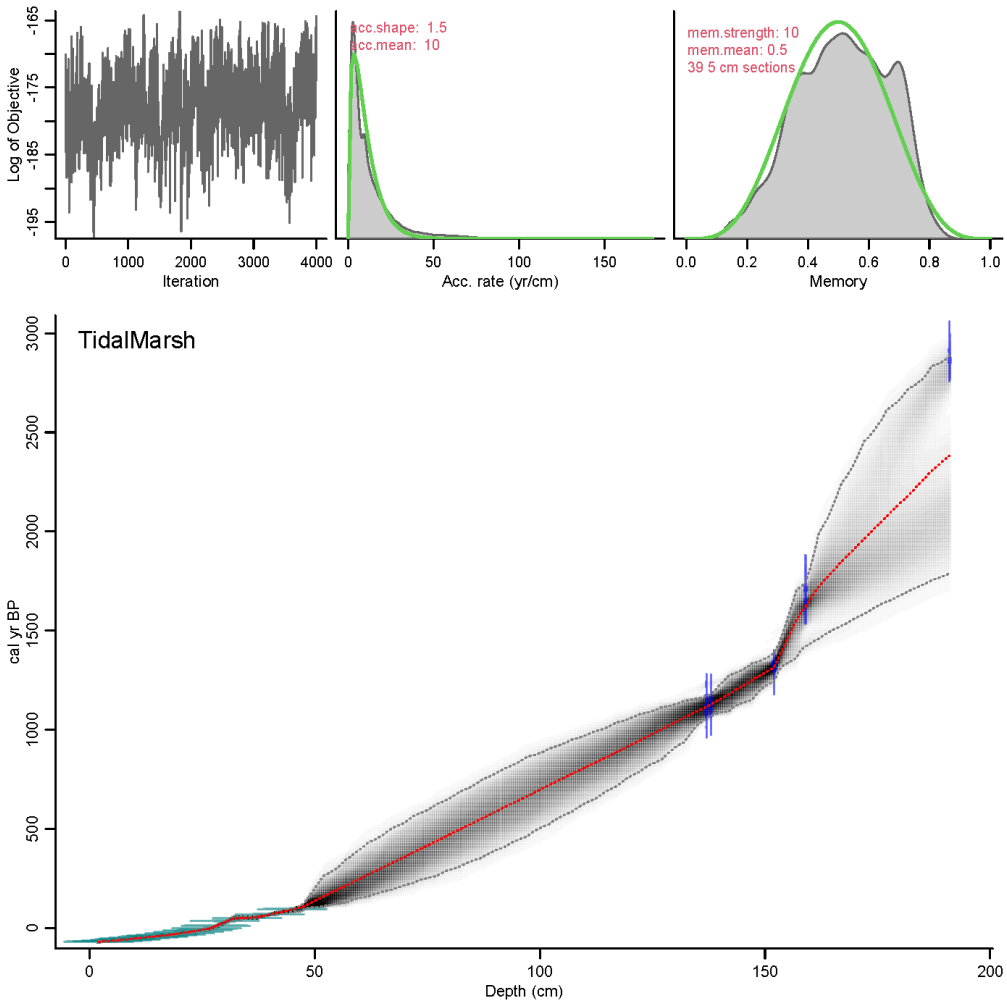

Figure E3. Figure generated using BACON program in R to compare ^{210}Pb and ^{14}C data without using bulk density in Tidal Marsh